



Norwegian University of
Science and Technology

Dynamic Response and Fatigue of Offshore Wind Turbines

Effect of Foundation Type and Modelling
Method Using Software FAST

Ingrid Bye Løken

Mechanical Engineering
Submission date: June 2017
Supervisor: Amir Kaynia, KT

Norwegian University of Science and Technology
Department of Structural Engineering



MASTER THESIS 2017

SUBJECT AREA: Structural Dynamics	DATE: 11.06.17	NO. OF PAGES: 26 + 112 + 31
--------------------------------------	-------------------	--------------------------------

TITLE:

Dynamic Response and Fatigue of Offshore Wind Turbines

Dynamisk Respons og Utmatting av Offshore Vindturbiner

BY:

Ingrid Bye Løken



SUMMARY:

This thesis presents dynamic response and fatigue analyses of several bottom-mounted offshore wind turbine models, simulated in the aero-hydro-servo-elastic simulation tool *FAST v8*. A 5 MW offshore wind turbine supported on a monopile was used as a reference model, and the effect of different foundation modelling methods, concepts and dimensions was studied.

Default modelling of the wind turbine foundation in *FAST* is by means of a rigid connection to the seabed, implying that foundation flexibility and soil-structure interaction are not considered. The first objective of this thesis was to study the effect of including foundation flexibility in the *FAST* model. The soil-foundation stiffness was represented by adding a fictive beam below the mudline, a procedure called the *apparent fixity method*. A simplified approach was implemented first, followed by the development of a more exact approach. The second objective was to perform sensitivity analyses of both monopile foundations and suction caisson foundations with different dimensions, with respect to dynamic response and fatigue damage.

It was concluded that foundation modelling is an important topic in offshore wind turbine research and development. Neglecting the flexibility of the foundation lead to underpredictions of structural dynamic response and fatigue damage, while modelling the foundation with the simplifications made in the first method lead to overpredictions. Furthermore, reducing the monopile subsoil length had no significant effect on the *FAST* output and the fatigue life, while reducing the monopile wall thickness lead to large increases in fatigue damage, and hence large reductions in fatigue life. Regarding both the suction caisson foundations and the monopile foundations, it was concluded that further analyses with respect to soil capacity and buckling would have to be performed to make valid conclusions on required dimensions.

RESPONSIBLE TEACHER: Amir M. Kaynia

SUPERVISOR(S): Amir M. Kaynia

CARRIED OUT AT: Department of Structural Engineering, Faculty of Engineering Science and Technology, Norwegian University of Science and Technology (NTNU)

Preface

This Master's thesis has been written as the final part of the five year Master of Science programme in Mechanical Engineering at the Norwegian University of Science and Technology (NTNU) in Trondheim. The work was conducted during the spring semester 2017 at the Department of Structural Engineering at the Faculty of Engineering Science and Technology. The author's specialization in Applied Mechanics has provided an interdisciplinary and broad background for the work presented in this thesis.

Acknowledgements

I would like to express my gratitude to my supervisor, Professor Amir M. Kaynia. I highly appreciate his availability by email and his motivating replies. His dedication, knowledge and curiosity throughout these months have been inspiring. Further, I want to thank fellow student Else Tjønn for entertaining discussions about both relevant and irrelevant issues. Finally, I wish to thank my family for supporting me throughout these years.

Trondheim, June 11, 2017



Ingrid Bye Løken

Abstract

This thesis presents dynamic response and fatigue analyses of several bottom-mounted offshore wind turbine models, simulated in the aero-hydro-servo-elastic simulation tool *FAST* v8. The distinction between the models is the foundations, which are modelled with different methods, concepts and dimensions. United States' National Renewable Energy Laboratory has developed a 5 MW reference turbine supported on a monopile, the *NREL 5MW*, which was used as a reference model in this thesis.

OWT foundations have in general been given low priority by researchers. Default modelling of the foundation in *FAST* is by means of a rigid connection to the seabed, meaning that foundation flexibility is not considered. Including the soil-foundation flexibility would give a softer model, which reduces the natural frequencies of the OWT system, shifting them closer to the frequencies of the environmental loads. This may lead to resonance effects and large cyclic loads in the structure, causing increased fatigue damage.

The flexibility of the monopile foundation was first included in the *FAST* model through the *simplified apparent fixity method*. This method represents the stiffness of the real soil-foundation system by adding a fictive beam below the mudline. Further, an improved method was developed, referred to as the *improved apparent fixity method*, adding *two* fictive beams below the mudline. *FAST* simulations showed significant differences in dynamic response between the two foundation methods; the simplified model gave a considerably softer behaviour. This concluded that the simplification made in the first method had an important impact on the response. Consequently, the improved AF method was chosen as the preferred modelling method.

Furthermore, sensitivity analyses of different monopile foundation dimensions were performed by simulating models with reduced subsoil pile lengths and pile wall thicknesses. The simulation outputs showed that large reductions in pile length lead to almost no change in dynamic response in *FAST*. Moreover, reduced wall thickness lead to moderate increases in mudline bending moments, implying large increases in bending stresses.

A relatively new alternative to the monopile foundation is the suction caisson foundation. Models of the *NREL 5MW* with caisson foundations of varying dimensions were simulated in *FAST* for sensitivity purposes. The results showed that a small caisson of 10 m \times 5 m gave the same dynamic response in *FAST* as the regular monopile foundation.

The final part of the thesis presents fatigue analyses of the different foundation models. 17 load cases were run in FAST for every model, and time series of mudline moment were used for fatigue analyses in the tool *MLife*. Fatigue damage, fatigue life and damage equivalent loads were calculated, as well as the relative fatigue contribution from each load case. The analyses showed that the time until failure was reduced by 22.1% for the flexible monopile model compared to the fixed base model, and that reducing the pile wall thickness by 1/3 reduced the fatigue life with 89.1%.

It was concluded that foundation modelling is an important topic in offshore wind turbine research and development. Neglecting the flexibility of the foundation lead to underpredictions of structural dynamic response and fatigue damage, while modelling it inaccurately gave overpredictions. There are possibilities for optimizing OWT foundations, both by means of concept and dimensions. However, further analyses regarding soil capacity and buckling would have to be performed to make valid conclusions on required dimensions, both for the monopile and the caisson foundation.

Sammendrag

Denne masteroppgaven presenterer analyser av dynamisk respons og utmatting av modeller av bunnfaste offshore vindturbiner, simulert i det aero-hydro-servoelastiske simuleringsverktøyet *FAST* v8. Forskjellen mellom modellene er fundamentene, som er modellert med ulike metoder, konsepter og dimensjoner. Det amerikanske *National Renewable Energy Laboratory* har utviklet en 5 MW referanseturbin på en monopelstruktur, kalt *NREL 5MW*, som har blitt brukt som en referansemodell i denne oppgaven.

Fundamentering av offshore vindturbiner har generelt blitt nedprioritert av forskere. *FAST* modellerer fundamentet fast innspent i havbunnen, noe som betyr at fundamentets fleksibilitet ikke er tatt i betraktning. Å inkludere fleksibiliteten i fundamentet gir en mykere modell, noe som reduserer egenfrekvensene til systemet, slik at de kommer nærmere frekvensene til naturlastene. Dette kan føre til resonsanseffekter og store sykliske laster i turbinstrukturen, noe som øker tretthetsskader.

Fleksibiliteten til monopelfundamentet ble først inkludert i *FAST*-modellen med den *forenklede apparent fixity-metoden*. Denne metoden reproduserer stivheten til jord-fundamentsystemet ved å legge inn en fiktiv bjelke under havbunnen. Videre ble en forbedret metode utviklet, referert til som den *forbedrede apparent fixity-metoden*, som legger inn *to* fiktive bjelker under havbunnen. *FAST* simuleringer viste tydelig forskjell i dynamisk respons mellom de to fundamentmodellene; den forenklete modellen viste betydelig mykere oppførsel. Fra dette kunne en konkludere med at forenklingen gjort i den første metoden hadde en betydelig innvirkning på responsen, og derfor ble den forbedrede metoden valgt som den foretrukne modelleringsmetoden.

Videre ble sensitivitetsanalyser og ulike monopeldimenssjoner gjennomført ved å simulere modeller med redusert lengde og veggtykkelse på pelen. Resultatene viste at store reduksjoner i lengde førte til nesten ingen endring i dynamisk respons i *FAST*. Redusert veggtykkelse førte til moderate økninger i bøyemoment ved havbunnen, som betyr store økninger i bøyepenninger.

Et relativt nytt alternativ til monopelfundamentet er et bøttfundament. Modeller av *NREL 5MW* med bøttfundamenter av ulike dimensjoner ble simulert i *FAST* for å undersøke sensitivitet. Resultatene viste at et lite bøttfundament på 10×5 m ga den samme dynamiske responsen i *FAST* som det vanlige monopelfundamentet.

I den siste delen av denne oppgaven blir utmattingsanalyser av de ulike fundamentmodellene presentert. 17 lasttilfeller ble simulert i FAST for hver model, og tidsserier av bøyemoment ved havbunnen ble brukt som utgangspunkt for utmattingsanalysene i verktøyet *MLife*. Tretthetsskader, levetid og skadetilsvarende laster ble beregnet, i tillegg til det relative utmattingsbidraget fra hvert lasttilfelle. Analysene viste at levetiden ble redusert med 22.1 % for den fleksible monopelmodellen sammenlignet med den fast innspente modellen, og at reduisering av veggykkelsen med 1/3 reduserte levetiden med 89.1%.

Det ble konkludert med at modellering av fundamenter er et viktig tema for utvikling av og forskning på offshore vind turbiner. Neglisjering av fundamentets fleksibilitet førte til underestimering av dynamisk respons og utmattingskader, mens unøyaktiv modellering ga overpredikeringer. Det er muligheter for å optimalisere vindturbinfundamenter, både med tanke på konsept og dimensjoner, men analyser vedrørende jordkapasitet og knekking må utføres for å trekke gyldige konklusjoner om nødvendige dimensjoner, både for monopelen og bøttefundamentet.

Contents

Preface	iii
Abstract	v
Sammendrag	vii
Nomenclature	xvii
1 Introduction	1
1.1 Motivation and Background	1
1.2 Objectives	2
1.3 Organization of the Thesis	2
2 Theory	5
2.1 Wind Energy History	5
2.2 Offshore Wind Turbines	5
2.2.1 Power Generation	6
2.2.2 Turbine Types	7
2.2.3 Dynamics of Offshore Wind Turbines	8
2.2.4 Support Structures	9
2.3 Offshore Wind Turbine Foundations	11
2.3.1 Foundation Concepts	12
2.3.2 Foundation Behaviour	13
2.4 Foundation Models	13
2.4.1 Stiffness Matrix	15
2.4.2 Coupled and Uncoupled Springs	15
2.4.3 Distributed Springs	15
2.4.4 Apparent Fixity	15
2.5 Environmental Loads	17
2.5.1 Random Data Analysis	17
2.5.2 Wind	19
2.5.3 Waves	22

2.6	Fatigue in Offshore Wind Turbines	28
3	Computational Tool: FAST	29
3.1	The FAST Model	29
3.2	FAST Modularization Framework	32
3.2.1	SubDyn	33
3.2.2	ElastoDyn	34
3.2.3	HydroDyn	35
3.2.4	InflowWind and TurbSim	36
3.2.5	AeroDyn	37
3.2.6	ServoDyn	38
3.3	BModes	39
4	NREL 5-MW Baseline Wind Turbine	41
5	Simplified Foundation Model	45
5.1	Soil-Pile Interaction	45
5.2	Implementing the Foundation Model in FAST	48
5.3	FAST Simulation Inputs	51
5.4	FAST Simulation Outputs	53
6	Improved Foundation Model	57
6.1	Simulation Outputs	60
6.2	Power Spectral Densities	64
6.3	Response to Different Wave Periods	69
7	Sensitivity Analyses of a Monopile	73
7.1	Shorter Pile	73
7.2	Smaller Pile Wall Thickness	76
8	Suction Caisson Foundations	81
8.1	Sensitivity Analyses of Caisson Foundations	83
9	Fatigue Analyses	89
9.1	Load Conditions and FAST Simulations	89
9.2	MLife Theory	93
9.3	MLife Analyses	96

9.4	Results	99
10	Conclusions and Recommendations for Further Work	103
10.1	Conclusions	103
10.2	Recommendations for Further Work	105
	Bibliography	107
A	FAST Input Files for the NREL 5MW OWT	113
A.1	FAST Main Input File	113
A.2	ElastoDyn Input File	114
A.3	ElastoDyn Tower File	116
A.4	SubDyn Input File	117
A.5	ServoDyn Input File	119
A.6	InflowWind File	121
A.7	AeroDyn Input File	122
A.8	HydroDyn Input File	124
B	TurbSim Input File	127
C	Input Files for the Simplified AF Model	128
C.1	SubDyn Input file	128
C.2	BModes Main Input File	130
C.3	BModes Tower Section Properties	132
C.4	ElastoDyn Tower File	133
D	Derivation of the Flexibility Relations for the Improved AF Method	134
E	SubDyn Input File for the Improved AF Model	136
F	SubDyn Input File for Monopile with $t_w=0.05$ m	138
G	SubDyn Input File for 12 m \times 6 m Caisson	140
H	MLife Input File for the Regular Monopile	142

List of Figures

2.1	Installed OWT capacity in Europe - Cumulative share by country (Wind Europe, 2017).	6
2.2	Upwind HAWT and VAWT (The Scottish Government, 2006).	8
2.3	Simplified power spectral density of the forcing frequencies (Lombardi et al., 2013).	9
2.4	Parts of the support structure of an OWT (Passon and Kühn, 2005).	10
2.5	Tower, sub-structure and foundations concepts for bottom-mounted OWTs (Passon and Kühn, 2005).	10
2.6	Share of substructure types for grid-connected wind turbines in Europe (Wind Europe, 2017).	11
2.7	Different foundations for bottom mounted OWTs. a) Gravity based foundation, b) Monopile foundation, c) Caisson foundation, d) Multipile foundation e) Multi caisson foundation and f) Jacket pile foundation (Kallehave et al., 2015).	12
2.8	Different foundation modelling methods.	14
2.9	Fixed-base foundation model (left) and flexible foundation model using the apparent fixity method (right) (Bush et al., 2008).	16
2.10	Wind speed profile (der Tempel, 2006)	20
2.11	Mean wind profile according to the logarithmic and power law. $z_0 = 0.001$, $U_{10}(z_r) = 12$ m/s, $z_r = 90$ m and $\alpha = 0.14$	21
2.12	Airy wave theory.	23
2.13	Pierson-Moskowitz spectrum ($\gamma = 1$) and JONSWAP spectrum ($\gamma = 3.3$) for $H_s = 1.5$ m and $T_p = 6$ s.	26
2.14	Slender vertical tower with hydrodynamic loads (der Tempel, 2006).	27
3.1	Global coordinate system (Damiani et al., 2015).	30
3.2	Layout and DOFs of a three bladed HAWT FAST model (Jonkman, 2015).	31
3.3	Support platform layout (Jonkman and Buhl, 2005).	32
3.4	FAST modularization framework for fixed-bottom offshore wind turbine systems (Jonkman and Jonkman, 2016).	33
3.5	Coordinates of a TurbSim wind field with 15° horizontal and 8° vertical mean flow angles (Jonkman and Kilcher, 2012).	37
3.6	Aerodynamic forces on a blade element (Moriarty and Hansen, 2005).	38

4.1	NREL 5-MW OWT (Aasen et al., 2016).	42
5.1	Soil profile (Passon, 2006).	45
5.2	Normalized tower mode shapes from BModes for the rigid and the AF model.	50
5.3	Wind field generated by TurbSim.	52
5.4	Wave elevation above sea level, generated by HydroDyn.	52
5.5	Mudline fore-aft shear force for the fixed base model and the simplified AF model.	54
5.6	Mudline fore-aft moment for the fixed base model and the simplified AF model.	54
5.7	Tower top fore-aft displacement for the fixed base model and the simplified AF model.	55
5.8	Mudline moment oscillations.	56
6.1	Improved apparent fixity method.	58
6.2	Bending stiffness relations for a cantilever beam.	59
6.3	Fore-aft mudline bending moment for the three foundation models.	61
6.4	Fore-aft mudline shear force for the three foundation models.	61
6.5	Tower top fore-aft displacement for the three foundation models.	62
6.6	Tower top fore-aft acceleration for the three foundation models.	62
6.7	Mudline moment oscillations for the three foundation models.	63
6.8	PSD from fore-aft mudline moment for the fixed base model, the simplified AF model and the improved AF model.	65
6.9	PSD from fore-aft tower top displacement for the fixed base model, the simplified AF model and the improved AF model.	66
6.10	PSD of blade root out-of-plane moment.	68
6.11	PSD of nonrotating yaw bearing pitch moment.	68
6.12	Mudline moment and tower top displacement for $H_s = 6$ m and $T_p = 15$ s.	69
6.13	Mudline moment and tower top displacement for $H_s = 6$ m and $T_p = 10$ s.	70
6.14	Mudline moment and tower top displacement for $H_s = 6$ m and $T_p = 5$ s.	70
6.15	Mudline moment and tower top displacement for simulations of the improved AF model with various T_p .	71
7.1	Fore-aft mudline moment for models with different monopile lengths.	74
7.2	Fore-aft tower-top displacement for models with different monopile length.	75
7.3	Fore-aft mudline moment for the models with different wall thickness.	77
7.4	Tower top fore-aft displacement the models with different pile wall thickness.	78

7.5	PSD from mudline fore-aft bending moment for the models with different wall thickness.	79
8.1	Illustration of an OWT with caisson foundation.	81
8.2	Caisson foundation geometry.	82
8.3	Time window of mudline fore-aft bending moment for different caisson dimensions, compared to the regular monopile and the fixed base model.	85
8.4	Time window of tower top fore-aft displacement for different caisson dimensions, compared to the regular monopile and the fixed base model.	85
8.5	PSD from mudline fore-aft bending moment for models with different caisson dimensions.	87
9.1	Mudline fore-aft bending moment for selected load cases of the monopile.	92
9.2	Details of mudline fore-aft bending moment for selected load cases for the improved AF model monopile.	92
9.3	Rainflow cycle-counting illustration (der Tempel, 2006).	93
9.4	Steps of the fatigue analyses	98
9.5	Short term DEL for the different load cases.	100
9.6	Relative short term DEL for the different load cases, weighted with probability of occurrence	101
D.1	Derivation of flexibility relations for the improved AF method	134

List of Tables

4.1	Properties of the NREL 5-MW baseline wind turbine.	41
4.2	The first natural frequencies of the NREL 5MW OWT from BModes.	43
5.1	The first natural frequencies and periods from BModes.	49
5.2	Maximum values of mudline moment, mudline shear force and tower top displacement for $U = 12$ m/s, $TI = 14\%$, $H_s = 6$ m and $T_p = 10$ s.	55
6.1	Properties of the two AF beams.	59
6.2	Maximum response values for $U = 12$ m/s, $TI = 14\%$, $H_s = 6$ m, $T_p = 10$ s . . .	64
6.3	Natural frequencies and corresponding periods from peaks in fore-aft moment PSD plot (figure 6.8).	67
7.1	Stiffness coefficients from PILES for different pile lengths.	73
7.2	Improved AF properties corresponding to different monopile lengths.	74
7.3	Stiffness coefficients from PILES for different pile wall thickness.	76
7.4	Improved AF properties corresponding to piles with different wall thicknesses. . .	77
7.5	Maximum response values from FAST simulations of the models with different pile wall thickness.	78
8.1	Stiffness coefficients from G123 for different caisson dimensions.	84
8.2	Improved AF properties of caisson models with different dimensions.	84
8.3	Maximum and mean values of mudline moment, mudline shear force and tower top displacement from 10 minutes FAST simulations of different caisson dimensions. .	86
9.1	Load cases from Fischer et al. (2010).	90
9.2	Results from MLife fatigue analyses.	99

Nomenclature

Abbreviations

AB4 4th-order Adams-Bashforth

ABM4 4th-order Adams Bashforth-Moulton

AF Apparent Fixity

BEM Blade Element Momentum

C – B Craig-Bampton

CAE Computer-Aided Engineering

DEL Damage Equivalent Load

DFT Discrete Fourier Transform

DLC Design Load Case

DLL Dynamic-Link-Library

DOE Department of Energy

DOF Degree of Freedom

FAST Fatigue, Aerodynamics, Structures and Turbulence

FE Finite Element

FEA Finite Element Analysis

FFT Fast Fourier Transform

HAWT Horizontal Axis Wind Turbine

IEC International Electrotechnical Commission

JONSWAP Joint North Sea Wave Project

LC Load Case

LFE Linear Frame Finite-Element Beam

MDOF Multi Degree of Freedom

MSL Mean Sea Level

NREL National Renewable Energy Laboratory

NWTC National Wind Technology Center

OWT Offshore Wind Turbine

PSD Power Spectral Density

PSF Partial Safety Factor

RCC Rainflow Cycle-Counting

RK4 4th-order Runge-Kutta

RNA Rotor Nacelle Assembly

SDOF Single Degree of Freedom

SSI Soil-Structure Interaction

TI Turbulence Intensity

TP Transition Piece

ULF Ultimate Load Factor

VAWT Vertical Axis Wind Turbine

Greek letters

α	Power Law Exponent	[-]
β	Direction of wave propagation	[degrees]
$\delta_{\theta\theta}$	Rotational flexibility coefficient	[rad/Nm]
$\delta_{u\theta}, \text{delta}_{\theta u}$	Coupled flexibility coefficients	[rad/N],[m/Nm]
δ_{uu}	Translational flexibility coefficient	[m/N]
$\eta(x, y, t)$	Sea surface elevation	[m]
γ	Peak-shape factor	[-]
λ	Wave length	[m]
λ_W	Weibull scale factor	[N/m]
ν	Poisson's Ratio	[-]
ω	Angular frequency	[rad/s]
ω_0	Fixed-base natural frequency	[rad/s]
ω_u	Translational natural frequency	[rad/s]
ω_θ	Rotational natural frequency	[rad/s]
ω_{eq}	Equivalent natural frequency	[rad/s]
ρ_{air}	Density of air	[kg/m ³]
ρ_{steel}	Density of steel	[kg/m ³]

ρ_{water}	Density of water	[kg/m ³]
σ	Spectral width parameter	[-]
σ^{ult}	Ultimate tensile strength	[N/m ²]
σ_b	Bending stress	[N/m ²]
σ_U	Standard deviation of wind speed	[m/s]
Θ	Phase angle	[degrees]
ε_k	Random phase angles	[degrees]

Lowercase letters

\ddot{x}	Water particle acceleration	[m/s ²]
\dot{x}	Water particle velocity	[m/s]
θ	In-plane rotation	[rad]
d	Water depth	[m]
f	Frequency	[Hz]
f^{eq}	DEL frequency	[Hz]
$f_j^{Life,eq}$	Lifetime cycle count extrapolation factor	[-]
f_j^{Life}	Cycle count extrapolation factor	[-]
f_p	Spectral peak frequency	[Hz]
k	Wave number	[-]
k_W	Wilbull shape factor	[-]

$k_{\theta\theta}$	Rotational stiffness coefficient	[Nm/rad]
$k_{u\theta}, k_{\theta u}$	Coupled stiffness coefficients	[N/rad, Nm/m]
k_{uu}	Translational stiffness coefficient	[N/m]
m	Wöhler exponent	[-]
$n^{Life,eq}$	Lifetime equivalent number of cycles	[-]
n_i	Number of load cycles in block i	[-]
n_j^{STeq}	Equivalent number of load cycles for time series j	[-]
n_{ji}	Number of cycles to failure for block i in time series j	[-]
n_{ji}^{Life}	Lifetime number of cycles from block i in time series j	[-]
t	Time	[s]
t_w	Monopile wall thickness	[m]
u	Horizontal in-plane translation	[m]
$u(z, t)$	Turbulent wind velocity	[m/s]
$x(t)$	Random process	[unit $_{x(t)}$]
x_r	Discrete sequence	unit $_{x_r}$]
y	Outer radius of cross section	[m]
z	Height above the ground or the MSL	[m]
z_0	Roughness parameter	[m]

Uppercase letters

$[C]$	Damping matrix	$[\text{Ns/m}], [\text{Ns/rad}], [\text{Nsm/m}], [\text{Nsm/rad}]$
$[F]$	Flexibility matrix	$[\text{m/N}], [\text{rad/N}], [\text{m/Nm}], [\text{rad/Nm}]$
$[F]_{PILES}$	Flexibility matrix from PILES	$[\text{m/N}], [\text{rad/N}], [\text{m/Nm}], [\text{rad/Nm}]$
$[K]$	Stiffness matrix	$[\text{N/m}], [\text{N/rad}], [\text{Nm/m}], [\text{Nm/rad}]$
$[K]_{PILES}$	Stiffness matrix from PILES	$[\text{N/m}], [\text{N/rad}], [\text{Nm/m}], [\text{Nm/rad}]$
$[M]$	Mass matrix	$[\text{kg}]$
$\ddot{U}(t)$	Acceleration vector	$[\text{m/s}^2], [\text{rad/s}^2]$
$\dot{U}(t)$	Velocity vector	$[\text{m/s}], [\text{rad/s}]$
A	Wave amplitude	$[\text{m}]$
A_r	Area swept by rotor	$[\text{m}^2]$
C_D	Drag coefficient	$[-]$
C_M	Inertia coefficient	$[-]$
D	Accumulated fatigue damage	$[-]$
d	Pile diameter	$[\text{m}]$
D^{Life}	Lifetime damage	$[-]$
D_c	Caisson diameter	$[\text{m}]$
D_j^{ST}	Short term damage from time series j	$[-]$
DEL^{Life}	Lifetime damage equivalent load	$[\text{Nm}]$
DEL_j^{ST}	Short term damage equivalent load	$[\text{Nm}]$
dF_D	Hydrodynamic drag load	$[\text{N/m}]$

dF_M	Hydrodynamic inertia load	[N/m]
$dF_{Morrison}$	Hydrodynamic load	[N/m]
E	Young's modulus	[N/m ²]
E_{AF}	Young's modulus of AF beam	[N/m ²]
EI	Flexural rigidity	[Nm ²]
F	Force	[N]
$F(t)$	Load vector	[N],[Nm]
G	Shear Modulus	[N/m ²]
G_{AF}	Shear modulus of AF beam	[N/m ²]
H	Wave height	[m]
H_s	Significant wave height	[m]
I	Area moment of inertia	[m ⁴]
$I_U(z)$	Turbulence intensity	[-]
I_{AF}	Area moment of inertia of AF beam	[m ⁴]
L^{MF}	Fixed load-mean	[Nm]
L^{ult}	Ultimate design load	[Nm]
L_1, E_1, I_1	Properties of improved AF beam 1	[m],[N/m ²],[m ⁴]
L_2, E_2, I_2	Properties of improved AF beam 2	[m],[N/m ²],[m ⁴]
L_c	Caisson depth	[m]
L_i^M	Load mean	[Nm]

L_i^{RF}	Load range about a fixed mean value	[Nm]
L_i^R	Load range	[Nm]
L_k	Integral length scale parameter	[m]
L_{AF}	Length of AF beam	[m]
M	Moment	[Nm]
M^{ult}	Ultimate design load	[Nm]
N_i	Number of cycles before failure for block i	[-]
N_j^{eq}	Equivalent number of cycles to failure for time series j	[-]
$N_{j,i}$	Number of cycles to failure for block i in time series j	[-]
P	Power in the wind	[W]
$S(f)$	Wave Spectrum	[m ² /Hz]
$S_U(f)$	Wind Spectrum	[(m/s) ² /Hz]
$S_x(f)$	Power Spectral Density function	[(unit _{<i>x_r</i>}) ² /Hz]
T	Wave period	[s]
T^{Fail}	Time until failure	[s]
T^{Life}	Design Lifetime	[s]
T_j	Elapsed time of time series j	[s]
T_p	Peak spectral period	[s]
T_z	Zero-crossing period	[s]
$U(t)$	Displacement vector	[m],[rad]

$U(z)$	Mean wind speed	[m/s]
U_{10}	Mean wind for stationary conditions	[m/s]
$V(z, t)$	Total Wind Velocity	[m/s]
$X(\omega)$	Fourier Transform of $x(t)$	[unit $_{x(t)}$ s]
$X_k(f)$	Discrete Fourier transform of x_r	[unit $_{x_r}$.s]
z_r	Reference Height	[m]
1P	Rotor loading frequency	[Hz]
3P	Blade passing frequency	[Hz]

1 Introduction

1.1 Motivation and Background

The world is threatened by climate change, and the focus on utilizing renewable energy sources has increased significantly over the last years. In 2015, the Paris Agreement was signed, bringing the world's nations into a common cause to take actions against climate change, with an aim of keeping the global temperature rise below 2 °C above pre-industrial levels. To reach this goal, moving the world's energy consumption away from fossil fuels is inevitable, and countries invest more than ever in renewable energy.

The offshore wind industry has grown remarkably over the last few years, a growth that has brought global offshore wind capacity to over 14 GW, which equals 3.7% of global electricity consumption (Global Wind Energy Council, 2017). Offshore wind turbines (OWTs) are costly and difficult to install and maintain, and have not yet been economically favourable. However, a main reason for the recent growth is the decreasing cost, making offshore wind a competitive energy source. According to Bloomberg New Energy Finance (2017a) energy from offshore wind became 28% cheaper in 2016 compared to the year before. In April 2017 it was announced that the first offshore wind farm to offer subsidy-free power will be built in Germany (Bloomberg New Energy Finance, 2017b).

An important research area is offshore wind foundations. The foundation system contributes to up to 20-25% of the capital costs for offshore wind turbines (Carswell et al., 2015). Hence, optimizing the support structure and foundation, by means of both design and installation method, has a great potential for the overall cost effectiveness of offshore wind farms. The monopile is by far the most common foundation type, but new concepts for larger water depths, like suction caissons, multipiles and moored floating structures are being introduced. Despite this, the monopile is expected to continue to have a large market share in the years to come.

Offshore wind turbines are long and slender structures that need to withstand large lateral loads from wind, waves and currents. The natural frequencies of the structure are close to both the operational frequencies of the rotor and wave frequencies, which can lead to resonance effects causing large cyclic loads in the structure and thereby fatigue damage. Knowledge on the dynamics

of the whole wind turbine structure, including the foundation, is therefore important to predict the dynamic response and fatigue damage.

Soil-Structure Interaction (SSI) plays a major role in bottom-mounted OWT support structure behaviour. Nevertheless, SSI of wind turbine foundations is a topic that is often overlooked by researchers for the benefit of other topics like blade aerodynamics and hydrodynamics. According to Passon and Kühn (2005), modelling capabilities of the foundation is very crude in most wind turbine simulation codes. In FAST, the software used in this thesis, the foundation is not even included; the default OWT model is limited to a rigid connection between the substructure and the seabed. Soil-foundation response can have high impact on the dynamics of the wind turbine, and correct modelling and analysis of this is important for the optimization of offshore wind turbine foundations. Increased knowledge on the effect of foundation modelling methods and foundation concepts may lead to conclusions either preventing fatigue damage or endorsing possible dimension reductions, which would both be highly economically favourable. Hence, studying and gaining knowledge on the effect of foundation modelling is inevitable in the development of both existing and new solutions for offshore wind turbine foundations.

1.2 Objectives

The main objectives of this Master's thesis are:

1. To study the effect of including foundation flexibility in an offshore wind turbine model, originally rigidly fixed to the seabed, in the simulation code FAST.
2. To compare different foundation modelling methods, foundation dimensions and two different foundation concepts with respect to dynamic response and fatigue damage of the offshore wind turbine structure.

1.3 Organization of the Thesis

In Chapter 2 relevant theory is presented. The chapter covers general theory on offshore wind turbines, theory used for mimicking foundation flexibility, as well as theory used for calculations of loads in the simulation tools used in this thesis. In Chapter 3, the main computational tool used in this thesis, FAST v8, is described. It includes introduction to the different modules of the

simulation code as well as the coupling between them. Chapter 4 describes the properties of the OWT model used as a reference model in this thesis; a 5MW OWT with a fixed base boundary at the seabed.

The first part of the analyses made in this thesis is regarding the method used for modelling foundation flexibility. In Chapter 5, the first foundation modelling method is explained and implemented in FAST, referred to as the *simplified apparent fixity method*. An improved version of this method is developed in chapter 6, referred to as the *improved apparent fixity method*, and FAST output time series of the two methods are studied and compared.

Furthermore, sensitivity analyses of monopile foundations with different dimensions are presented in chapter 7. Chapter 8 introduces a new foundation concept, the suction caisson foundation, and FAST simulations with varying dimensions are run.

The final topic in this thesis is fatigue analyses of all the preceding foundation models, carried through and presented in chapter 9. Finally, in chapter 10 the results of the analyses made in the previous chapters will be connected to the objectives of the thesis, and recommendations for further work is presented.

2 Theory

2.1 Wind Energy History

Utilizing the energy from wind goes far back in history. Already around the tenth century the first windmills were developed in Asia, and a few centuries later the technology spread to Europe. The traditional windmills were used for mechanical tasks like grinding grains and pumping water, and were a major source of mechanical energy before the industrial revolution, where steam turbines and electric power took over. But the developments in electrical energy inspired engineers to the idea of using wind to generate electricity, and one of the first windmills used for driving an electrical generator was made in Ohio in 1888 (Lynn, 2012). Further research was conducted during the following years, but cheap energy from fossil fuels put a brake on the development of the wind power industry. However, in the mid 1970s the world faced the first oil crisis, and attention was drawn to renewable energy sources. This marked a turning point for the wind industry, which has developed remarkably over the last decades and now delivers vast amounts of clean, renewable power to the world.

The winds at sea are stronger and more stable than onshore. This led to the beginning of offshore wind energy research in the late 1970s. In 1991 the world's first offshore wind farm, *Vindeby*, was built in Denmark (Schaffarczyk, 2014), with 11 turbines with a total capacity of 5 MW. Since then, other coastline countries have joined in on the development of offshore wind farms. After 25 years of delivering clean energy and pioneering the offshore wind industry, *Vindeby* farm finished its duty in March 2017 and is currently being replaced by wind farms in the gigawatt scale.

2.2 Offshore Wind Turbines

According to Global Wind Energy Council (2016), at the end of 2015, more than 90% of all offshore wind installations were located in Europe. Over 40% of the installed European capacity is in the UK, followed by Germany and Denmark, see figure 2.1. However, countries outside Europe are currently setting ambitious targets for offshore wind and have started development and installation, with China leading ahead.

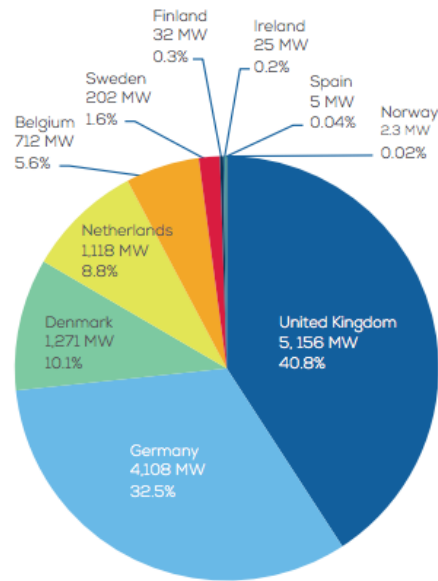


Figure 2.1: Installed OWT capacity in Europe - Cumulative share by country (Wind Europe, 2017).

According to numbers by Wind Europe (2017), in 2016, the average offshore wind turbine size in Europe waters was 4.8 MW, the average water depth of wind farms was 29 meters, and the average distance to shore was 44 kilometers. These numbers are currently growing. Developments in wind turbine technology are constantly increasing the size, power rating and efficiency, which decrease the cost per MW. 8 MW turbines have already been installed, and turbines of up to 10 MW are currently being developed, sizes which are well-suited offshore. Other contributing factors for moving wind farms offshore are the increasing difficulty in locating new sites for onshore wind farms and the fact that they move out of sight of the population.

2.2.1 Power Generation

The power P intercepted by a wind turbine rotor in a steady airstream is defined as:

$$P = 0.5\rho_{air}A_rU^3 \quad (2.1)$$

where ρ_{air} is the density of the air, A_r is the area swept by the rotor and U is the speed of the wind.

This power relate to the power in the wind and is not the same as the power actually extracted by a turbine rotor. The difference between the two is determined by the rotor efficiency, and large modern turbines can capture up to about 50% of the wind's power.

Another case related to the amount of power generated is the capacity factor. A 5 MW wind turbine does not generate 5 MW all the time, this is the full rated power, which is only generated when the wind reaches a certain speed, called the *rated* wind speed. Most of the time it produces considerably less power. The capacity factor is the ratio of the actual amount of power produced over a period of time to the rated turbine power. According to (Lynn, 2012), offshore sites have a capacity factor of approximately 40%, which is higher than onshore sites.

The cubic relationship between wind speed and power is the most important factor affecting wind turbine design and performance. Strong winds generate many times more energy than moderate winds, meaning that a site with short strong wind gusts generally will produce disproportionately more annual electricity than a steady site with the same average wind speed. At the same time, extreme winds can damage the turbine. Therefore, wind turbines are designed to have certain *cut-in* and *cut-out* wind speeds determining the lower and upper limits for power generation.

2.2.2 Turbine Types

Several different turbine types have been proposed over the past century. The two main classes of wind turbines are *horizontal axis wind turbines* (HAWTs) and *vertical axis wind turbines* (VAWTs), shown in figure 2.2. HAWTs have two- or three-bladed rotors mounted upwind (facing the wind) or downwind (away from the wind) of their towers, while VAWTs have their rotors set transverse of the wind direction. The vast majority of wind turbines today is upwind three-bladed HAWTs, and this is the type referred to for the rest of this thesis.

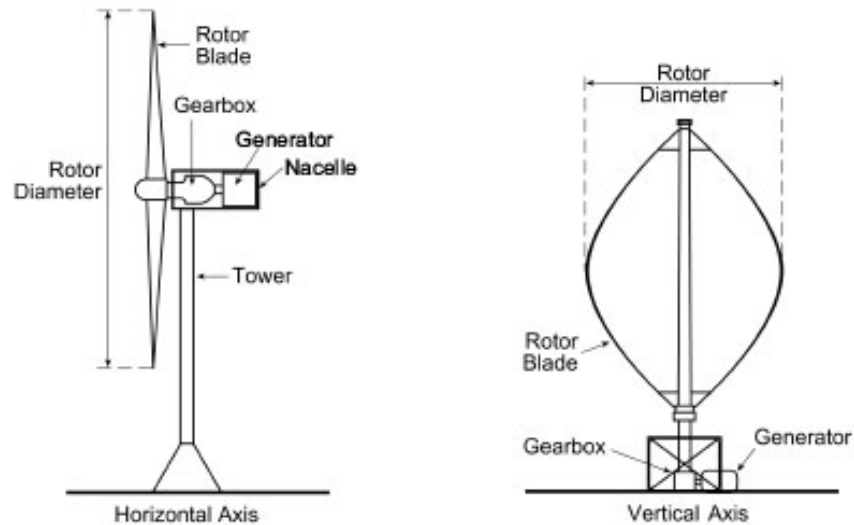


Figure 2.2: Upwind HAWT and VAWT (The Scottish Government, 2006).

2.2.3 Dynamics of Offshore Wind Turbines

Offshore wind turbines are subjected to a combined set of loading conditions: Environmental loads from wind and waves and operational loads from the rotating rotor. Wind turbines have natural frequencies directly related to their operational states. For a three-bladed wind turbine these operational natural frequencies are referred to as 1P and 3P. The rotor loading frequency 1P is associated with the cyclic loading generated by mass imbalance in the rotating blades. The blade passing frequency 3P is due to the shadowing effect from the wind each time a blade passes the tower (Andersen et al., 2012).

The magnitude of the response of a wind turbine strongly depends on the frequency of the excitation. If the natural frequencies of the wind turbine tower coincide with the natural frequencies of either the wind, waves or the forces set up by the rotor, resonance will occur. Hence, to avoid this, the overall system must be designed to have natural frequencies kept away from the frequency content of the applied loads (Lombardi et al., 2013). Only the lowest, or fundamental, natural frequency of the wind turbine is normally of concern here, as it is the one that is closest to the operating frequency and the wave frequencies.

Consequently, three classical design approaches for the turbine tower is defined:

1. Soft-soft design: The tower fundamental frequency is less than 1P

2. Soft-stiff design: The tower fundamental frequency lies between 1P and 3P
3. Stiff-stiff design: The tower fundamental frequency is higher than 3P

Figure 2.3 shows simplified *power spectral densities* (PSDs) of the wind forces, wave forces as well as the operational natural frequency ranges for a typical three-bladed 3.6 MW OWT with an operational speed of 5-13 rpm. PSDs represent energy distribution of the loads over different frequencies, and will be explained further in section 2.5. Figure 2.3 shows that typical wave frequencies are around 0.1 Hz, which is close to the rotor frequency 1P, especially at lower rotor speed.

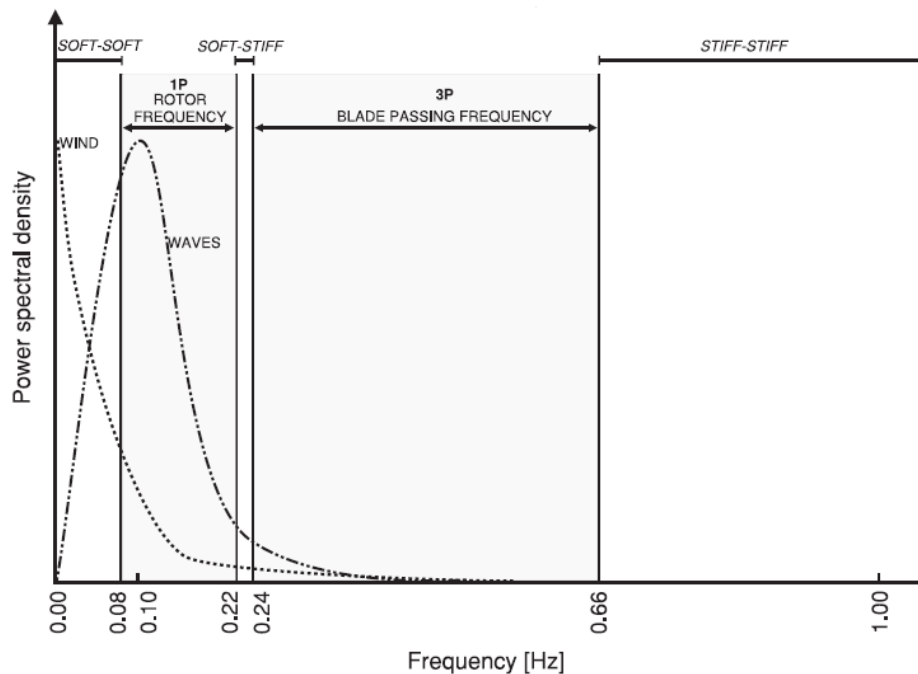


Figure 2.3: Simplified power spectral density of the forcing frequencies (Lombardi et al., 2013).

2.2.4 Support Structures

A HAWT can be divided into two main parts: the *rotor nacelle assembly* (RNA) and the support structure. The RNA consists of the rotor, the hub, the blades and the nacelle, containing the generator and the drivetrain. In addition to supporting the RNA, the main task of the support structure is to transfer loads into the seabed. The support structure consists of the tower, the platform, the transition piece, the substructure and the foundation, illustrated in figure 2.4. The

terminology in OWT literature can be inconsistent. The terms transition piece (TP) and platform are often not distinguished, and the terms foundation and substructure are used interchangeably. The denotations from figure 2.4 will be used in this thesis. Figure 2.5 illustrates tower, substructure and foundation concepts and how the terminology is distinguished for bottom-mounted OWTs.

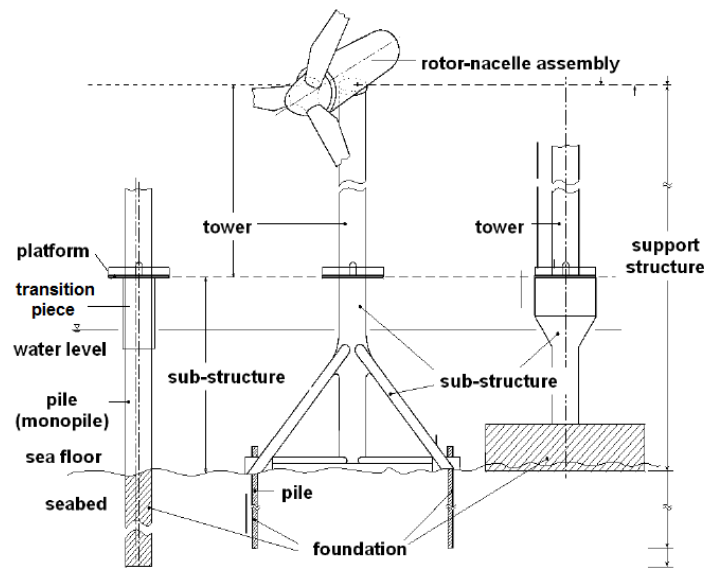


Figure 2.4: Parts of the support structure of an OWT (Passon and Kühn, 2005).

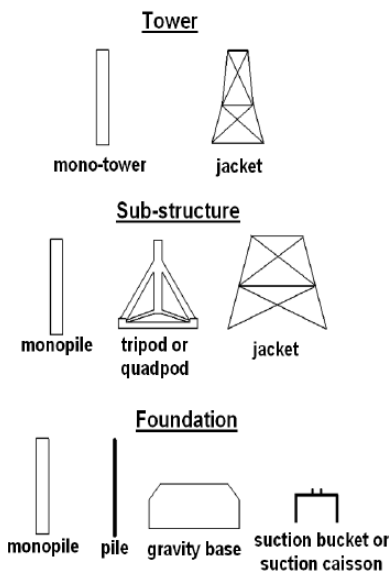


Figure 2.5: Tower, sub-structure and foundations concepts for bottom-mounted OWTs (Passon and Kühn, 2005).

The monopile is by far the most common substructure type, accounting for over 80% of all installed OWTs (Wind Europe, 2017). It is simple in fabrication and installation, and is suitable for water depths up to approximately 30 meters. For larger water depths, other substructures like tripods, jackets, moored floating structures or suction caissons may be preferable. Figure 2.6 shows the cumulative European market share of substructures in 2016.

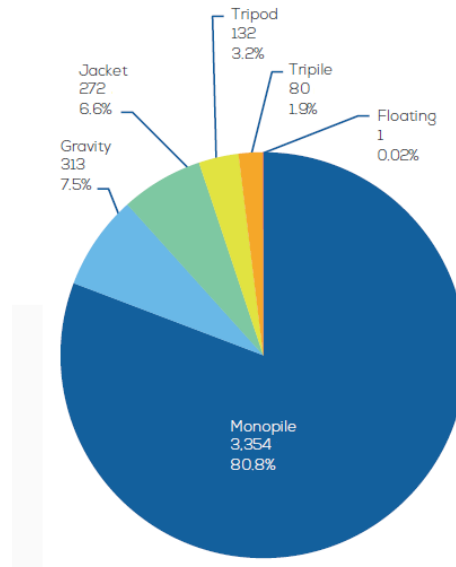


Figure 2.6: Share of substructure types for grid-connected wind turbines in Europe (Wind Europe, 2017).

2.3 Offshore Wind Turbine Foundations

The harsh environmental conditions offshore make design and construction of turbine foundations challenging. The foundations must take account of turbine weight and height, the depth of water, the wind, wave and current loads and the soil type at the particular site. The combination of relatively low weight and large horizontal loading produce large overturning moments at the base. The foundation has to resist the loads transferred from the structure above and remain functional and stable throughout the whole lifetime of the OWT. As the conditions offshore are highly site-dependent, a single OWT sometimes requires a unique foundation design.

2.3.1 Foundation Concepts

Bottom-mounted OWT substructures are founded on several different types of foundations; the four main ones being the monopile, multiple, gravity base and suction bucket or suction caisson. Figure 2.7 shows different substructures and foundations for bottom-mounted OWTs.

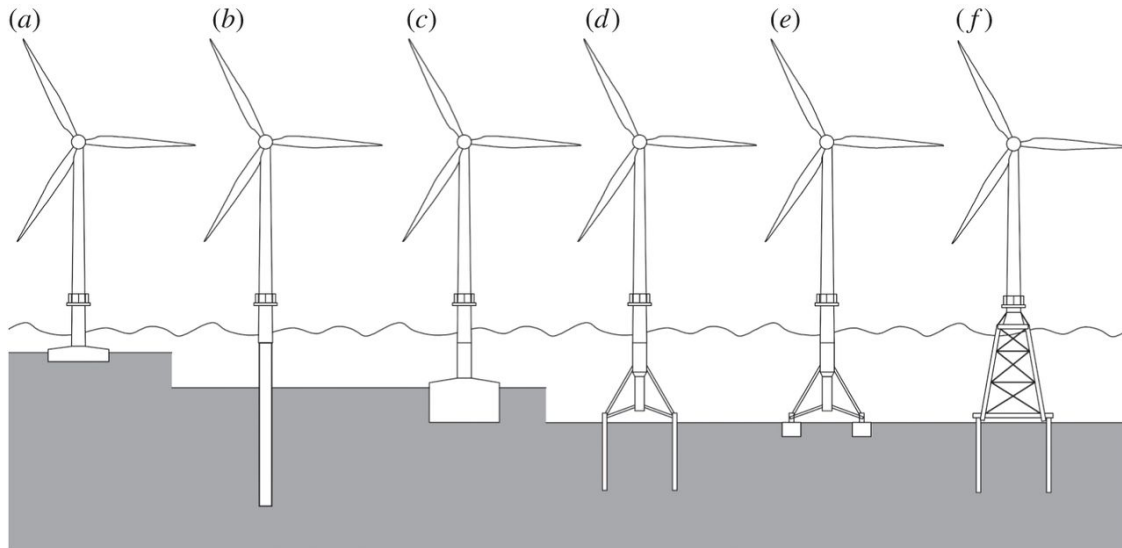


Figure 2.7: Different foundations for bottom mounted OWTs. a) Gravity based foundation, b) Monopile foundation, c) Caisson foundation, d) Multipile foundation e) Multi caisson foundation and f) Jacket pile foundation (Kallehave et al., 2015).

The *monopile foundation* is a cylindrical steel tube driven a certain depth into the seabed, depending on the environmental and soil conditions. Reasons why the monopile is the most commonly chosen foundation type are the simplicity of installation and the proven success of driven piles for oil and gas platforms (Lombardi et al., 2013). Even though existing knowledge from the oil and gas industry is highly relevant in structural analysis of OWTs, there are several important differences. Firstly, wind loading plays a much more significant role for an OWT due to higher elevations. Secondly, the diameter of OWT monopiles are much larger than the piles used for oil platforms, and the existing design methods may not yield accurate results. Lastly, monopile-supported OWTs must withstand large lateral loads and moments, as opposed to oil and gas platform foundation loads which are mainly vertical. The tripod and jacket substructures are normally supported on multiple piles, or *multipiles*, which will experience additional axial loads.

The *gravity foundation* is normally a concrete based structure, designed to avoid tensile loads

between the support structure and the seabed (Det Norske Veritas, 2014). It is not driven into the seabed like the monopile, but relies on its own weight to maintain the stable (Lynn, 2012). Hence, to handle the overturning moments of the turbine loads, the base area has to be large, and additional dead load may be added. The gravity foundation is easier to install than the monopile, as it does not need heavy installation vessels. However, it is only competitive when the environmental loads are relatively modest.

The *suction caisson* is a relatively new foundation concept, suitable for both shallow and larger water depths. It is an upturned steel bucket that is installed by means of suction and sticks to the seafloor when the water inside is pumped out. The main advantages of the suction caisson is the ease of installation and the requirement of less steel than the monopile (Bloomberg New Energy Finance, 2017a). The suction caisson is described further in chapter 8.

2.3.2 Foundation Behaviour

The behaviour of the soil-foundation configuration is influenced by the soil surrounding it, and is highly dependant in soil type. Soils show nonlinear behaviour during loading, as well as different stiffness during loading, unloading and reloading (Bush and Manuel, 2009).

An OWT experiences four main types of damping: Aerodynamic damping, hydrodynamic damping, structural damping and soil damping. In general, aerodynamic damping is the largest contributor to the total damping in an OWT. Further, there are two types of soil damping; radiation damping and hysteretic damping. Radiation damping may be neglected for frequencies below 1 Hz, and as the majority of wind and wave loads have frequencies below 1 Hz, the main foundation damping contribution comes from hysteretic damping. Hysteretic damping is a function of load level, and represents energy loss because of inelastic behaviour of the soil, i.e. plastic deformations (Aasen et al., 2016). Soil damping, or foundation damping, is most important when the OWT is parked or idling, as aerodynamic damping is reduced in these cases. Different foundation modelling methods and simulation codes treat the soil-foundation behaviour and its nonlinearities variously.

2.4 Foundation Models

Modelling of OWT foundations and SSI has in general been put in the shade of other simulation topics in wind turbine analysis software. Simplified foundation models, neglecting a certain

amount of interactions, may be appropriate for some analyses, but the lack of research on foundation models may lead to both underpredictions and overpredictions of structural response. Underpredictions of loads in the wind turbine structure may lead to fatal consequences and failure, while overpredictions may indicate possibilities of dimension reduction and design optimization.

An important effect of SSI is the reduction in natural frequencies of the soil-structure system compared to a fixed base system. The equivalent natural frequency for a Single Degree of Freedom (SDOF) system with SSI is presented in Kramer (1996) as

$$\frac{1}{\omega_{eq}^2} = \frac{1}{\omega_0^2} + \frac{1}{\omega_u^2} + \frac{1}{\omega_\theta^2} \quad (2.2)$$

where ω_{eq} is the equivalent natural frequency, ω_0 is the fixed-base natural frequency, ω_u is the horizontal translational natural frequency and ω_θ is the rotational natural frequency of the foundation. Consequently, when foundation flexibility is included in an OWT model, the first natural frequencies of the structure is shifted closer to wave frequencies and operational frequencies, which may increase resonance effects.

Four different methods for modelling foundation flexibility of an OWT monopile is represented in figure 2.8, and will be described below. Even though these methods are described for a monopile foundation, they may be applied to other types of foundations as long as the soil-foundation stiffness can be obtained.

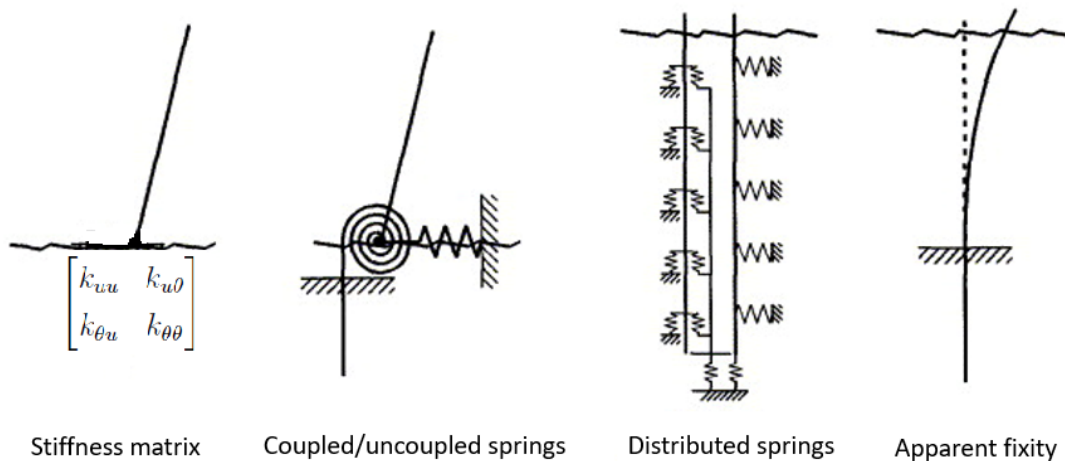


Figure 2.8: Different foundation modelling methods.

2.4.1 Stiffness Matrix

In the *stiffness matrix* method, a full Finite Element model (FE model) of the foundation and soil is made. A static analysis of this model for different load cases is used to obtain a stiffness matrix located at the mudline, representing the stiffness of the true soil-pile system (Zaaijer, 2006). The stiffness matrix is then directly applied at a single point on the turbine at the mudline. This type of modelling is the most accurate; however, it requires a wind turbine software allowing this direct application of a stiffness matrix. The software used in this thesis does not support this method.

2.4.2 Coupled and Uncoupled Springs

The *coupled springs* and *uncoupled springs* methods model the foundation flexibility as a set of translational and rotational springs positioned at the mudline. Coupled springs means that a lateral load leads to both lateral displacement and rotation, while an uncoupled springs model is simplified to have independent springs for each relevant degree of freedom. The spring stiffness constants are derived to give the same response as the true soil-foundation system at the mudline.

2.4.3 Distributed Springs

The *distributed springs* method models the foundation flexibility through a free-free beam with lateral springs distributed along the subsoil part of the monopile (Jonkman and Musial, 2010). The beam has the real properties of the monopile both above and below the mudline, including the real subsoil length. The spring stiffnesses vary along the pile to represent the behaviour of the soil profile. The stiffness of the soil at a specific depth under a certain load condition can be determined by p-y curves, or load deflection curves, which is then used to compute the spring stiffnesses.

2.4.4 Apparent Fixity

The principle behind the *apparent fixity* (AF) method is to reproduce the stiffness of the true soil-pile system with a fictive cantilevered beam, fixed at a certain point below the mudline, as shown in figure 2.9.

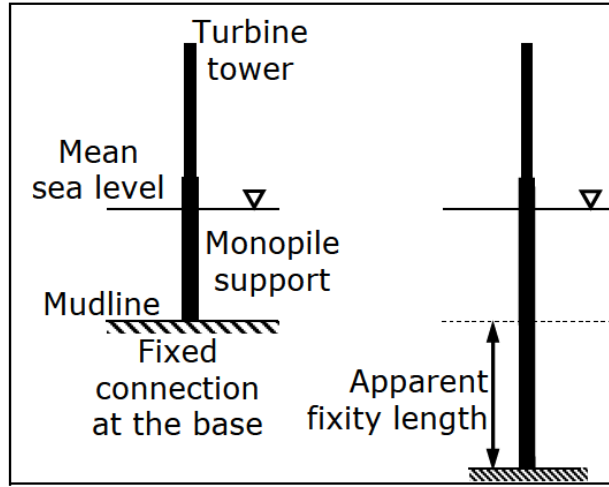


Figure 2.9: Fixed-base foundation model (left) and flexible foundation model using the apparent fixity method (right) (Bush et al., 2008).

The length and the properties of the fictive beam, referred to as the *AF beam*, are calculated so that the deflections and rotations at the mudline represent the response of the true soil-pile system. For the response in a horizontal direction, the stiffness relation at the mudline is shown in equation 2.3, represented by a coupled stiffness matrix with two degrees of freedom (DOFs).

$$\begin{bmatrix} k_{uu} & k_{u\theta} \\ k_{\theta u} & k_{\theta\theta} \end{bmatrix} \begin{bmatrix} u \\ \theta \end{bmatrix} = \begin{bmatrix} F \\ M \end{bmatrix} \quad (2.3)$$

F and M are the force and moment at the mudline, u is the horizontal in-plane translational DOF, θ is the in-plane rotational DOF, k_{uu} is the stiffness in u -direction, $k_{\theta\theta}$ is the rotational stiffness and $k_{u\theta}$ and $k_{\theta u}$ are the coupled stiffness coefficients.

To calculate the required length L_{AF} and the flexural rigidity EI_{AF} of the AF beam, the stiffness matrix from equation 2.3 is matched to the stiffness matrix of a Bernoulli beam:

$$K = \begin{bmatrix} k_{uu} & k_{u\theta} \\ k_{\theta u} & k_{\theta\theta} \end{bmatrix} = \begin{bmatrix} \frac{12EI_{AF}}{L_{AF}^3} & -\frac{6EI_{AF}}{L_{AF}^2} \\ -\frac{6EI_{AF}}{L_{AF}^2} & \frac{4EI_{AF}}{L_{AF}} \end{bmatrix} \quad (2.4)$$

The apparent fixity method is the method used to model flexibility of the soil-foundation system in this thesis, and will be described further in chapter 5. The AF method is chosen mainly because it is the only method that is possible to implement in FAST v8. In the previous version of FAST,

FAST v7, springs could be implemented, but this is no longer available in FAST v8. The interested reader is referred to Krathe and Kaynia (2016) regarding implementation of a nonlinear coupled springs foundation model in FAST v7.

2.5 Environmental Loads

The environment at sea is generally rougher than onshore, and offshore wind turbine structures need to withstand strong winds, waves and currents. Environmental loading, and consequently responses of offshore wind turbines, vary in time, and can be classified as *stochastic*, or random, processes. A stochastic process is the collection of all possible single time histories from a random phenomenon (Bendat, 2011). A random physical phenomenon can not be described by an explicit mathematical relationship because every representation of the phenomenon will be unique. However, a random process is said to be *stationary* if the stochastic properties of the process do not change with time (Newland, 2005). Hence, assuming wind and waves to be stationary processes over a certain period of time makes it possible to describe them with mathematical relationships and models. Using wind and wave models representative of the real environmental conditions is essential in the design and analysis of offshore wind turbines. A complete review of random data theory is seen as out of scope of this thesis, but to understand how random processes like waves and wind are treated, an introduction to the most relevant tools for random data analysis will be presented in the following section, followed by sections on wind and wave theory.

2.5.1 Random Data Analysis

For a Multi Degree of Freedom (MDOF) system, the equation of motion is defined as

$$[M]\{\ddot{U}(t)\} + [C]\{\dot{U}(t)\} + [K]\{U(t)\} = \{F(t)\} \quad (2.5)$$

Where $\{F(t)\}$ is the external load vector at time t , $\{U(t)\}$, $\{\dot{U}(t)\}$ and $\{\ddot{U}(t)\}$ are displacements, velocities and accelerations, respectively, and $[M]$, $[C]$ and $[K]$ are mass, damping and stiffness matrices, respectively. This relationship between load and response implies clearly that a random load will give a random response. In this thesis, analysis of the random response of an offshore wind turbine due to stochastic wind and wave loading will be analyzed.

Fourier Transform and Power Spectral Density

An essential tool when analyzing processes that are randomly distributed in space and time is the *Fourier transform*. Taking the Fourier transform of a time history $x(t)$ converts the process from the time domain to the frequency domain. The Fourier transform $X(\omega)$ of a periodic function $x(t)$ and the inverse Fourier transform $x(t)$ is defined as

$$X(\omega) = \frac{1}{2\pi} \int_{-\infty}^{\infty} x(t)e^{-i\omega t} dt \quad (2.6)$$

$$x(t) = \int_{-\infty}^{\infty} X(\omega)e^{i\omega t} d\omega \quad (2.7)$$

where $\omega = 2\pi f$ is the relation between angular frequency in rad/s and ordinary frequency in Hz. Since most measured time histories are obtained in a discrete form with values taken over equally spaced intervals in time, it is convenient to describe the Fourier transform accordingly. A discrete time record of total length T is sampled at a time step $\Delta t = T/N$, where N is the total number of time steps. The *discrete Fourier transform* (DFT) is the Fourier transform of a discrete sequence, $x_r, r = 0, 1, 2, \dots, (N - 1)$ and is defined in Newland (2005) as

$$X_k(f) = \frac{1}{N} \sum_{r=0}^{N-1} x_r e^{-i\pi kr/N} \quad k = 0, 1, 2, \dots, (N - 1). \quad (2.8)$$

Moreover, the *fast Fourier transform* (FFT) is a computer algorithm for calculating DFT's (Newland, 2005). The DFT's are then used to estimate the power spectral density (PSD). The PSD of a random process, also called *spectral density* or just *spectrum*, gives a statistical representation of a stationary random process in the frequency domain. In other words; the PSD describes how the power of the time series is distributed over frequency. Power, in this sense, is what the time series represent, for example wave height or wind speed. Spectral models are essential for representing wind and wave fields, which will be described further in section 2.5.2 and 2.5.3. The PSD function can be determined from the DFT as follows:

$$S_x(f) = \lim_{T \rightarrow \infty} \frac{1}{T} E[|X_k(f)|^2] \quad (2.9)$$

where $E[|X_k(f)|^2]$ is the mean value of $|X_k(f)|^2$.

One application of the FFT is the *Welch method*. The time series data is partitioned into n_d segments, called hanning windows, each of length $T_h = N\Delta T$. The Welch method then takes the FFT of each segment and computes the total spectral density through an ensemble averaging operation over the n_d segments (Welch, 1967). The advantage of dividing the time series into shorter windows instead of just estimating the spectrum directly from the whole data record is that it decreases the variance of the estimate, and hence makes the spectrum more accurate. The reason for this is that the method uses non-rectangular windows, which reduces the weighting of the end samples of segments. This means that it extracts the most important part of each window before the average is computed.

2.5.2 Wind

Wind speed at any location varies in space, time and direction, variations with a time scale from seconds to years. Inter-annual, seasonal and daily changes in the wind must be taken into account when making predictions for offshore wind farm sites. Further, the wind velocity fluctuates randomly over short periods of time, which is known as turbulence.

Turbulence and Shear

Wind speed can be divided into a quasi-static part and a fluctuating part:

$$V(z, t) = U(z) + u(z, t) \quad (2.10)$$

where $V(z, t)$ is the total wind velocity at height z above the ground, or above the *mean sea level* (MSL) for offshore applications, at time t , $U(z)$ is the mean wind velocity and $u(z, t)$ is the turbulent wind velocity. The mean wind over a short period of 10 minutes to 1 hour can be considered as constant. Det Norske Veritas (2010) describes that the arbitrary wind speed under stationary 10-minute conditions follows a Gaussian probability distribution with mean value U_{10} and standard deviation σ_U .

A parameter describing a turbulent wind field is the *turbulence intensity* (TI). It increases with higher roughness of the terrain and decreases with height, and is defined as

$$I_U(z) = \frac{\sigma_U(z)}{U_{10}(z)} \quad (2.11)$$

Wind speed is also affected by friction on the earth's surface, an effect known as *wind shear*. Wind shear reduces the wind speed from its undisturbed speed above the atmospheric boundary layer to almost zero at the earth's surface. Figure 2.10 shows the effect of both turbulence and shear on the mean wind speed profile.

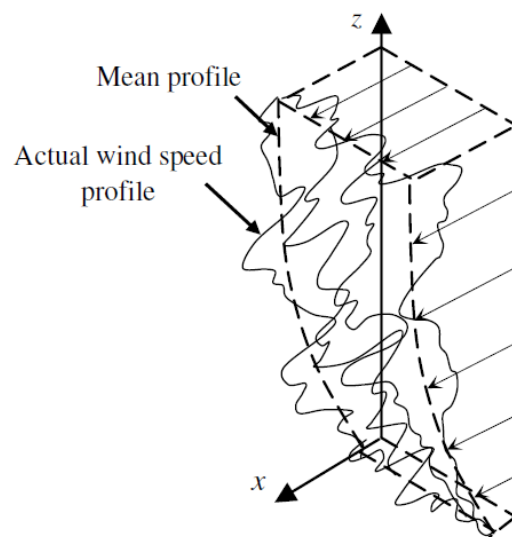


Figure 2.10: Wind speed profile (der Tempel, 2006)

Mean Wind Profiles

Two models are mainly used to describe the mean wind speed profile. The *logarithmic profile* states that

$$U(z) \propto \ln \frac{z}{z_0} \quad (2.12)$$

where z_0 is a roughness parameter, which for offshore locations depends on the wind speed, the distance to land, the water depth and the wave field. As mentioned earlier, an advantage of moving wind turbine farms offshore is that the winds are stronger and more stable than onshore, due to less surface roughness across the ocean than on land. According to Det Norske Veritas (2010), z_0

varies between 0.0001 m in open seas to 0.01 m in coastal areas with onshore wind.

Another common way of representing the wind speed profile is through the *power law*:

$$U(z) = U_{10}(z_r) \left(\frac{z}{z_r} \right)^\alpha \quad (2.13)$$

where $U_{10}(z_r)$ is the 10-minute mean wind speed at reference height z_r . Usually, the reference height associated with the mean wind is $z_r = 10$ m, while wind turbine software, like FAST, normally demand the wind speed at hub height as input. The power law exponent α depends on the surface roughness, $\alpha = 0.14$ is recommended for offshore locations.

A comparison of the two mean wind speed profiles is shown in figure 2.11, for $z_r = 90$ m, which is the hub height of the wind turbine model used in this thesis, $z_0 = 0.001$, $\alpha = 0.14$ and $U_{10}(z_r) = 12$ m/s. Note that the reference height input is important, as this is where the wind profiles have the same value.

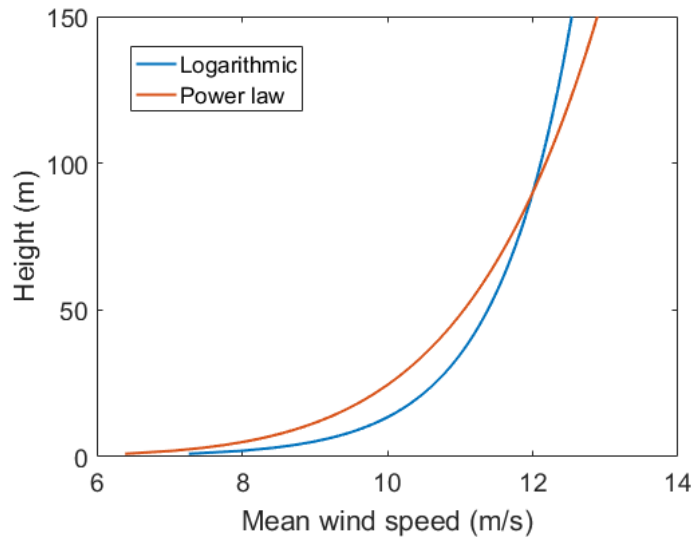


Figure 2.11: Mean wind profile according to the logarithmic and power law. $z_0 = 0.001$, $U_{10}(z_r) = 12$ m/s, $z_r = 90$ m and $\alpha = 0.14$.

Wind Spectra

The stationary short term wind climate can be represented by a wind spectrum, or a PSD function, which expresses how the energy of the wind at a specific point in space is distributed across various

frequencies. Several model spectra exist, which generally agree in the high frequency range, but differ significantly in the low frequency range. Most wind spectra are based on measurements over land, like the well known *Von Kármán spectrum* and the *Davenport spectrum*. The spectral density of the wind speed for offshore wind applications may be presented by a *Kaimal spectrum*:

$$S_U(f) = \sigma_U^2 \frac{4 \frac{L_K}{U_{10}}}{\left(1 + 6 \frac{f L_k}{U_{10}}\right)^{(5/3)}} \quad (2.14)$$

in which f is frequency and L_k is an integral length scale parameter with the following values:

$$L_k = \begin{cases} 5.67 \text{ m for } z < 60 \text{ m} \\ 340.2 \text{ m for } z \geq 60 \text{ m} \end{cases} \quad (2.15)$$

The standard deviation of the wind speed can be found by integrating the spectrum function (Strømme, 2010):

$$\sigma_U^2 = \int_0^{\infty} S_U(f) df \quad (2.16)$$

Wind spectra represent the short term stationary wind conditions. The long term probability distributions for the wind climate parameters U_{10} and σ_U obtained from measurement data can be represented in terms of generic distributions or in terms of scatter diagrams. According to Det Norske Veritas (2014), unless data indicate otherwise, a Weibull distribution can be assumed for the arbitrary mean wind at a given height above the ground or the MSL. A scatter diagram, or a scattergram, gives the frequency of occurrence of given combinations of U_{10} and σ_U .

2.5.3 Waves

The most important types of wave loads relate to wind-induced waves, or surface waves, which build up with time and distance from shore. Even though wave climate and wind climate are correlated, the wave height and direction do not necessarily coincide with the local wind patterns, as wave patterns can travel thousands of kilometers across the ocean. Waves travelling on an ocean surface are irregular and random in shape, height, length and speed of propagation, and several models and theories have been developed to describe sea states.

Wave Theories and Wave Kinematics

A wave theory describes the relationship between the wave period T and the wave length λ and the water particle motion throughout the flow. Wave patterns are often divided into three classes: Regular or Airy waves, irregular waves and random waves.

Linear wave theory, or *Airy wave theory*, is the simplest wave theory describing regular waves, and applies when the wave height is assumed to be much smaller than both the wave length and the water depth. The surface elevation η is given in Det Norske Veritas (2010) as:

$$\eta(x, y, t) = \frac{H}{2} \cos \Theta \quad (2.17)$$

where H is the wave height, $\Theta = k(x \cos \beta + y \sin \beta) - \omega t$ is the phase angle, β is the direction of propagation, $\omega = \frac{2\pi}{T}$ is the angular frequency and $k = \frac{2\pi}{\lambda}$ is the wave number. For Airy waves, the wave height equals twice the wave amplitude, $H = 2A$. Figure 2.12a describes the general characteristics of a regular wave. The wave period T is the time interval between two consecutive zero-upcrossings, and the wave length λ is the distance between two consecutive zero-upcrossings. Underneath the surface, the water particles move in circles according to the harmonic wave, illustrated in figure 2.12. For small water depths, the circular motion is transformed into elliptical motions.

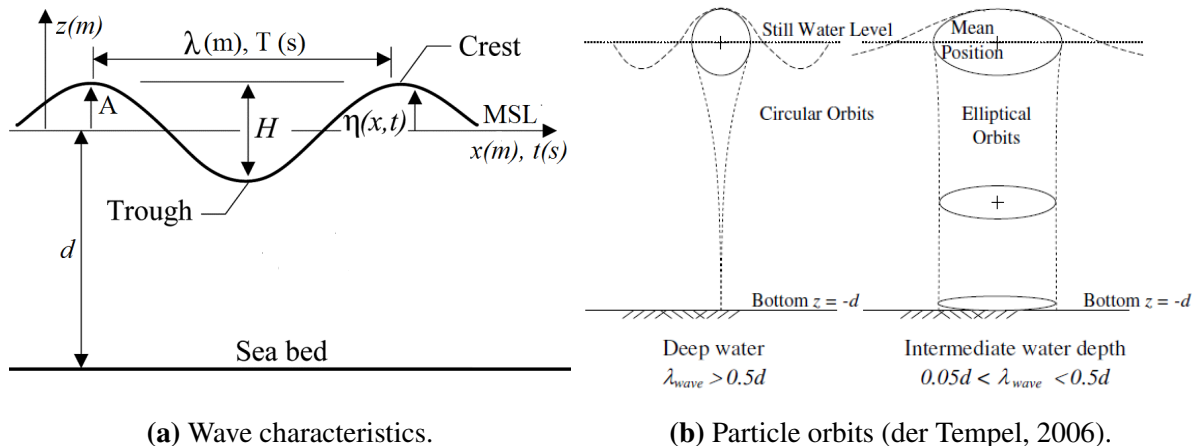


Figure 2.12: Airy wave theory.

Stokes wave theory is used for high waves, and is an expansion of the surface elevation in powers of the linear wave height. A first-order Stokes wave is identical to an Airy wave, while second-

or higher order Stoke waves are asymmetric, with crest height A_C larger than wave trough height A_H . Other wave theories are *Stream function theory*, used for a broad range of water depths, *Boussinesq higher-order theory*, used for shallow water waves, and *Solitary wave theory* used for waves in particularly shallow water (Det Norske Veritas, 2014).

In irregular or random waves, the free surface elevation η is a random process. Kinematics of irregular waves can be obtained through summation of kinematics from linear wave components. The surface elevation is thus given by

$$\eta(t) = \sum_{k=1}^N A_k \cos(\omega_k t + \varepsilon_k) \quad (2.18)$$

where ε_k are random, independent phase angles uniformly distributed between 0 and 2π and A_k are random amplitudes with frequency ω_k .

Airy linear wave theory and Stokes wave theory is only valid up to the still water level, and does not describe the kinematics in the wave top (der Tempel, 2006). To correct for this, different wave stretching methods can be applied. The *Wheeler stretching method* is widely used, and is based on the observation that the fluid velocity at the still water level is reduced compared with linear theory. The velocity for each frequency component is computed using linear theory, and for each time step the vertical coordinate is stretched according to the following equation:

$$z = \frac{z_s - \eta}{1 + \frac{\eta}{d}} \quad (2.19)$$

where d is the water depth.

Wave Spectra

For structural analysis purposes, wave conditions may be described either by deterministic or stochastic approaches. The stochastic representation of a sea state is a wave spectrum, or a PSD function, obtained from a time series of measurements of surface elevation at a single point. The wave spectrum is a function of significant wave height H_s and spectral peak period T_p , and expresses how the energy of the sea elevation is distributed across various frequencies. The significant wave height H_s is defined by Faltinsen (1990) as the mean of the one third highest waves in the time series, which is equal to 4 times the standard deviation of the surface elevation. It is

a measure of the intensity of the wave climate and the variability in arbitrary wave heights. The peak spectral period T_p is related to the mean zero-crossing period T_z through a function depending on spectrum type and wave conditions. Sea states are generally assumed to be stationary for a reference period of 3 hours, meaning that H_s and T_p are assumed constant during that period.

A commonly used spectral shape is the Pierson-Moskowitz wave spectrum, which describes the sea surface elevation for fully developed sea for a certain wind condition. Further measurements of wave spectra in the *Joint North Sea Wave Project* resulted in the JONSWAP spectrum, which is a modification of the Pierson-Moskowitz spectrum and represents sea states that are still developing. Det Norske Veritas (2014) specifies that, unless data indicate otherwise, the sea state at an offshore wind farm location should be represented by a JONSWAP spectrum:

$$S(f) = \frac{\alpha g^2}{(2\pi)^4} f^{-5} \exp\left(-\frac{5}{4} \left(\frac{f}{f_p}\right)^{-4}\right) \gamma^{\exp\left(-0.5 \left(\frac{f-f_p}{\sigma f_p}\right)^2\right)} \quad (2.20)$$

where

$$\alpha = 5 \left(\frac{H_s^2 f_p^4}{g^2} \right) (1 - 0.287 \ln \gamma) \pi^4 \quad (2.21)$$

$f = \frac{1}{T}$ is the wave frequency, $f_p = \frac{1}{T_p}$ is the spectral peak frequency and g is the acceleration of gravity. γ is the *peak-shape factor*, and is dependant on T_p and H_s . A typical value is $\gamma = 3.3$. When $\gamma = 1$ the JONSWAP spectrum is equal to the Pierson-Moskowitz spectrum. σ is the spectral width parameter:

$$\begin{aligned} \sigma &= 0.07 \text{ for } f \leq f_p \\ \sigma &= 0.09 \text{ for } f > f_p \end{aligned} \quad (2.22)$$

For a JONSWAP spectrum, the relation between T_z and T_p is defined as

$$T_z = T_p \sqrt{\frac{5 + \gamma}{11 + \gamma}} \quad (2.23)$$

Figure 2.13 shows a typical JONSWAP spectrum compared to the Pierson-Moskowitz spectrum.

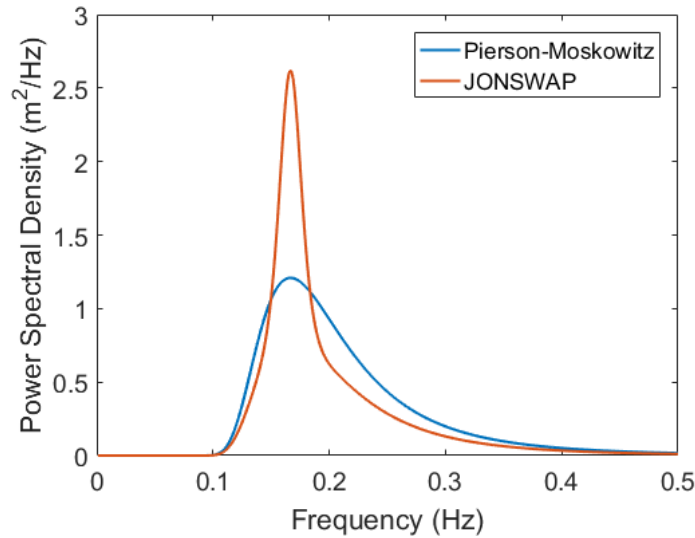


Figure 2.13: Pierson-Moskowitz spectrum ($\gamma = 1$) and JONSWAP spectrum ($\gamma = 3.3$) for $H_s = 1.5\text{m}$ and $T_p = 6\text{s}$.

The long-term probability distributions for the wave climate parameters can be represented in the same way as described for wind in section 2.5.2; either as a Weibull distribution or in a scatter diagram with frequency of occurrence of given combinations of H_s and T_p .

Wave Loads

The wave loads on a cylindrical, slender structure, like an OWT monopile, can be calculated with *Morison's equation* and *strip theory*. The structure is divided into a number of strips, shown in figure 2.14, and the horizontal force on a vertical strip dz at level z is defined by Morison's equation as:

$$dF_{Morison} = dF_M + dF_D \quad (2.24)$$

where the hydrodynamic inertia load, dF_M , is defined as

$$dF_M = C_M \rho \frac{\pi d^2}{4} \ddot{x} dz \quad (2.25)$$

and the hydrodynamic drag load, dF_D , is defined as

$$dF_D = C_D \rho_{water} \frac{d}{2} |\dot{x}| \ddot{x} dz \quad (2.26)$$

C_M and C_D are inertia and drag coefficients, respectively, D is the diameter of the cylinder, ρ_{water} is the density of water, and \dot{x} and \ddot{x} are the horizontal water particle velocity and acceleration, respectively. The resulting horizontal force is obtained by integrating equation 2.24 from $z = -d$ to $z = \eta(t)$.

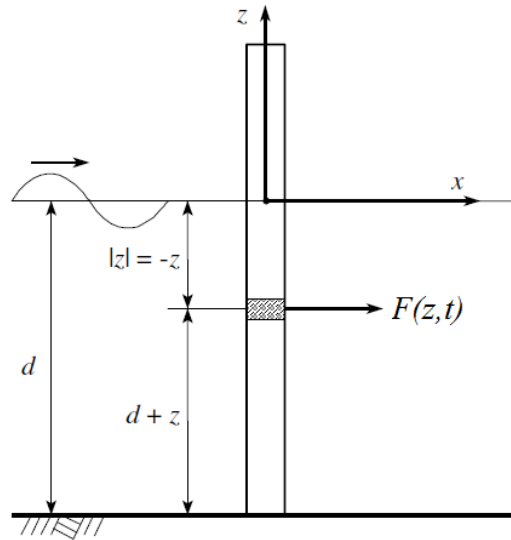


Figure 2.14: Slender vertical tower with hydrodynamic loads (der Tempel, 2006).

Morison's equation is applicable when the effects of *diffraction* are negligible (Jonkman et al., 2016b). Diffraction is the effect a structure has on a wave field, and can be incorporated in equation 2.25 through a correction factor dependent on the ratio D/λ .

Other sea loads to consider for an OWT monopile are currents, breaking wave loads, ice induced loads and loads from marine growth, and the reader is referred to Det Norske Veritas (2010) and Det Norske Veritas (2014) for details regarding these.

2.6 Fatigue in Offshore Wind Turbines

Fatigue is the process of gradual damage done to materials when these are subjected to cyclic loading (der Tempel, 2006). Even though the stresses acting on offshore wind turbine support structures are far below the yield stress limit of the material, fatigue occurs when small stresses are applied a sufficient number of times. The *Palmgren-Miner rule* predicts fatigue damage under the assumptions of linear cumulative damage, and is given as

$$D = \sum_i \frac{n_i}{N_i} \quad (2.27)$$

Where D is the fatigue damage in the structural detail considered, n_i is the number of stress cycles at stress level i and N_i is the number of cycles to failure at stress level i . Failure occurs when $D \geq 1$.

Wind turbines are designed for a lifetime of 20 years. Compared to other structures, the contribution of the turbine's self-weight in stress calculations is small, while the contribution from bending moment caused by wind and waves is large. According to Schaffarczyk (2014), the wind turbine structure is subjected to approximately 500 million load cycles during its lifetime, and must be able to withstand these loads for 20 years without failure. Hence, fatigue is an unavoidable topic when simulating the loads acting on wind turbines. A detailed overview of the theory and equations used for fatigue analyses in this thesis is given in chapter 9.

3 Computational Tool: FAST

Reliable and accurate *computer-aided engineering* (CAE) tools are essential for the wind energy industry to develop new technology. The software used to model the offshore wind turbine in this thesis is called FAST, which is short for Fatigue, Aerodynamics, Structures and Turbulence (Jonkman and Buhl, 2005). It is an open-source aero-hydro-servo-elastic CAE tool for modelling horizontal axis wind turbines, developed by the United States' National Renewable Energy Laboratory (NREL) through the U.S. Department of Energy (DOE). FAST enables fully coupled non-linear aero-hydro-servo-elastic simulations in the time domain by coupling structural dynamics, hydrodynamics, aerodynamics and control and electrical system dynamics models. FAST enables analysis of a range of horizontal axis wind turbine configurations, including two or three-bladed, land-based, offshore fixed bottom and offshore floating turbines. The open-source code is written in the programming language Fortran v90.

FAST v8 is the most recent version of the tool, and is the version used in this thesis. FAST v8 differs significantly from previous versions in its modularity. Features that previously were a part of one FAST module is now split out as callable modules with separate input files and source codes. The individual modules are interconnected under the same framework to solve for the global response of the whole wind turbine system. The new FAST Modularization Framework is developed to transform FAST to a more powerful and flexible tool which enables further improvements from a large number of developers without the need to recode established modules (Jonkman, 2013b).

3.1 The FAST Model

As mentioned above, FAST enables analysis of a range of onshore and offshore HAWTs; both two or three bladed, upwind or downwind rotor, and lattice and tubular towers can be modelled.

The FAST model employs a combined modal and multi-body dynamics formulation. The multi-body formulation applies to the support platform, nacelle, generator, gears, hub and tail, while the modal formulation applies to the blades and the tower. FAST relies on an assumed modes approach, implying that the blade and tower mode shapes are required as input.

Figure 3.1 shows the global coordinate system of the FAST model, here illustrated with a lattice

type substructure. When the main environmental load component is in the x-direction, the most excited motions of the turbine structure is fore-aft displacement, called surge, and fore-aft rotation, called pitch. Other words for the side-to-side displacement and rotation are sway and roll, respectively.

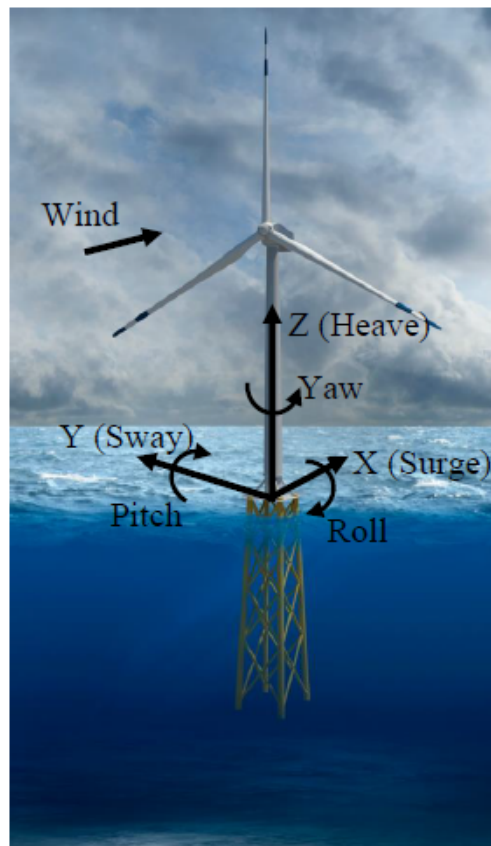


Figure 3.1: Global coordinate system (Damiani et al., 2015).

The three-bladed wind turbine model, which is used in this thesis, utilizes 24 degrees of freedom (DOFs), shown in figure 3.2. Figure 3.3 shows the support platform layout. Note that FAST does not distinguish between the terms platform and transition piece, both refer to the red part in figure 3.3. Six DOFs account for the platform translational (surge, sway and heave) and rotational (roll, pitch and yaw) motions. Four DOFs relate to tower motion; two are longitudinal modes and two are lateral modes, and nine DOFs are for the flapwise and edgewise blade modes. The last five DOFs are related to the generator, nacelle and rotor-and tail furl.

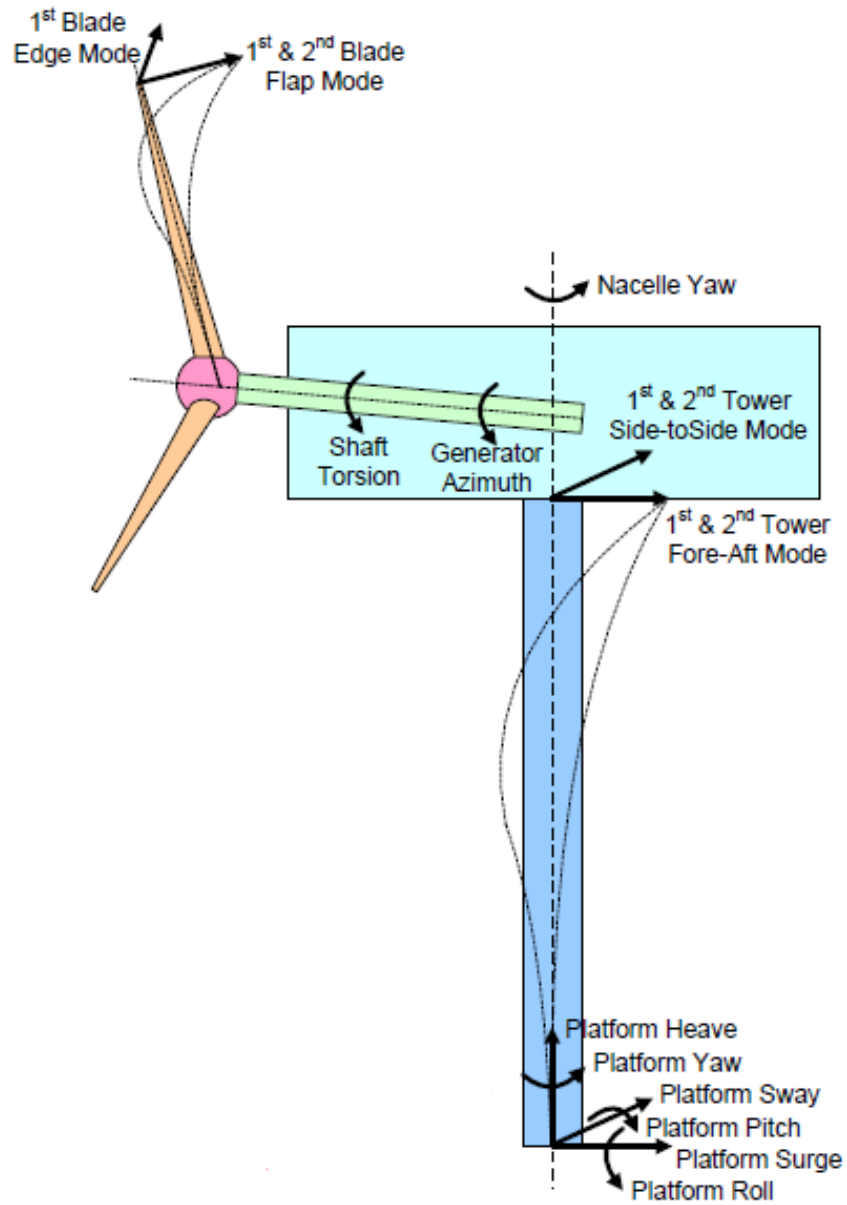


Figure 3.2: Layout and DOFs of a three bladed HAWT FAST model (Jonkman, 2015).

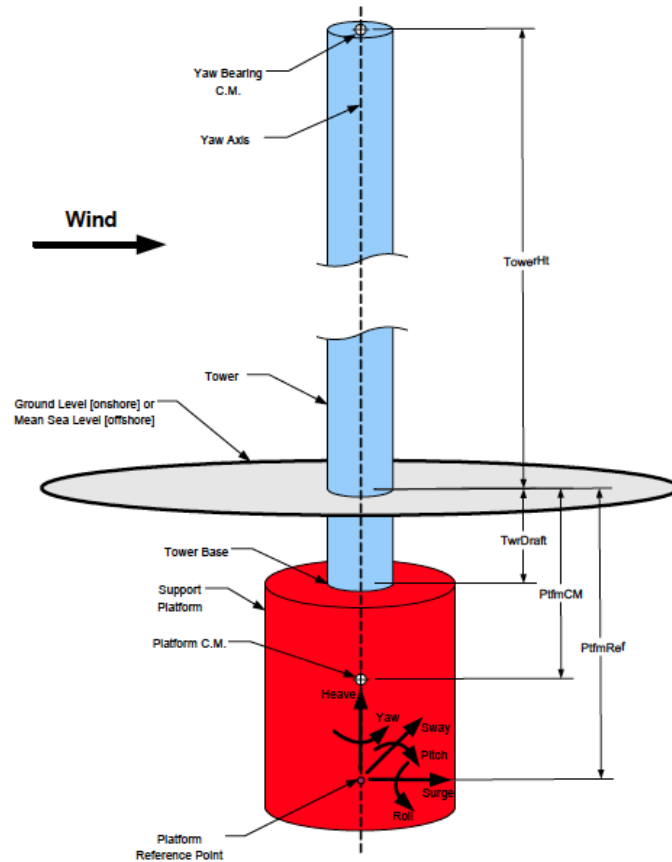


Figure 3.3: Support platform layout (Jonkman and Buhl, 2005).

3.2 FAST Modularization Framework

FAST is an open source code downloaded from the NREL website (National Renewable Energy Laboratory, 2016) together with an archive containing all the modules required for performing full aero-hydro-servo-elastic analyses of an OWT. The main modules in FAST are *SubDyn* and *ElastoDyn* for the structural dynamics, *ServoDyn* for the power generation, and *InflowWind*, *HydroDyn* and *AeroDyn* for external conditions and applied loads. These are the modules used in this thesis. Their different modelling purposes and coupling are illustrated in Figure 3.4, and will be explained further in the next subsections.

The FAST archive also contains the modules *BeamDyn* for blade structural dynamics, *MoorDyn* for modelling of moorings of floating OWTs, and *IceDyn* and *IceFloe* for modelling of surface

ice. These modules are not used in this thesis and will not be explained further, but prove the great modelling opportunities of the FAST code.

Structural loads and responses are transferred between the modules via the FAST driver program, which handles the time and spatial coupling across the modules. Sharing of data between modules is performed with a predictor-corrector approach, which allows for either implicit or explicit time integration within each module. The FAST main input file, *filename.fst*, calls the different modules to be run in the analysis and their individual input files. The FAST main input file, along with input files for the different modules used in this thesis can be found in Appendix A.

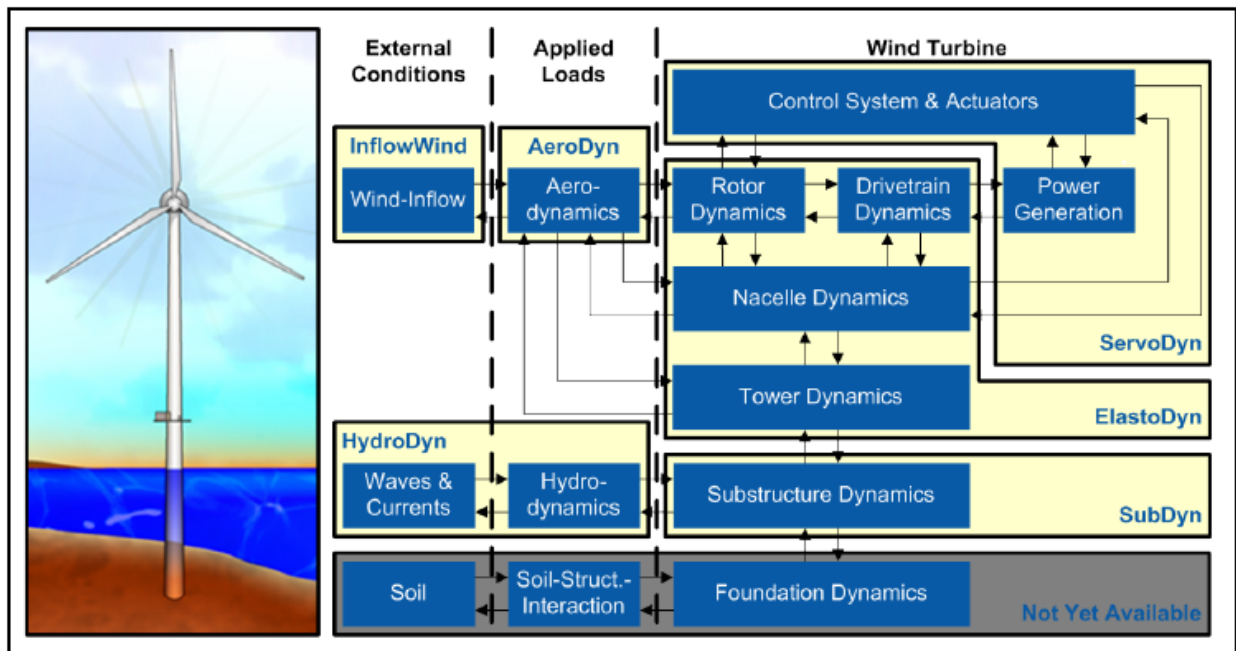


Figure 3.4: FAST modularization framework for fixed-bottom offshore wind turbine systems (Jonkman and Jonkman, 2016).

3.2.1 SubDyn

SubDyn is a time-domain structural-dynamics module for fixed-bottom substructures, and is the most important module for this thesis. SubDyn models the structure from the seabed up to the TP, while the TP and the tower is modelled in ElastoDyn. Unlike previous versions of FAST, which could only model monopiles, SubDyn also enables modelling of tripods, jackets and other lattice-type multimember substructures. SubDyn can be driven as a standalone code independent of FAST

to compute the natural frequencies and structural response of only the substructure.

Damiani et al. (2015) describes the theory behind the SubDyn module. SubDyn uses a *linear frame finite-element beam* (LFEB) model, where the user can choose between Euler-Bernoulli and Timoshenko beams. Further, the SubDyn input file contains information about the substructure geometry, material properties, integration type, finite element model and modal damping coefficients. The substructure is modelled by defining joint coordinates connected with members. A member is refined into a number of elements with nodes located at the element ends. The geometry of a member is defined by its outer diameter and wall thickness, and the material properties are defined by Young's modulus E , shear modulus G and mass density ρ . In addition to the hydrodynamic loads from HydroDyn, self-weight loads are applied by SubDyn at all nodes.

For beam frame substructures, like the tripod or jacket, the number of DOFs in the equation of motion (equation 2.5) can easily grow to thousands. For this reason, SubDyn performs a dynamics system reduction via the Craig-Bampton (C-B) method, to recharacterize the substructure finite-element model into a reduced DOF model that maintains the fundamental low-frequency response modes of the structure. C-B reduction is not applied for simple substructures like monopiles.

Loads and responses are transferred between SubDyn, HydroDyn and ElastoDyn via the FAST driver program to enable hydro-elastic interaction at each coupling time step. The displacements, velocities and accelerations of the six TP DOFs are inputs to SubDyn from ElastoDyn, while the reaction loads at the TP are outputs from SubDyn to ElastoDyn. Outputs from SubDyn to HydroDyn are nodal displacements, velocities and accelerations in order to calculate hydrodynamic loads, which then become inputs to SubDyn from HydroDyn.

SubDyn is currently limited to rigid connections between the substructure and the seabed, which implies that foundation flexibility and SSI is disregarded. Figure 3.4 illustrates that this is "not yet available" in FAST. However, foundation flexibility can be represented through the apparent fixity method, as described in section 2.4.4. The fictive AF beam is included in the FAST model through the SubDyn input file, a procedure that will be described in detail in chapter 5.

3.2.2 ElastoDyn

ElastoDyn is a structural dynamics module, modelling the tower and platform, as well as the rotor, drivetrain and nacelle. The ElastoDyn input file contains information on a number of parameters, ranging from what degrees of freedom to enable or disable to initial conditions and information

on the turbine configuration. Tower and blade structural properties are also written to ElastoDyn through separate input files. The tower structural input file, *ElastoDyn_Tower.dat*, contains information on tower distributed properties and assumed mode shapes. The *ElastoDyn_Tower* file requires input on four mode shapes: the two first fore-aft modes and the two first side-to-side modes of the tower, specified as polynomial coefficients. The mode shapes have to be obtained outside of FAST, and the software BModes is primarily used for this purpose. An introduction to BModes will be given in section 3.3.

Straight Euler-Bernoulli beams are used for the ElastoDyn model, which implies no axial or torsional DOFs and no shear deformation. Otherwise, all terms include full nonlinearity: The mode shapes are used as shape functions in a nonlinear beam model, using Rayleigh Ritz method (Jonkman, 2013a).

The user specifies what time integration method to use; either explicit 4th-order Runge-Kutta (RK4), 4th-order Adams-Bashforth (AB4) multi-step explicit, or 4th-order Adams-Bashforth-Moulton (ABM4) multi-step predictor-corrector integration method. In this thesis the ABM4 integration method is used.

3.2.3 HydroDyn

HydroDyn models hydrodynamics using a combination of incident-wave kinematics and hydrodynamic loading models. HydroDyn uses first-order linear Airy or first- plus second-order wave theory to generate waves, with the option to include wave directional spreading. Second-order terms are calculated using the first-order wave-component amplitudes with additional energy added to the wave spectrum. Enabling second-order terms includes nonlinearities of real surface waves, which permits more accurate modelling of the hydrodynamic loads. In earlier versions of FAST, wave stretching was possible, but this is not yet possible in FAST v8, and the waves are only computed in the domain between the seabed and the MSL.

HydroDyn requires inputs on environmental conditions, wave and current conditions, as well as inputs regarding the model's support structure and hydrodynamic coefficients. HydroDyn allows for complex modelling of hydrodynamics, but only the most important features used for modelling wave loads is presented in this section. Further information can be found in the HydroDyn manual by Jonkman et al. (2016b).

The user can choose between several different wave kinematics models, including regular waves,

JONSWAP or Pierson-Moskowitz spectra, white noise or other user-defined spectra. Other important inputs are H_s , T_p , γ , wave cut-off frequencies and wave spreading direction. Lower and upper cut-off frequencies tell what domain of frequencies to include in the wave spectrum. To ensure that the wave kinematics and hydrodynamic loads are realistic, and to minimize computational expense, it is important to set proper wave-cut off frequencies.

In HydroDyn, a fixed-bottom structure subjected to hydrodynamic loads is modelled with strip theory using Morison's equation, described in section 2.5.3, and the geometry is defined using joints and members. When modelling a floating platform, potential-flow theory, strip theory or a combination may be used.

3.2.4 InflowWind and TurbSim

TurbSim is a stochastic, full-field, turbulent-wind simulator used to create wind-fields. TurbSim is not included in the FAST framework, but is the software recommended by NREL for generating wind-field files. InflowWind, however, is the FAST module used for processing wind-inflow data generated by TurbSim.

TurbSim simulates time series of three-component wind speed vectors in a two-dimensional vertical rectangular grid that is fixed in space, as shown in figure 3.5 (Jonkman and Kilcher, 2012). The time series are produced through spectra of the velocity and spacial coherence in the frequency domain, converted to the time domain through an inverse Fourier transform, as explained in section 2.5.1).

The TurbSim input file requires information about model specifications, including dimensions of the grid and the wind turbine, as well as analysis time specifications and seed number. The seed number is used to create random phases for the velocity time series. Moreover, in the input section called *Meteorological Boundary Conditions* the spectral model, the wind speed profile, the turbulence characteristics and the mean wind speed are specified. The user can choose between several different spectral models. Among them are the Kaimal and von Kármán spectrum, as well as several spectral models developed by NREL. Turbulence intensity is specified either by standard categories A, B and C, defined by International Electrotechnical Commission (IEC), or in percentage.

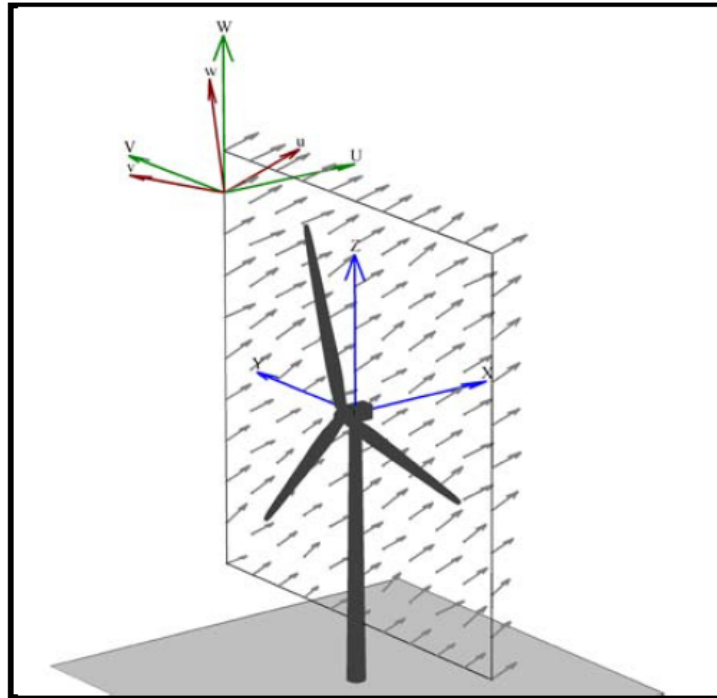


Figure 3.5: Coordinates of a TurbSim wind field with 15° horizontal and 8° vertical mean flow angles (Jonkman and Kilcher, 2012).

3.2.5 AeroDyn

AeroDyn is a time-domain rotor aerodynamics module, which uses wind inflow from InflowWind to calculate wind forces, namely lift, drag and pitching moments. The calculations of the influence of the wake on the turbine rotor aerodynamics is based on quasi-steady *blade element momentum* (BEM) theory. BEM theory originates from the blade element theory and the momentum theory. It assumes that the blades can be divided into small two-dimensional elements with elemental forces, which are integrated across the length of the blade to obtain the total aerodynamic loads. These blade elements trace out annular regions as they rotate in the rotor plane, across which momentum theory assumes momentum balance. Figure 3.6 shows the resultant aerodynamic forces on a blade element and their components perpendicular and parallel to the rotor plane.

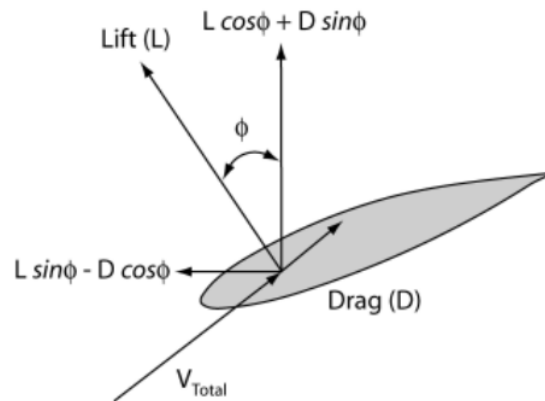


Figure 3.6: Aerodynamic forces on a blade element (Moriarty and Hansen, 2005).

The BEM iteration uses static airfoil data, supplied to the AeroDyn main input file through individual files for each airfoil, containing information about lift force, drag force and pitching moment versus angle of attack. Furthermore, the AeroDyn input file contains information about parameters such as environmental conditions and tower properties, as well as file names calling separate files about blade geometry and discretization.

Like the blades, the tower is also discretized with nodes distributed across its length. The influence of the tower on the wind is based on a potential-flow model, using the analytical solution for flow around a cylinder, and/or a tower shadow model, accounting for the tower wake influence on downwind rotors. The wind load on the tower is based directly on the tower diameter and drag coefficient and the local relative wind velocity at each tower node.

3.2.6 ServoDyn

ServoDyn is the control and electrical-drive module. It includes control and electrical-drive models for blade pitch, generator torque, nacelle yaw, high-speed shaft brake and blade-tip brakes. Bladed-style dynamic link library (DLL) is the default blade pitch control mode in FAST v8. A more detailed description of ServoDyn is seen as out of scope for this thesis, but can be found in Jonkman (2014). The default ServoDyn input file provided by NREL is used for all the simulations in this thesis, and can be found in Appendix A.5.

3.3 BModes

As described in section 3.1 and 3.2.2, assumed mode shapes are required as input to *ElastoDyn*, and *BModes* is the software primarily used to obtain them. *BModes* is a finite-element code that provides coupled modes for the wind turbine tower or blades. It is not a part of the FAST modularization framework and has to be run as a separate program, but according to Bir (2007) there are plans to eventually integrate *BModes* with FAST to enable tower and blade modes to change during a simulation.

For obtaining the tower modes, inputs to *BModes* are tower structural properties, including mass and stiffness matrices. These matrices change with the boundary conditions, that is when flexibility of the foundation is implemented in *SubDyn*, and the user must adjust this. Rotor speed and blade pitch angles are automatically set to zero for tower modal analysis. Output from *BModes* are natural frequencies of the support structure, and displacements and rotations along the normalized tower length. This deflection data can be converted to a polynomial representing the mode shape, whose coefficients can be written to the *ElastoDyn_Tower* file. A detailed description on how to obtain mode shapes from *BModes* when the foundation properties, and hence the boundary conditions, change is given in section 5.2.

4 NREL 5-MW Baseline Wind Turbine

NREL has developed a reference turbine with detailed specifications representative of a typical utility-scale multimegawatt turbine, known as the *NREL 5-MW offshore baseline wind turbine*. It is a three-bladed upwind HAWT with a monopile support structure, developed for researches to have a common reference model for studies of offshore wind technology. It has been used in several international research projects, and will be used for the analyses in this thesis, referred to as NREL 5MW. The size of 5MW was chosen by NREL because it was concluded that offshore wind turbines need to be of at least this size to be cost-effective, and because of access to previous research on this size. In the FAST archive, NREL provides input files for different standard simulations of the NREL 5MW. The specifications of the turbine are described in Jonkman et al. (2009), and a collection of the properties are presented in table 4.1.

Table 4.1: Properties of the NREL 5-MW baseline wind turbine.

Rating	5 MW
Rotor orientation, configuration	Upwind, 3 blades
Rotor diameter, hub diameter	126 m, 3 m
Hub height	90 m
Cut-in, rated, cut-out wind speed	3 m/s, 11.4 m/s, 25 m/s
Cut-in, rated rotor speed	6.9 rpm, 12.1 rpm
Rated tip speed	80 m/s
Rotor mass	110,000 kg
Nacelle mass	240,000 kg
Tower mass	347,460 kg
Tower height	87.6 m
Tower top diameter, wall thickness	3.87 m, 0.019 m
Tower base diameter, wall thickness	6.0 m, 0.027 m
Substructure base diameter, wall thickness	6.0 m, 0.06 m
Support structure steel density	8500 kg/m ³
Steel Young's modulus	210 GPa
Steel Shear modulus	80.8 GPa
Support structure structural-damping ratio (all modes)	1 %

The heights in the table are measured from the MSL, which is set to 20 meters above the mudline. The point defined as the tower base, or the connection between the tower and the substructure, is 10 meters above the MSL. Notice that the hub height, i.e. the vertical distance from the turbine platform to the rotor centre, and tower height are not the same, there is a 2.4 meters vertical distance between them. The diameter and wall thickness of the steel tower decreases linearly from the tower top to the substructure base at the seabed. Structural damping is given as a percentage of critical damping, and follows recommendations from Det Norske Veritas (2014) of 1%.

Figure 4.1 illustrates the dimensions of the NREL 5MW. The support structure has a perfectly fixed boundary at the mudline, illustrated by shading the subsoil part of the turbine, which means that neither lateral nor rotational movements are allowed here. Due to this fixed base seabed connection, this model will subsequently be referred to as the *fixed base model*.

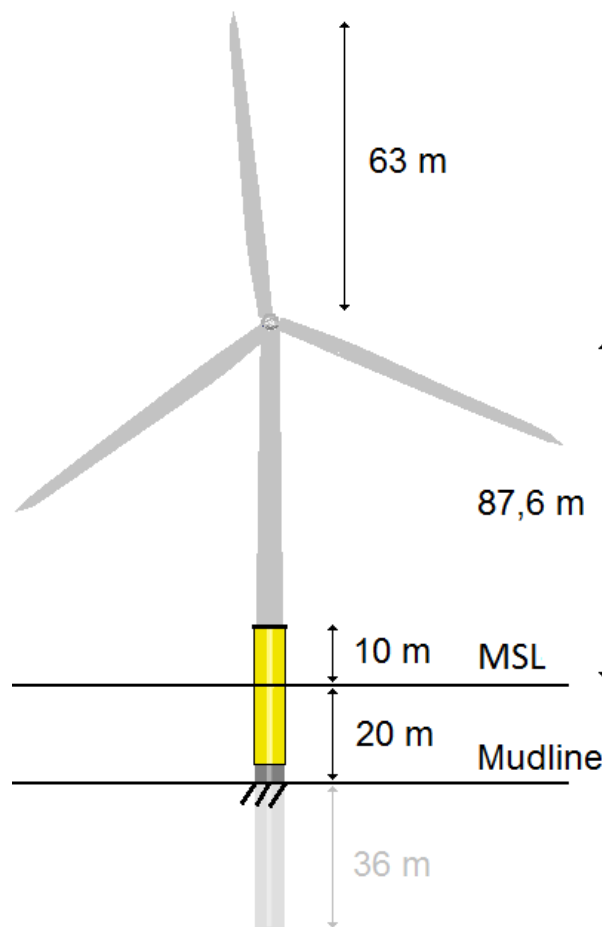


Figure 4.1: NREL 5-MW OWT (Aasen et al., 2016).

In Jonkman et al. (2009), only the natural frequencies of the land-based version of the NREL 5MW is presented. Therefore, the natural frequencies of the offshore turbine were calculated using BModes, and are presented in table 4.2.

Table 4.2: The first natural frequencies of the NREL 5MW OWT from BModes.

Mode	Frequency (Hz)
1st fore-aft	0.280
1st side-to-side	0.373
2nd fore-aft	1.860
2nd side-to-side	2.049

In addition, as described in section 2.2.3, a wind turbine has operational natural frequencies of 1P and 3P. In this case, where the turbine is operating at its rated rotor speed of 12.1 rpm, the operational natural frequencies and their corresponding natural periods become:

$$1P = \frac{12.1 \text{ rpm}}{60 \text{ s/min}} = 0.202 \text{ Hz}$$

$$T = \frac{1}{0.202} = 4.959 \text{ s}$$

$$3P = 3 \times 0.202 \text{ Hz} = 0.605 \text{ Hz}$$

$$T = \frac{1}{0.605} = 1.653 \text{ s}$$

Referring to figure 2.3, it is evident that the wind turbine tower has a soft-stiff design, since the natural frequency of the first tower mode lies between 1P and 3P.

All the FAST input files required to run simulations of the NREL 5MW fixed base OWT model are provided by NREL in the downloaded FAST archive. The main input file as well as the input files for the different FAST modules are presented in Appendix A.

5 Simplified Foundation Model

In this chapter, soil-foundation flexibility is introduced in the the FAST model through the apparent fixity method.

5.1 Soil-Pile Interaction

As introduced in section 2.4, the principle behind the apparent fixity method, or the *AF method*, is to reproduce the stiffness of the soil-pile system with a fictive cantilevered beam, fixed at its lower end at a certain point below the mudline. To obtain the properties of the AF beam, the properties of the real monopile and the soil surrounding it are needed. The monopile penetration depth of the NREL 5MW was set to 36 meters, which is the length used in Jonkman and Musial (2010), and the soil profile is the one described in Passon (2006), shown in figure 5.1.

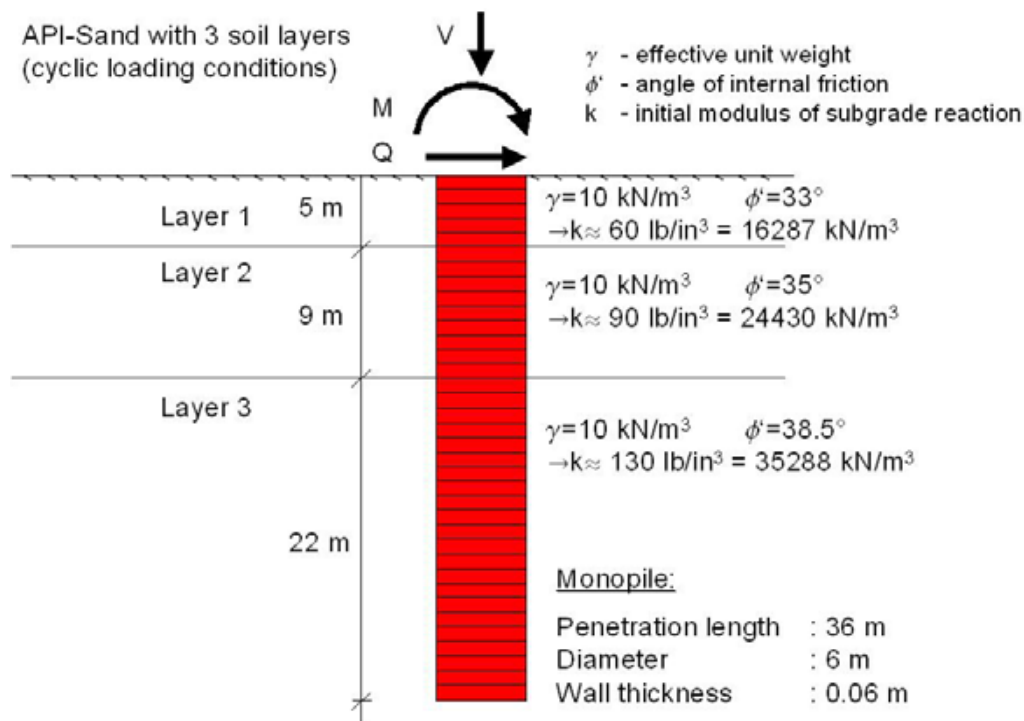


Figure 5.1: Soil profile (Passon, 2006).

There are mainly two possible procedures to obtain the required properties of the AF beam, i.e. the apparent fixity length L_{AF} and the flexural rigidity EI_{AF} . Both procedures are based on obtaining the stiffness relation of the true soil-pile system in figure 5.1 from a geotechnical software, and comparing it with the stiffness relation of a two DOF cantilevered Bernoulli beam, shown in equation 5.1. The differences between the two procedures are the assumptions made on the foundation behaviour.

$$\begin{bmatrix} \frac{12EI}{L^3} & -\frac{6EI}{L^2} \\ -\frac{6EI}{L^2} & \frac{4EI}{L} \end{bmatrix} \begin{bmatrix} u \\ \theta \end{bmatrix} = \begin{bmatrix} F \\ M \end{bmatrix} \quad (5.1)$$

Passon (2006) and Bush et al. (2008) have both studied foundation models for the NREL 5MW using the soil profile in figure 5.1. They used a nonlinear soil-pile lateral load analysis programme called *LPILE* to calculate deflection u and rotation θ at the mudline for specified levels of shear force F and moment M . Two drawbacks of this method will be presented here. Firstly, *LPILE* relies on a distributed springs approach developed for piles with fairly small diameters compared to an OWT monopile. The spring stiffnesses are believed to not be accurate for larger piles like a monopile (Kaynia, 2017). Secondly, assumptions have to be made regarding the level of shear force and moment in the structure, since they naturally are unknown in the beginning of the analyses, and because the nonlinear soil behaviour makes mudline forces change with the foundation flexibility. Bush et al. (2008) used multiple ten-minute FAST simulations of a fixed base OWT model, like the fixed base model described in chapter 4, to obtain values for F and M to use as input to *LPILE*. *LPILE* calculates u and θ , which are then used to find L_{AF} and EI_{AF} from equation 5.1. As the mudline loads from the simulations apply to a fixed base model, they are not representative of the actual forces and moments that will occur in the flexible foundation model. However, there is particularly one interesting discovery from Bush et al. (2008). When comparing three mudline force cases; one using the mean value from the time series of mudline force, one using the "mean plus one standard deviation" values, and one using maximum values, the AF properties were only slightly different. This suggests that the soil behaviour is almost linear for the pile and soil properties studied here for the range of environmental loads simulated. With this in mind, another approach was chosen in this thesis to find L_{AF} and EI_{AF} .

To calculate the stiffness of the soil-pile system in figure 5.1, the geotechnical software *PILES* (Kaynia, 1982) was used. This is a linear soil-pile analysis software not accounting for any non-linear load-displacement behaviour of the soil. Hence, it is independent on load level, and the only inputs required by *PILES* are the soil profile, the pile properties and the boundary conditions. The

mass per meter pile was set to include the mass of the soil inside the pile. The output from PILES is a 6 x 6 stiffness matrix located at the mudline, representing stiffness coefficients of the soil-pile system in the two horizontal DOFs, the vertical DOF, two rotational DOFs and one torsional DOF. Soil behaviour is assumed to be isotropic, which implies that the stiffness coefficients in the two horizontal directions, surge and sway, are identical ($k_{xx} = k_{yy} = k_{uu}$), as well as the rotational stiffness coefficients related to pitch and roll, ($k_{x\theta} = k_{\theta x} = k_{y\theta} = k_{\theta y} = k_{u\theta} = k_{\theta u}$). Considering that the vertical, or axial, stiffness is not considered in FAST, and that torsion is not significant for the analysis in this thesis, the stiffness matrix can be reduced to a 2 x 2 matrix:

$$[K]_{PILES} = \begin{bmatrix} k_{uu} & k_{u\theta} \\ k_{\theta u} & k_{\theta\theta} \end{bmatrix} = \begin{bmatrix} 2.84 \times 10^9 & -1.56 \times 10^{10} \\ -1.56 \times 10^{10} & 1.93 \times 10^{11} \end{bmatrix} \quad (5.2)$$

The units of k_{uu} , $k_{u\theta}$, $k_{\theta u}$ and $k_{\theta\theta}$ are N/m, N/rad, Nm/m and Nm/rad, respectively.

The stiffness matrices in equations 5.1 and 5.2 were matched with each other while neglecting the off-diagonal terms, which is common practice in general geotechnical research (Kaynia, 2017). There are mainly two reasons for disregarding the off-diagonal stiffness terms. Firstly, because the system of three equations with two unknowns, EI and L , is inconsistent, meaning that there is no solution satisfying all three equations. Secondly, because in regular pile constructions, the off-diagonal terms are normally small compared to the diagonal terms and do not affect the total structural response of the system significantly. As this is a recognized method used for soil-pile modelling and analysis, it is the provisional approach in this chapter, but the effect of disregarding the off-diagonal stiffness terms will be investigated further in chapter 6. Due to this simplification, the method described in this chapter will be referred to as the *simplified AF method*.

L_{AF} and EI_{AF} of the fictive beam were calculated straightforwardly from the stiffness matrices, and the results are as follows:

$$\begin{aligned} L_{AF} &= 14.28 \text{ m} \\ EI_{AF} &= 6.889 \times 10^{11} \text{ Nm}^2 \end{aligned}$$

As described in section 3.2.1, the inputs required by SubDyn to describe beams are the Young's modulus and the length, along with shear modulus, material density, pile diameter and wall thickness. It was chosen to let the AF beam be a hollow cylinder, just like the real monopile. Using the same diameter d and wall thickness t_w as the real monopile, 6 m and 0.06 m respectively, to calculate the area moment of inertia

$$I_{AF} = 5.089 \text{ m}^4,$$

the Young's modulus was found to be

$$E_{AF} = 1.354 \times 10^{11} \text{ N/m}^2$$

The shear modulus is required as input to FAST, and was calculated using the relation

$$G_{AF} = \frac{E_{AF}}{2(1 + \nu)} = 5.206 \times 10^{10} \text{ N/m}^2 \quad (5.3)$$

where $\nu = 0.3$ is the FAST default value of the Poisson's ratio for steel. The material density was kept the same as the monopile above the mudline, namely $\rho_{steel} = 8500 \text{ kg/m}^3$.

5.2 Implementing the Foundation Model in FAST

This section will go through the changes made in the FAST code in order to include the foundation with the simplified apparent fixity method described in the previous section.

The AF beam was implemented in FAST by modifying the SubDyn code. In the original SubDyn input file for the NREL 5MW fixed base model, the mudline joint is constrained in all six DOFs, making the substructure rigidly connected to the seabed. These DOFs were enabled, and a new joint was added at a length $L_{AF} = 14.28 \text{ m}$ below the mudline. The new joint was connected to the NREL 5MW substructure through a beam member with the cross sectional properties calculated in the previous section. The joint below the mudline was constrained in all DOFs, making the new foundation model fixed to this point and free to move in all directions at the mudline. This model was now able to reproduce mudline rotations and displacement caused by the soil-foundation flexibility. The new SubDyn input file can be found in Appendix C.1.

Implementing the fictive beam below mudline in SubDyn changes the boundary conditions of the support structure and consequently affects the mode shapes. Hence, since FAST relies on an assumed modes approach, new mode shapes had to be calculated using BModes and be written to the ElastoDyn code for the flexible foundation model. BModes was originally developed to be used with previous versions of FAST, which did not divide the wind turbine modelling into one module for the substructure and one module for the tower, so the mode shape input was supposed to be for the tower and substructure as one. However, in FAST v8 the mode shape input needed

is only for the tower, that is from the platform and up. The effect of the substructure, and hence also the foundation, is accounted for by introducing additional stiffness and mass matrices in the BModes input file. These matrices are automatically calculated while running the SubDyn module, and can be directly substituted from the SubDyn output file into the BModes input file as *hydro_K* and *hydro_M*. The BModes input file and the tower properties input file are presented in Appendix C.2 and C.3, respectively. As the only mode shapes required by ElastoDyn are the two first fore-aft and side-to-side modes, one would not want torsional, axial and shear modes to disturb the output file. Hence, as proposed by NREL's National Wind Technology Center's forum, NWTC (2017), the tower properties input parameters *edge_iner* and *flp_iner* were set to very small numbers, and *tor_stff* and *axial_stff* were set to very high numbers.

The resulting natural frequencies from BModes are shown in Table 5.1 with their corresponding natural periods, compared to the natural frequencies and periods of the fixed base model.

Table 5.1: The first natural frequencies and periods from BModes.

Mode	Fixed base model		Simplified AF model	
	Frequency (Hz)	Period (s)	Frequency (Hz)	Period (s)
1st fore-aft	0.280	3.566	0.236	4.234
1st side-to-side	0.373	2.680	0.365	2.738
2nd fore-aft	1.860	0.538	1.446	0.692
2nd side-to-side	2.049	0.488	2.034	0.492

One would expect the fore-aft and side-to-side mode frequencies of a long and slender tower to be almost identical, but for an OWT the differences seen in table 5.1 is due to the center of mass offset and differences in inertias of the RNA (NWTC, 2017).

These frequencies are valuable for investigating the difference in structural dynamics of the models, and to check if the effect of introducing foundation flexibility leads to the expected amount of reduction in natural frequencies. However, BModes and FAST model the connection to the RNA differently, so the values in table 5.1 do not represent the correct natural frequencies of the full-system model. This will be investigated further in section 6.2.

BModes' output file contains deflection data along the normalized tower length, while the mode shape input required by ElastoDyn is in the format of a sixth order polynomial. This conversion was done in the Excel workbook *Modeshapepolyfitting.xls*, provided by NREL with the FAST

archive. This workbook creates normalized polynomial coefficients to fit the data, projected onto a line that is tangent to the deflection at the bottom, here being the rigid connection between the tower and the platform. This means that deflection and rotation in the platform are not shown in the calculated mode shapes. Figure 5.2 shows normalized plots of the estimated mode shapes for the fixed base model compared to the estimated mode shapes for the flexible AF model.

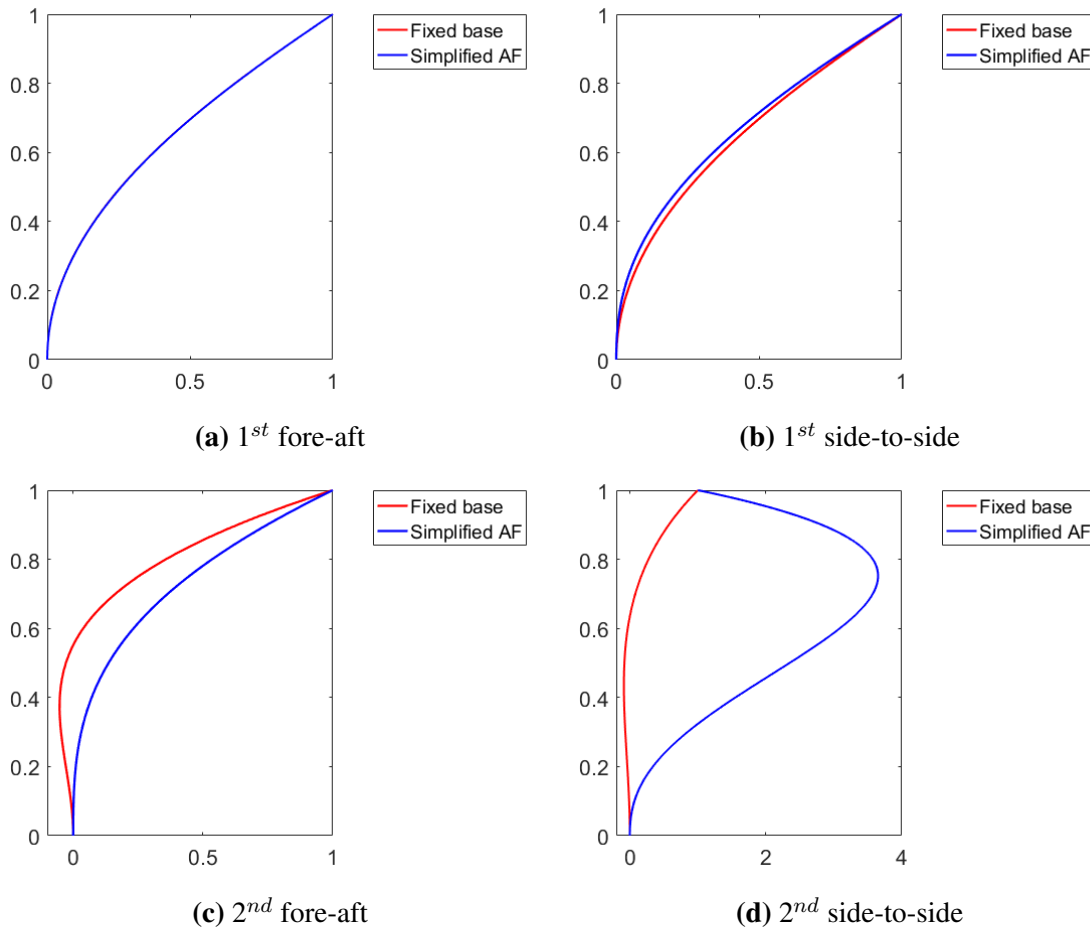


Figure 5.2: Normalized tower mode shapes from BModes for the rigid and the AF model.

As can be seen from figure 5.2, the first mode shapes are almost identical for the two models, but the second side-to-side mode differs significantly. The reason for this, explained by Jonkman (2017), is that the second tower modes are particularly sensitive to the boundary conditions at the base. The new mode shape polynomial coefficients were written to the *ElastoDyn_tower* file, which can be found in Appendix C.4.

In this section, the FAST files provided by NREL for the standard 5MW OWT with a rigidly

connected the seabed has been modified to include the foundation through the simplified apparent fixity method. The list below summarizes what has been done:

1. The SubDyn input file was changed to include an AF beam below the seabed.
2. The SubDyn module was run to obtain a stiffness matrix and a mass matrix for the new substructure configuration.
3. The stiffness and mass matrices were provided to the BModes input file, so that BModes accounts for the foundation flexibility when calculating the mode shapes.
4. The deflection output from BModes was converted to polynomials with the Excel workbook *modeshapepolyfitting.xls*.
5. The polynomial coefficients were provided to the *ElastoDyn_Tower* file.
6. A FAST v8 simulation was ready to be run.

5.3 FAST Simulation Inputs

The wind load applied in the simulation was generated with TurbSim and sent as input to the InflowWind FAST module. A full-field turbulent wind field was created using the Kaimal spectral model and the power law wind profile. The mean wind velocity at hub height was set to 12 m/s with a turbulence IEC characteristics B, representing a turbulence intensity of 14%. The size of the wind field grid was set to 145 m \times 145 m. The TurbSim input file for this simulation can be found in Appendix B. A time series of the wind velocity in horizontal directions (x- and y-direction) and vertical direction (z-direction) can be seen in figure 5.3, showing fluctuations around 12 m/s in the x-direction and around zero in the y- and z-directions.

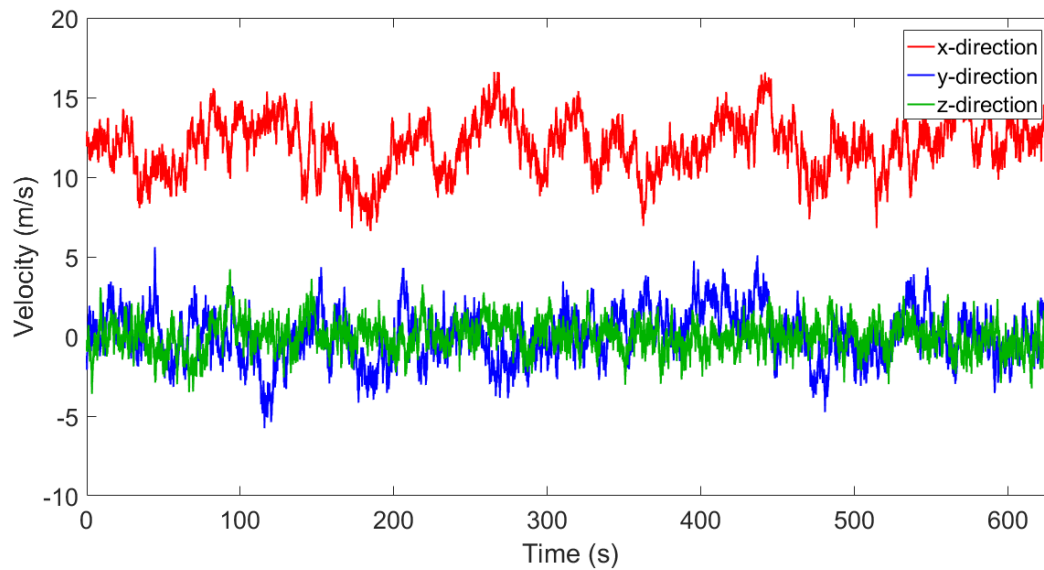


Figure 5.3: Wind field generated by TurbSim.

The hydrodynamic loads were generated by HydroDyn using an irregular JONSWAP wave spectrum with significant wave height H_s of 6 m and spectral wave period T_p of 10 s. The incident wave propagation heading was set in the x-direction, or the fore-aft direction of the OWT. No current was applied. The HydroDyn input file for this simulation is presented in Appendix A.8. A time series of the wave elevation above MSL is shown in figure 5.4.

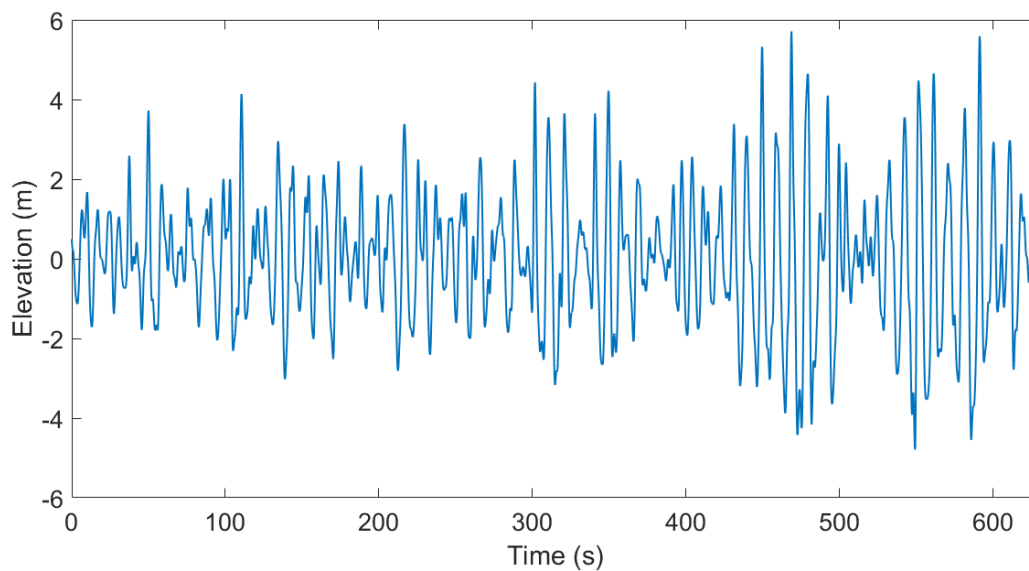


Figure 5.4: Wave elevation above sea level, generated by HydroDyn.

FAST simulations with the input described above were run for both the fixed base model and the simplified apparent fixity model. A simulation time of 630 seconds was chosen to get results from a 10 minute interval, ignoring the first 30 seconds to allow the transient effects associated with starting from rest to damp out (Jonkman and Buhl, 2005). The output time step of 0.05 s equals a sampling frequency of 20 Hz, and was chosen to make sure frequency domain processing of the time domain data would be accurate enough (der Tempel, 2006).

5.4 FAST Simulation Outputs

Large horizontal loads will act on the OWT structure, and the long tower makes the horizontal loads produce large overturning moments, especially in the foundation. The point of maximum moment is normally at a point right below the mudline, but this location is not exactly the same for different foundation models. Hence, the bending moment in the structure at the mudline is usually the major issue in the design of offshore wind turbine foundations, and will be given the most attention in the analyses in this thesis.

The highest shear forces in the structure also occur in the foundation, and the largest displacements occur at the tower top. As the applied mean wind and waves are in the x-direction, the fore-aft direction is the most excited DOF. Therefore, time histories of mudline fore-aft shear force, mudline fore-aft bending moment and tower top fore-aft displacement are shown in figure 5.5, 5.6 and 5.7, respectively.

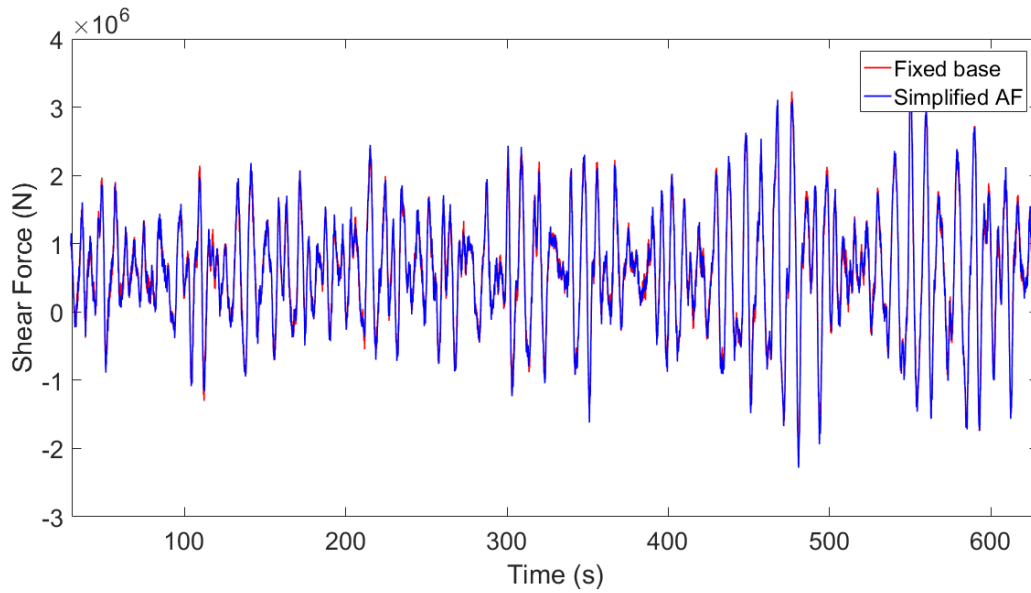


Figure 5.5: Mudline fore-aft shear force for the fixed base model and the simplified AF model.

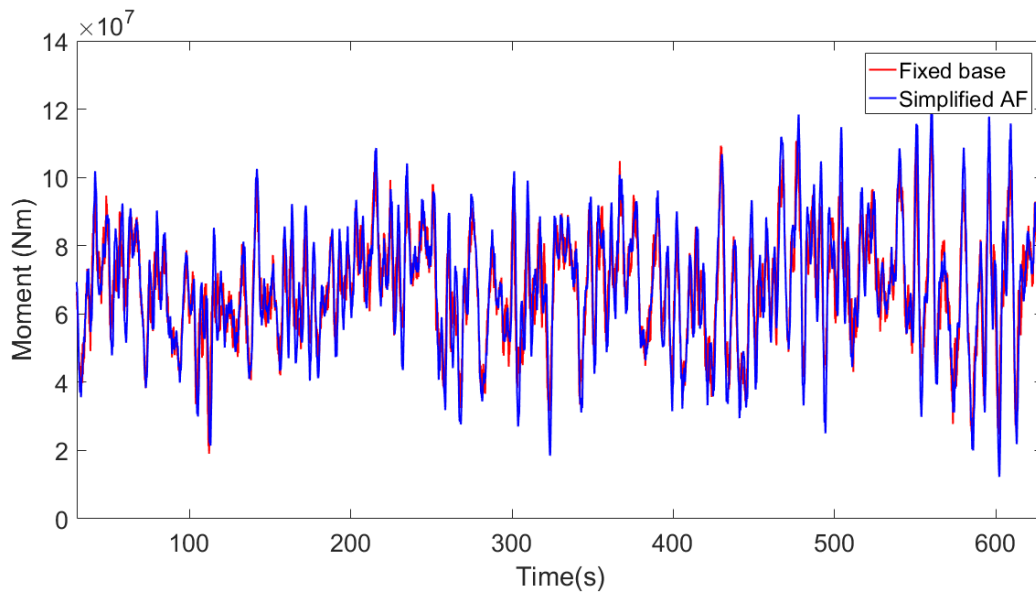


Figure 5.6: Mudline fore-aft moment for the fixed base model and the simplified AF model.

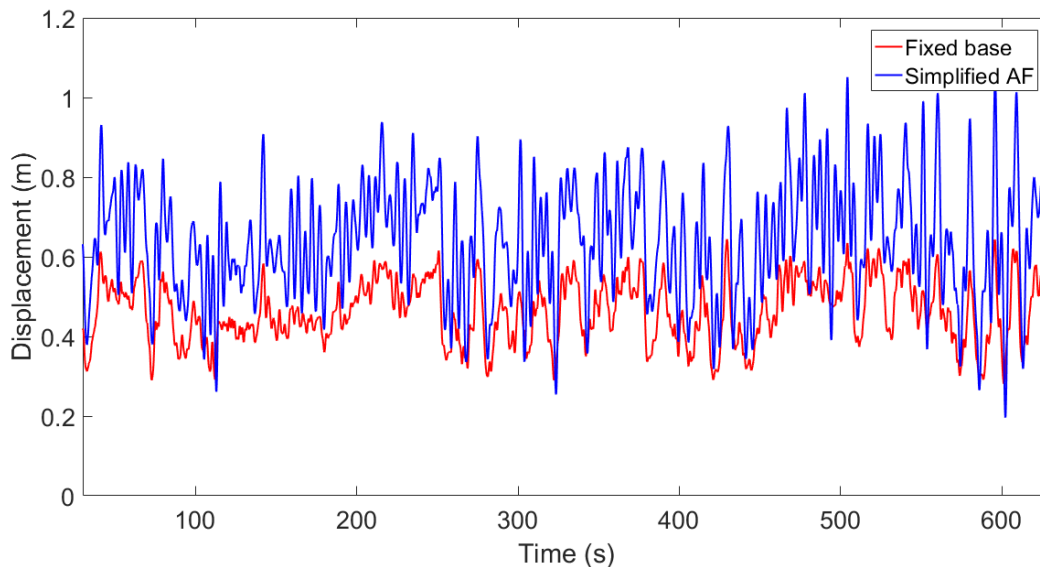


Figure 5.7: Tower top fore-aft displacement for the fixed base model and the simplified AF model.

Table 5.2: Maximum values of mudline moment, mudline shear force and tower top displacement for $U = 12$ m/s, $TI = 14\%$, $H_s = 6$ m and $T_p = 10$ s.

Foundation model	Max. Moment (MNm)	Max. Shear Force (MN)	Max. Displacement (m)
Fixed base	114.50	3.632	0.644
Simplified AF	121.10	3.555	1.056

As expected, the tower top displacement increases significantly when a flexible foundation is introduced. The plots also show higher values for the shear force and moment at mudline. One might expect forces and moments to be reduced by a softer foundation, due to less resistance of motion. However, as explained in section 2.4, a softer foundation reduces the natural frequencies of the structure and move them closer to both wave frequencies and operational frequencies. This leads to resonance effects and increased loads in the structure. In addition, an increase in tower top displacement leads to an increase in moment arm and consequently a larger mudline moment. Modelling the foundation too stiff, like the fixed base default in FAST, may give too low estimates of the forces and moments.

Looking closer on the mudline moment graphs in figure 5.8 shows large differences in structural

response between the two foundation models. Oscillations at high frequencies in addition to the oscillations at the wave frequencies are evident. The fixed base model vibrates with a high frequency, while there is less high-frequency energy seen for flexible foundation model, which is expected. A vibration period of approximately 0.4 seconds is identified for the fixed base model from the the plot in figure 5.8. This will be studied further in the next chapter.

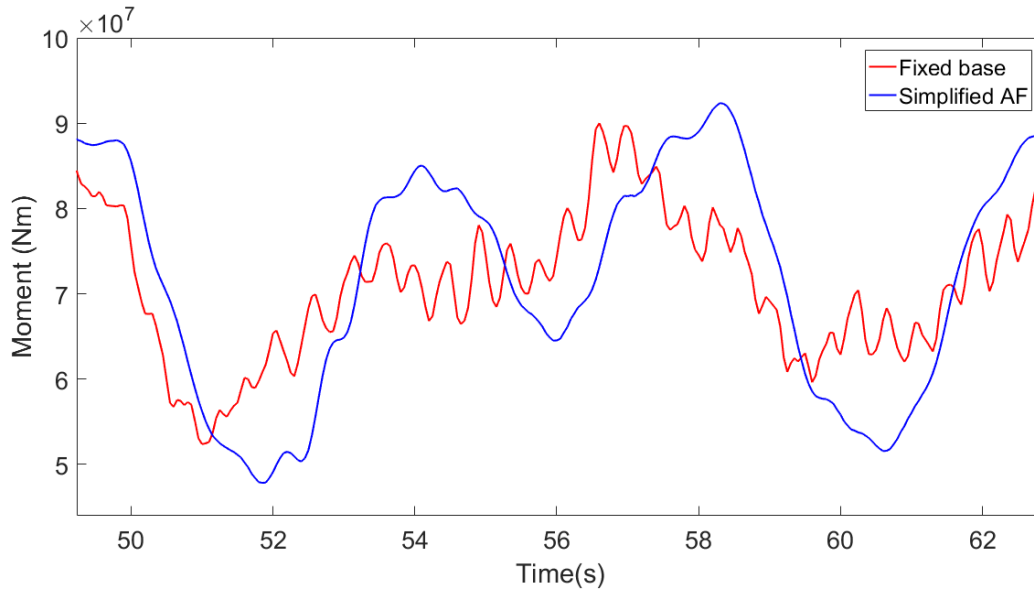


Figure 5.8: Mudline moment oscillations.

6 Improved Foundation Model

In the calculation of the properties of the apparent fixity beam, described in section 5.1, the off-diagonal terms, or cross terms, of the stiffness matrix of the soil-pile system were ignored. This approach was based on common practice of SSI of ordinary piles, where the piles normally are small and the effect of the off-diagonal terms is insignificant for the response of the whole structure. Hence, it is currently unclear whether this approach gives acceptable results for large piles like OWT monopiles. When comparing the calculated AF length and flexural rigidity to the two stiffness matrices from equation 5.1 and 5.2, it is clear that the off-diagonal terms do not match, due to the inconsistent set of equations. In this chapter, the effect of the coupled stiffness terms on the representation of foundation flexibility will be studied.

Fortunately, there are methods to accurately reproduce the whole stiffness matrix. One of them is by introducing a rigid link between the monopile and the AF beam and attach translational and rotational springs to account for the off-diagonal terms. This method is described in Carswell et al. (2015). As mentioned earlier, it is not possible to implement springs in FAST v8. Therefore, a second method was developed in this thesis, which enables to include the whole stiffness matrix in FAST v8. This was done by replacing the single AF beam with *two* beams, creating a system of three equations with three unknowns, including the off-diagonal stiffness terms in the equation system. This method allows for exact reproduction of the stiffness matrix of the monopile. The only source of inaccuracy in this method is that it uses the elastic stiffness matrix of the pile calculated with PILES; that is it ignores the minor nonlinearity of the soil. This new method of including foundation flexibility in the OWT model, referred to as the *improved apparent fixity method* or just the *improved AF method*, will be explained further and implemented in FAST in this chapter, with the purpose of studying whether it makes a significant difference in the outputs of the FAST simulation.

Instead of adding one fictive beam below the mudline, like in chapter 5, two beams were added on top of each other to be able to correctly represent the stiffness matrix of the true soil-pile system. Beam 1 is rigidly connected to a certain point below the mudline and to beam 2, which is rigidly connected to the monopile at the mudline. This configuration is shown in figure 6.1.

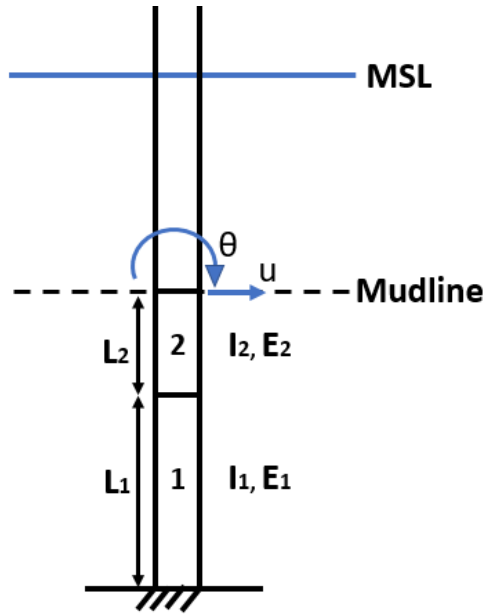


Figure 6.1: Improved apparent fixity method.

Assuming radial symmetry and neglecting the vertical and torsional DOFs, like described in section 5.1, the two-beam system is reduced to a two-dimensional system with two DOFs; deflection u and rotation θ at the mudline. There are several ways of solving this system. The chosen method consists of obtaining a flexibility matrix $[F]$ at the mudline, and comparing it to the flexibility matrix from PILES, $[F]_{PILES}$, representing the true soil-pile system. $[F]_{PILES}$ was found from the stiffness matrix from section 5.1 through the following relation:

$$[F]_{PILES} = [K]_{PILES}^{-1} = \begin{bmatrix} 6.33 \times 10^{-10} & 5.12 \times 10^{-11} \\ 5.12 \times 10^{-11} & 9.32 \times 10^{-12} \end{bmatrix} \quad (6.1)$$

To find the flexibility matrix $[F]$ of the two beam system in figure 6.1, stiffness relations for a cantilevered beam, shown in figure 6.2, were used and combined for the two DOFs. The derivation of equations 6.3, 6.4 and 6.5 is presented in Appendix D.

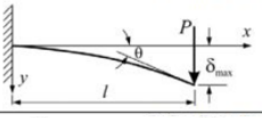
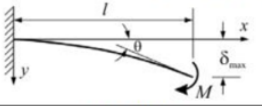
BEAM TYPE	SLOPE AT FREE END	DEFLECTION AT ANY SECTION IN TERMS OF x	MAXIMUM DEFLECTION
1. Cantilever Beam – Concentrated load P at the free end			
	$\theta = \frac{Pl^2}{2EI}$	$y = \frac{Px^2}{6EI}(3l-x)$	$\delta_{\max} = \frac{Pl^3}{3EI}$
5. Cantilever Beam – Couple moment M at the free end			
	$\theta = \frac{Ml}{EI}$	$y = \frac{Mx^2}{2EI}$	$\delta_{\max} = \frac{Ml^2}{2EI}$

Figure 6.2: Bending stiffness relations for a cantilever beam.

$$[F] = \begin{bmatrix} \delta_{uu} & \delta_{u\theta} \\ \delta_{\theta u} & \delta_{\theta\theta} \end{bmatrix} \quad (6.2)$$

where

$$\delta_{uu} = \frac{1}{E_1 I_1} \left(\frac{L_1^3}{3} + L_1^2 L_2 + L_2^2 L_1 \right) + \frac{L_2^3}{3E_2 I_2} \quad (6.3)$$

$$\delta_{u\theta} = \delta_{\theta u} = \frac{1}{E_1 I_1} \left(\frac{L_1^2}{2} + L_1 L_2 \right) + \frac{L_2^2}{2E_2 I_2} \quad (6.4)$$

$$\delta_{\theta\theta} = \frac{L_1}{E_1 I_1} + \frac{L_2}{E_2 I_2} \quad (6.5)$$

The diameter and wall thickness of the two fictive beams were kept the same as for the monopile at the mudline, 6 m and 0.06 m respectively, which implies that the area moment of inertia is known, and $I_1 = I_2 = I$. Assigning the length of the upper fictive beam L_2 to be a certain value leaves the length of the lower beam, L_1 , and the Young's modulus' of the two beams, E_1 and E_2 , as the three unknown parameters.

Comparing the flexibility matrices in 6.2 and 6.1 gives a system of three equations with three unknowns. Choosing an arbitrary value of L_2 , $L_2 = 5$ m, and solving the equation system lead to the results presented in table 6.1. The corresponding shear modulus G was also calculated for each beam, as this is required by FAST.

Table 6.1: Properties of the two AF beams.

Beam number	L (m)	d (m)	t_w (m)	I (m ⁴)	E (N/m ²)	G (N/m ²)
1	19.88	6.00	0.06	5.089	1.743×10^{12}	6.702×10^{11}
2	5.00	6.00	0.06	5.089	1.388×10^{11}	5.339×10^{10}

The new system was implemented in SubDyn as two beam members below the mudline with the properties from table 6.1 and the boundary conditions from figure 6.1. All the DOFs of the lower end of beam 1 were constrained to make it rigidly connected to a point at a distance $L_1 + L_2$ below the mudline. The procedure of including this in the SubDyn input file is described in section 5.2. The new SubDyn input file for the improved AF model can be found in Appendix E.

The assumed mode shapes that are required as input to FAST were kept the same as for the simplified AF model. This decision was based on a comparison of two analyses. A simulation of the simplified AF model with the mode shapes obtained for the fixed base model was run and compared with a simulation with updated mode shapes for the flexible model. The results showed that there was no noticeable difference in the response output for the two simulations, from which one can conclude that adjusting the assumed mode shapes is not necessary in the FAST analyses conducted in this thesis. This is a useful finding, as the procedure of updating the mode shapes, described in section 5.2, is time consuming for the researcher. This might, however, not be the case for analyses with larger differences in tower base boundary conditions.

A FAST simulation of 630 seconds was run for the improved AF method, with the same load input as presented in section 5.3; $U = 12$ m/s, $TI = 14$ %, $H_s = 6$ m and $T_p = 10$ s.

6.1 Simulation Outputs

Time series of the mudline bending moment, shear force, tower top displacement, as well as the tower top acceleration for the improved AF model, compared to the simplified AF model and the fixed base model, are plotted in figure 6.3, 6.4, 6.5 and 6.6, respectively.

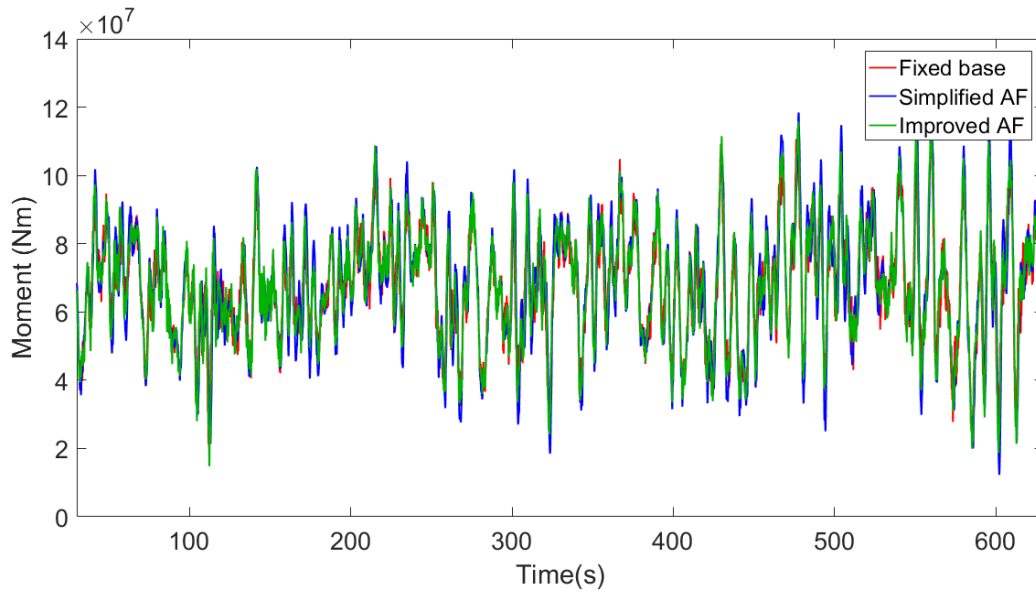


Figure 6.3: Fore-aft mudline bending moment for the three foundation models.

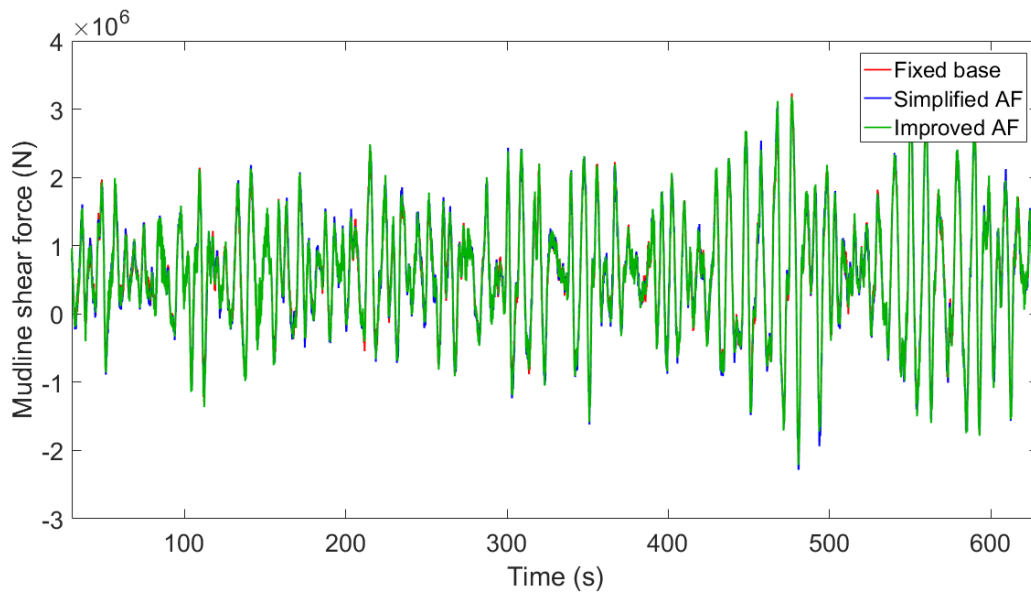


Figure 6.4: Fore-aft mudline shear force for the three foundation models.

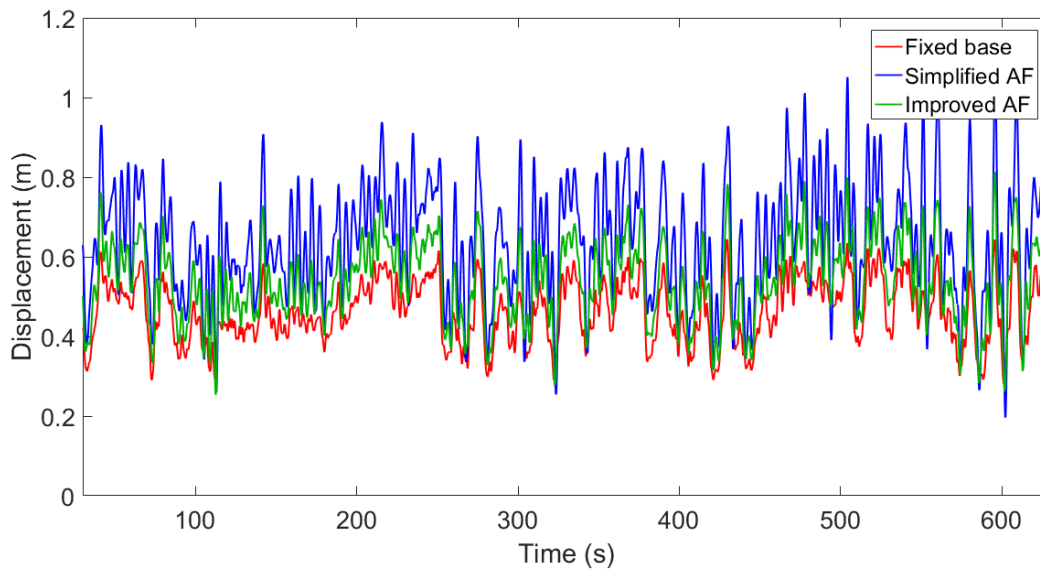


Figure 6.5: Tower top fore-aft displacement for the three foundation models.

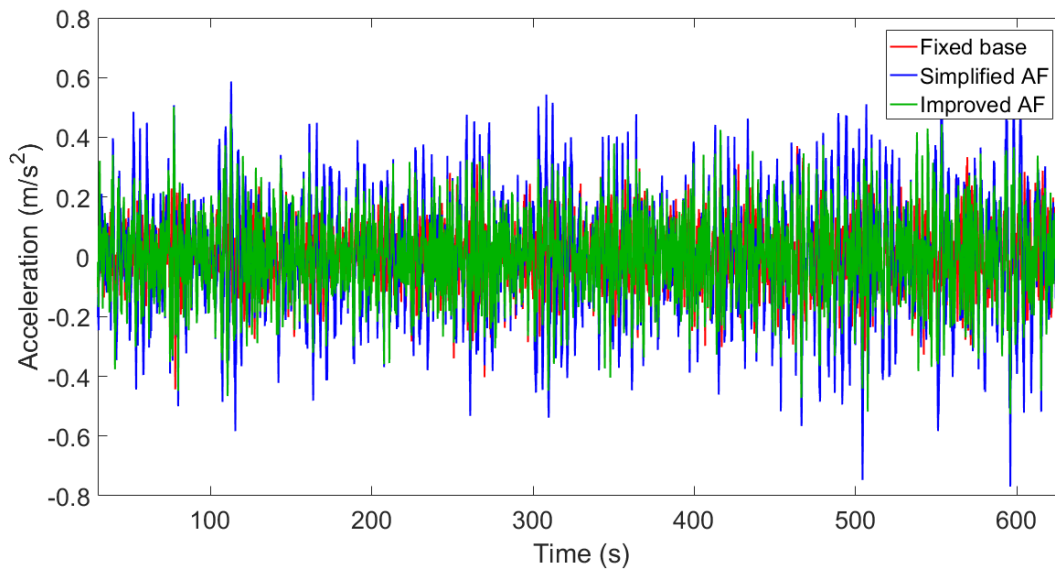


Figure 6.6: Tower top fore-aft acceleration for the three foundation models.

The plots show significant differences in response for the two flexible foundation models, especially figure 6.5 and figure 6.6. The improved AF model is much stiffer than the simplified AF model, and the behaviour of the former is closer to the fixed base model. A close-up on the mud-line moment plot in figure 6.7 shows similar response for the fixed base and the improved AF

model, but with higher vibration period and hence lower vibration frequency for the improved AF model.

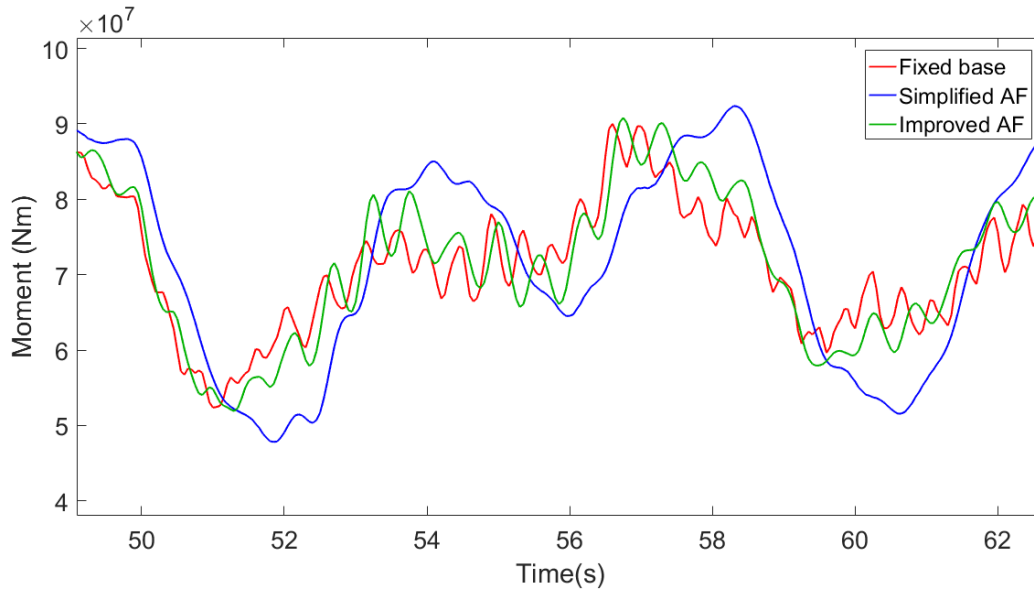


Figure 6.7: Mudline moment oscillations for the three foundation models.

From figure 6.7 it is evident how significant small adjustments in the implementation of the foundation are. Surprisingly enough, the off-diagonal terms of the soil-foundation stiffness matrix play a much more significant part than first thought, and by neglecting them you get a model that is too soft and does not represent the true behaviour of the turbine structure. The differences between a model with a fixed base and a model with foundation flexibility is no longer as great as first thought when the flexibility was modelled inaccurately in chapter 5. Using this discovery, the improved AF model will be the main focus from this point, but the simplified AF model will be brought in occasionally for comparison.

Table 6.2 lists maximum, minimum and mean values, as well as standard deviation (Std), of the moment, shear force and displacement from the FAST outputs of the three foundation models. These results underline the differences stated above, that the simplified AF method overpredicts the loads in the structure.

Table 6.2: Maximum response values for $U = 12$ m/s, $TI = 14\%$, $H_s = 6$ m, $T_p = 10$ s

Foundation model		Mudline fore-aft moment (MNm)	Mudline fore-aft shear force (MN)	Tower-top fore-aft displacement (m)
Fixed base	Max	114.50	3.632	0.644
	Mean	67.39	0.596	0.462
	Min	19.05	-2.104	0.280
	Std	15.30	0.813	0.079
Simplified AF	Max	121.10	3.555	1.056
	Mean	67.87	0.595	0.641
	Min	12.29	-2.283	0.196
	Std	17.87	0.833	0.143
Improved AF	Max	115.80	3.616	0.813
	Mean	67.62	0.596	0.540
	Min	14.79	-2.216	0.253
	Std	16.29	0.824	0.102

6.2 Power Spectral Densities

To validate the three foundation models and compare their dynamic response, it is convenient to obtain the full system natural frequencies from FAST simulations and evaluate whether they are reasonable. These natural frequencies can then be compared to the natural frequencies calculated by BModes for the fixed base and the simplified AF model in table 5.1. An important fact when identifying and comparing the natural frequencies is that the RNA is modelled rigidly in BModes, but flexible in FAST. This coupling between the rotor and tower is especially important for the second tower bending modes, and will make the frequencies from BModes differ from the true full system natural frequencies with the flexible RNA from FAST (NWTC, 2017).

Earlier versions of FAST had a linearization functionality which was used to obtain the natural frequencies. FAST v8 does not support linearization, and hence, the preferred method of identifying the natural frequencies of the models is to compute the PSD by performing a FFT of a FAST output time series. The peaks in the spectrum correspond to the natural frequencies of the OWT model.

To get clear peaks in the PSD for the natural frequencies, it is convenient to excite the structure with white noise only. White noise excitation has a constant spectral density (Newland, 2005), which means that the applied load frequency will not disturb the natural frequency peaks in the spectrum. In the FAST input file, the wind field was disabled, the wave spectrum in HydroDyn was set to *irregular white noise spectrum*, and second order waves were disabled to ensure that the white noise waves have equal energy across all frequencies (NWTC, 2017).

630 seconds FAST simulations were run for both the fixed base, the simplified AF and the improved AF model with the new load input of white noise. The response time series of the fore-aft tower top displacement and fore-aft mudline moment were used for the analysis. The PSDs were obtained using Welch method, explained in section 2.5.1, through MATLAB's *cpsd* function. The results are plotted on logarithmic axes in figure 6.8 and 6.9.

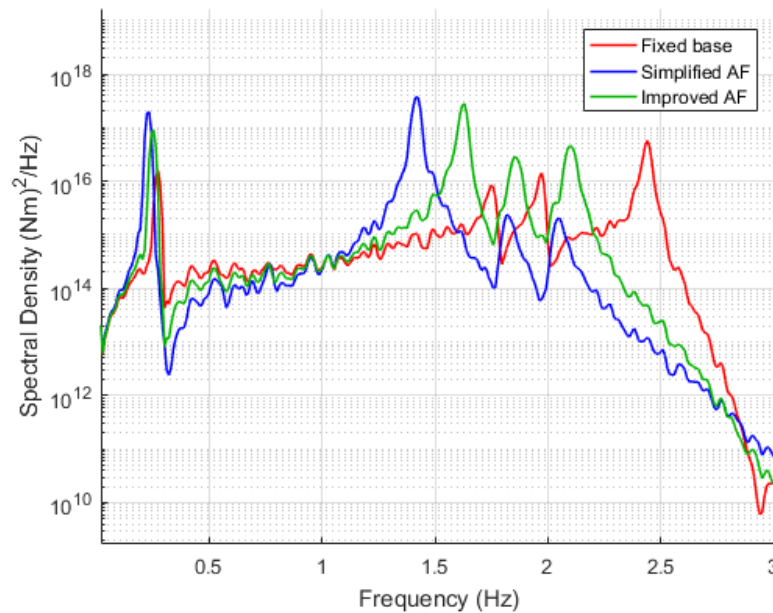


Figure 6.8: PSD from fore-aft mudline moment for the fixed base model, the simplified AF model and the improved AF model.

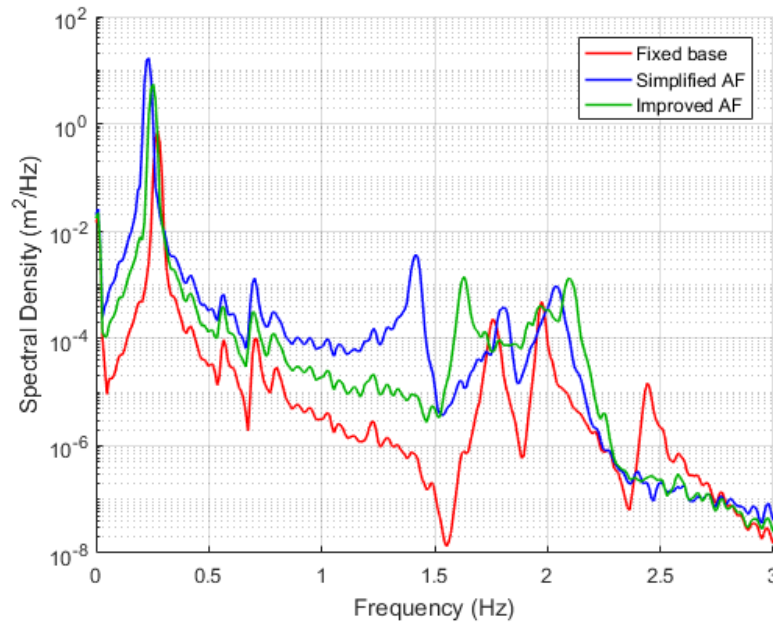


Figure 6.9: PSD from fore-aft tower top displacement for the fixed base model, the simplified AF model and the improved AF model.

The peaks in the PSD plots coincide well with what is expected from the output time series in the previous section, and underline that the improved AF model's structural dynamic response, and hence structural stiffness and natural frequencies, is between the fixed base model and the simplified AF model. The fixed base model has more high frequency contents than the two flexible models. One peak at ≈ 2.4 Hz is clearly visible in the PSD for the fixed base model, exactly at the frequency of the oscillations seen in the mudline moment time series of period ≈ 0.4 s, seen in figure 5.8 and 6.7. It has been confirmed by Jason Jonkman in NWTC (2017) that the fixed base NREL 5MW OWT is expected to have a second tower bending mode at around 2.4 Hz, representing this period of 0.4 s.

There are clearly visible peaks close to the first natural frequencies of the simplified AF model and the fixed base model calculated by BModes, listed in table 5.1. As mentioned above, the different coupling between the rotor and the tower in BModes and FAST is more important for the second tower bending modes than the first, and explains why the higher frequency peaks in the PSD plots differ from the second tower bending frequencies from BModes. Disabling the DOFs in the rotor, drivetrain and nacelle of the FAST model before running a simulation will move the frequency peaks of the second tower modes closer to the values from BModes. However, as the real RNA is flexible, as modelled in FAST, correct natural frequencies of the full system are the ones obtained

through the peak picking method in the PSD plots from the FAST outputs, which are listed in table 6.3. Note that even though the maximum values of moment, shear force and displacement from table 6.2 were close for the fixed base and the improved AF model, the natural frequency of the second tower fore-aft bending mode is significantly lower for the latter.

Table 6.3: Natural frequencies and corresponding periods from peaks in fore-aft moment PSD plot (figure 6.8).

	Fixed base model		Simplified AF model		Improved AF model	
	Frequency (Hz)	Period (s)	Frequency (Hz)	Period (s)	Frequency (Hz)	Period (s)
1	0.273	3.658	0.234	4.266	0.254	3.939
2	1.748	0.572	1.416	0.706	1.631	0.613
3	1.973	0.507	1.816	0.551	1.855	0.539
4	2.441	0.410	2.051	0.488	2.100	0.476

To further validate the models, study their structural behaviour and make sure they represent the same operational state, the operational natural frequencies are studied. To identify the operational natural frequencies of the models, moment in one of the blade roots and in the yaw bearing was extracted from the output files of the FAST simulations with the load input from section 5.3. The yaw bearing is the connection between the nacelle and the tower, a position which is highly affected by rotor frequency. PSDs were obtained from these moment time series, and are plotted in figure 6.10 and figure 6.11.

In chapter 4, the operational natural frequency 1P of the NREL 5MW OWT operating at 12.1 rpm was calculated to be 0.202 Hz. In figure 6.10, a peak at rotor frequency 1P = 0.202 Hz is evident, along with 2P, 3P, 4P etc due to a phenomenon called Doppler frequency shifting. In short, this frequency shifting is due to circular motions, called eddies, in the turbulent wind flow. The rotor period is often shorter than the time taken for an eddy to pass through the rotor plane, which means that the rotor will periodically sample the eddy with each rotation until the eddy has passed. This phenomenon is described in detail in Halfpenny (1998).

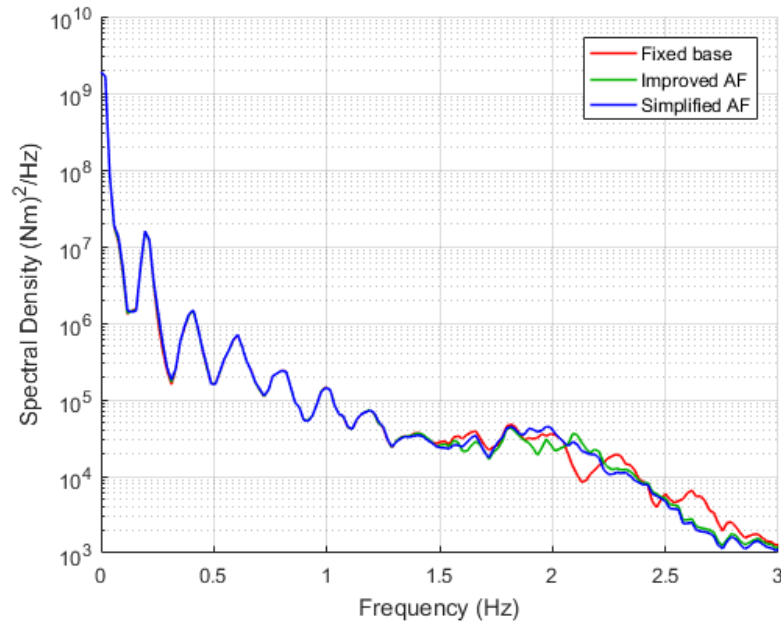


Figure 6.10: PSD of blade root out-of-plane moment.

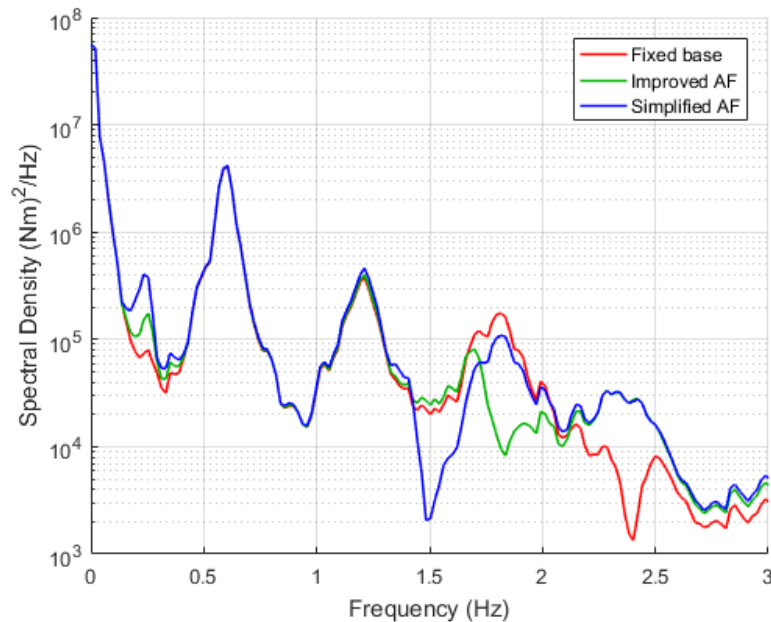


Figure 6.11: PSD of nonrotating yaw bearing pitch moment.

Figure 6.11 shows the frequencies the tower is experiencing from the blade passing frequency. The peak at ≈ 0.6 Hz represents $3P$, the next peak equals $6P$, then $9P$, and so on. These frequency peaks

are due to three blades passing the turbulent eddies with each rotation, leading to a thrust force in the tower with three times the rotor frequency. Figure 6.10 and 6.11 prove that the three models represent the same operational state.

6.3 Response to Different Wave Periods

In this section, the effect of changing the wave spectral peak period is studied. Since the operational natural periods and the first structural natural periods of the OWT are not too far from wave periods, it is relevant to investigate how increasing and decreasing wave periods affect the structural response. In addition to the simulations from section 6.1, with $H_s = 6$ m and $T_p = 10$ s, FAST simulations were run with $T_p = 15$ s and $T_p = 5$ s, where the latter equals the operational natural period. The wave spectrum and the wind field were kept the same as described in chapter 5, and $H_s = 6$ m. The combination of a large 6 m wave with a short 5 s period is not realistic, but H_s was unchanged to focus on the response to changing wave periods and to reveal potential differences between the foundation models more clearly. The mudline fore-aft bending moment and the tower top fore-aft displacement is plotted on axes with the same scale in figure 6.12, 6.13 and 6.14 for $T_p = 15$ s, $T_p = 10$ s and $T_p = 5$ s, respectively.

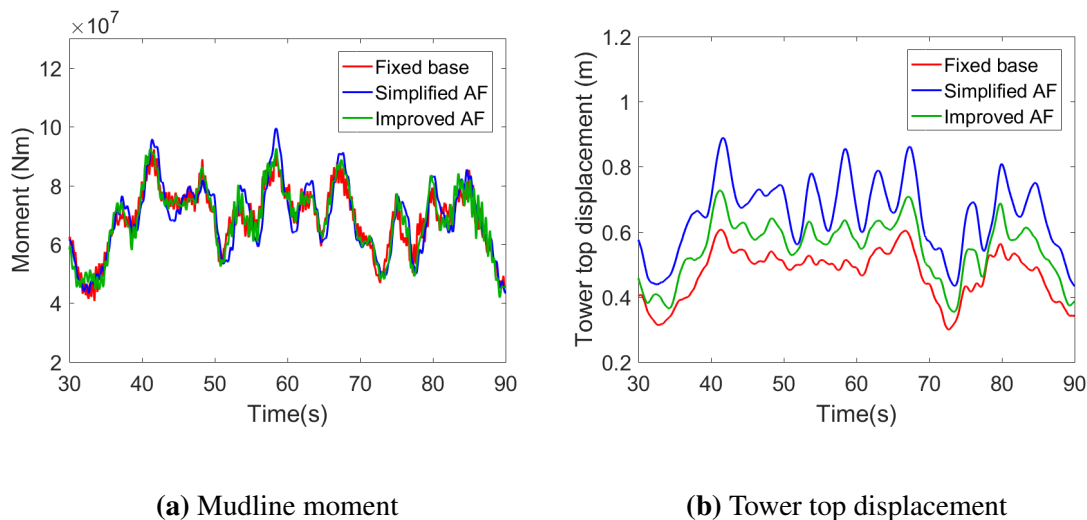


Figure 6.12: Mudline moment and tower top displacement for $H_s = 6$ m and $T_p = 15$ s.

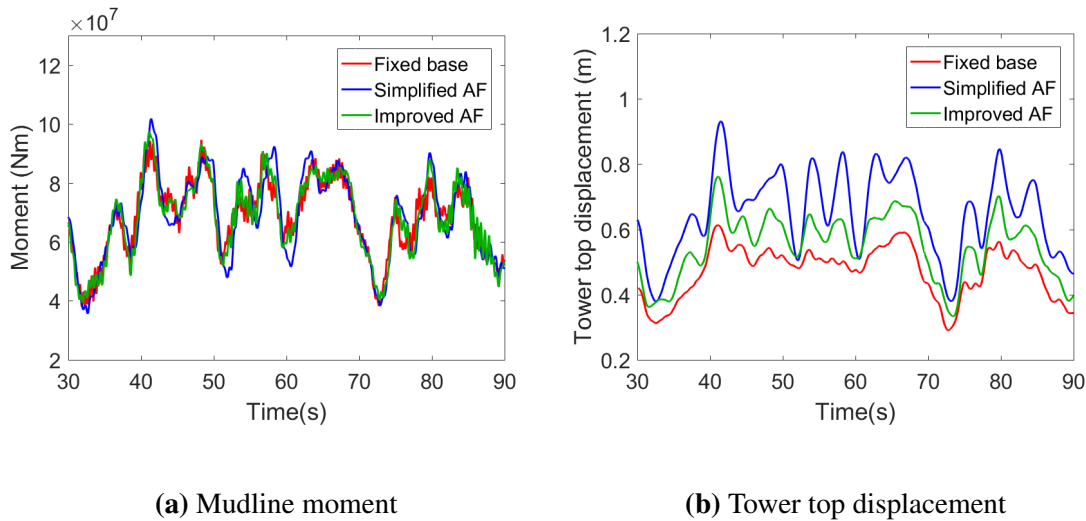


Figure 6.13: Mudline moment and tower top displacement for $H_s = 6$ m and $T_p = 10$ s.

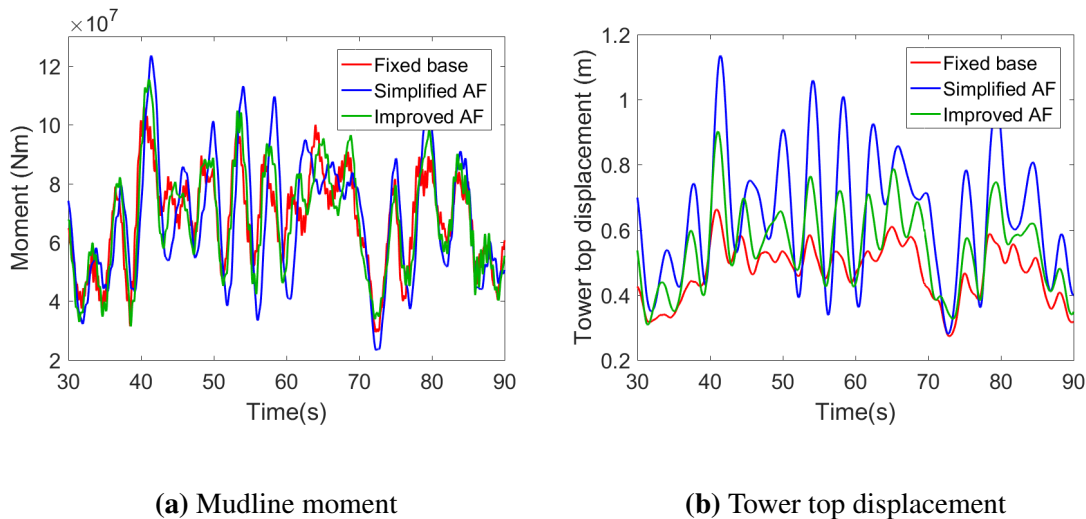


Figure 6.14: Mudline moment and tower top displacement for $H_s = 6$ m and $T_p = 5$ s.

The plots reveal that large resonance effects are present for all three foundation models when the wave period is decreased towards the operational and structural natural frequencies. This resonance effect was investigated further for the improved AF model. A new FAST simulation was run with wave spectral peak period equal to the exact value of the first natural period of the structure, $T_p = 3.939$ s, taken from table 6.3. The rest of the input parameters were the same as before. The structural response of the improved AF model for this wave period, along with the wave periods presented above, is plotted in figure 6.15.

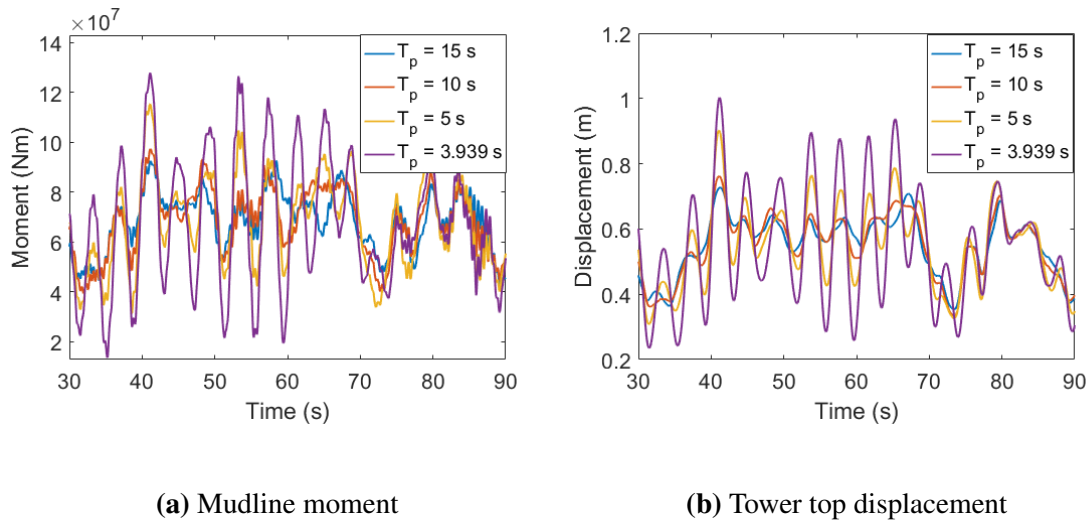


Figure 6.15: Mudline moment and tower top displacement for simulations of the improved AF model with various T_p .

Figure 6.15 show significant amplification of the response when the wave period is reduced to the OWTs natural period. Even a small reduction from 5 s to 3.939 s yields a large change. When T_p is decreased from 15 s to 5 s, the maximum mudline moment from the 90 seconds simulation is increased from 92.64 MNm to 115.4 MNm. Reducing T_p further to 3.939 s gives a maximum moment of 127.8 MNm. Equivalently, the maximum tower top displacement is increased from 0.727 for $T_p = 15$ s to 1.003 m for $T_p = 3.939$ s.

Firstly, these results underline the importance of designing OWT structures to have natural frequencies that do not coincide with wave frequencies, which was discussed in section 2.2.3 and shown in figure 2.3. Secondly, it underlines the importance of correct foundation modelling to ensure that the natural frequencies of the OWT structure are present in the simulations. This is especially important for short wave periods.

7 Sensitivity Analyses of a Monopile

Researchers believe that monopile foundations used for today’s OWTs have overly conservative designs due to lack of research on the topic (Kaynia, 2017). Increased focus on correct foundation modelling in OWT analyses and simulation codes can lead to more reliable models supporting the reduction of foundation dimensions and hence large cost reductions.

In this chapter, sensitivity analyses of the NREL 5MW monopile foundation with different dimensions are presented. The subsoil length and the pile wall thickness were changed to study their effects on the structural response. The new foundation properties were implemented in SubDyn using the improved AF method, and a 10 minutes FAST simulation with $U = 12\text{m/s}$, $TI = 14\%$, $H_s = 6\text{ m}$ and $T_p = 10\text{s}$ was run for each model. The regular monopile with pile wall thickness $t_w = 0.06\text{ m}$ and pile length $L = 36\text{ m}$ modelled through the improved AF method will from now on be referred to as the *regular monopile* or just the *monopile*.

7.1 Shorter Pile

Two new foundation models were simulated in this section; one where the monopile length was reduced to 26 m and one with a monopile length of 16 m. The rest of the OWT model and the soil profile were kept the same as before. Implementing the new lengths in PILES gave the stiffness coefficients in table 7.1, presented together with the values for the original 36 meter pile for comparison.

Table 7.1: Stiffness coefficients from PILES for different pile lengths.

Pile length	k_{uu} (N/m)	$k_{u\theta}$ (N/rad)	$k_{\theta\theta}$ (Nm/rad)
36 m	2.84×10^9	-1.56×10^{10}	1.93×10^{11}
26 m	2.80×10^9	-1.54×10^{10}	1.91×10^{11}
16 m	2.69×10^9	-1.56×10^{10}	1.88×10^{11}

Table 7.1 show that even with large reductions in pile length, the stiffness at the mudline is almost unchanged. Consequently, the properties of the fictive AF beams below the mudline will not

change significantly for the three models. Nevertheless, the improved AF properties were calculated from the stiffness values, keeping I constant and setting $L_2 = 5$ m as before, and presented in table 7.2.

Table 7.2: Improved AF properties corresponding to different monopile lengths.

Pile length	AF beam	L (m)	d (m)	t_w (m)	I (m ⁴)	E (N/m ²)	G (N/m ²)
36 m	1	19.88	6.00	0.06	5.089	1.743×10^{12}	6.702×10^{11}
	2	5.00	6.00	0.06	5.089	1.388×10^{11}	5.339×10^{10}
26 m	1	19.94	6.00	0.06	5.089	1.731×10^{12}	6.658×10^{11}
	2	5.00	6.00	0.06	5.089	1.375×10^{11}	5.289×10^{10}
16 m	1	18.98	6.00	0.06	5.089	1.201×10^{12}	4.618×10^{11}
	2	5.00	6.00	0.06	5.089	1.344×10^{11}	5.169×10^{10}

Only very small differences in AF properties are seen for the 26 m pile compared to the 36 m pile, which is expected to give no noticeable effect on the response. For the 16 meter pile, the properties differ more, but still just slightly, considering that the pile length is reduced by 20 meters, more than half of its original length. The AF properties were implemented in SubDyn and FAST simulations of the three models were run. The mudline fore-aft bending moment and the tower top fore-aft displacement are plotted in figure 7.1 and 7.2.

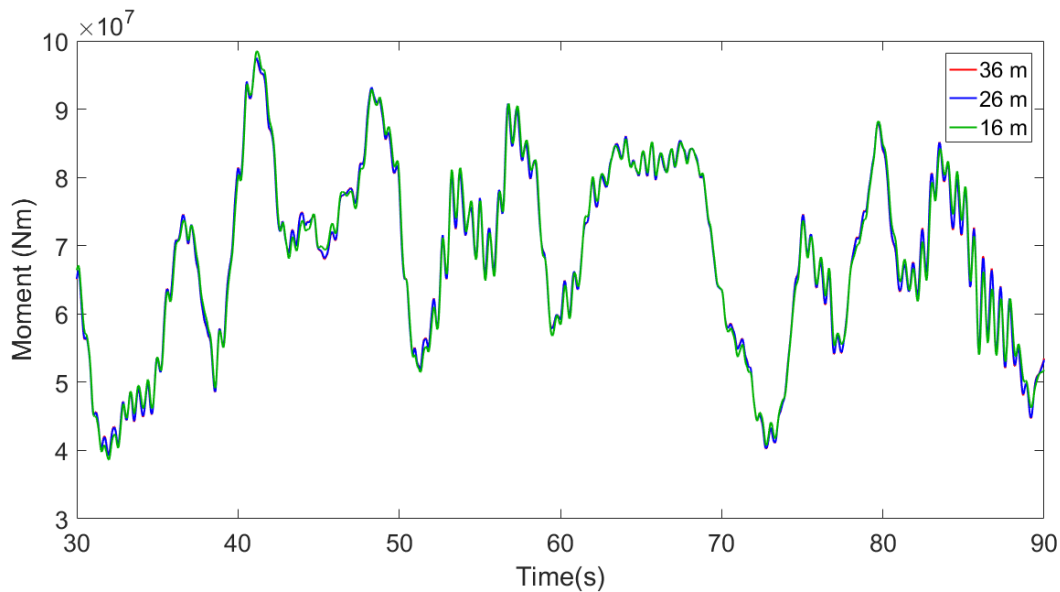


Figure 7.1: Fore-aft mudline moment for models with different monopile lengths.

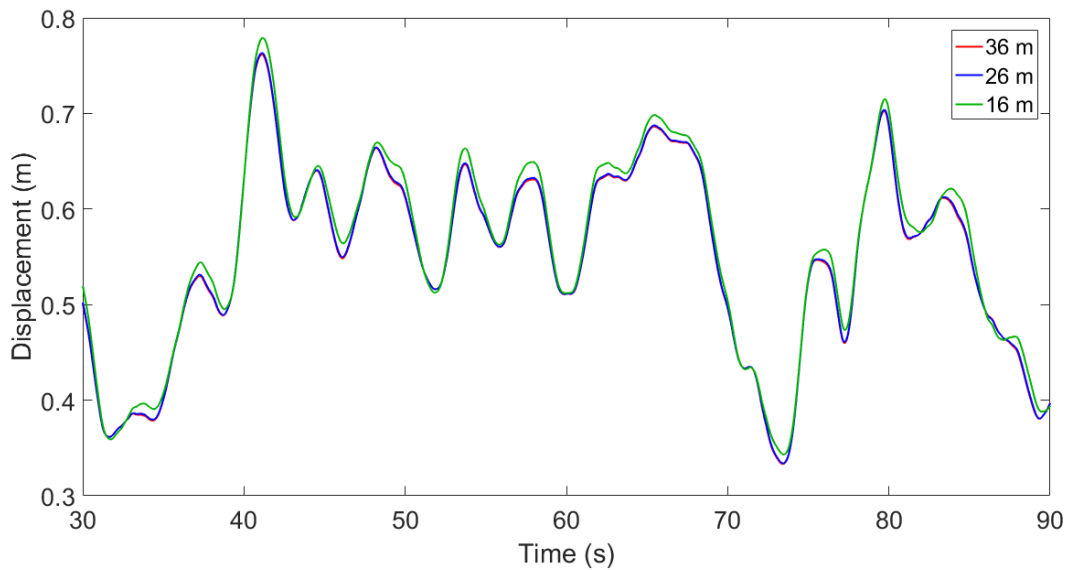


Figure 7.2: Fore-aft tower-top displacement for models with different monopile length.

Figure 7.1 and 7.2 prove the final point that reductions in monopile lengths do not make a large difference in the structural dynamic response obtained from FAST simulations. The 26 meters pile does not give any change at all, while the 16 meters pile give slightly larger displacements and moments. The 10 minute analysis gave a maximum moment of 116.3 MN for the 16 m model, compared to 115.8 for both the 26 m and the 36 m models. However, this result does not imply directly that the pile can be designed to be 26 or 16 meters instead of 36 meters, which would be very economically favorable. In addition to structural response, the capacity has to be taken into account; the pile need to be able to carry the weight of the whole turbine with sufficient safety margin. The soil capacity and plastic deformations of the soil are not taken into account, and a monopile without sufficient length may sink, slip or tip over. Capacity analysis is a geotechnical issue and is out of the scope of this thesis. But the result from this section is a step in the optimization of OWT foundations.

The effect on the fatigue life of shortening the pile to 16 m will be studied in chapter 9.

7.2 Smaller Pile Wall Thickness

Two new models of the monopile were simulated; one where the wall thickness was changed from $t_w = 0.06$ m to $t_w = 0.05$ m, and one with $t_w = 0.04$ m. The flexural rigidity EI of the pile, which is required as input to PILES, changes with wall thickness. Reducing the thickness to 0.05 m, i.e. reducing it by 1/6, means that I is reduced by approximately 1/6, and hence, since E is constant for the material, EI is reduced by approximately 1/6. Equally, when t_w is reduced by 1/3, EI is reduced by 1/3. The flexural rigidities for the reduced wall thickness models become:

$$EI_{t_w=0.05} \approx EI_{t_w=0.06} \times \frac{5}{6} = 1.05 \times 10^{12} \text{ Nm}^2 \times \frac{5}{6} = 8.75 \times 10^{11} \text{ Nm}^2 \quad (7.1)$$

$$EI_{t_w=0.04} \approx EI_{t_w=0.06} \times \frac{2}{3} = 1.05 \times 10^{12} \text{ Nm}^2 \times \frac{2}{3} = 7.00 \times 10^{11} \text{ Nm}^2 \quad (7.2)$$

The pile diameter, pile length and the rest of the pile and soil properties were kept the same as described in section 5.1. The axial rigidity EA of the pile will also change with reduced t_w , but this has no effect as the vertical motions are insignificant. Reduced wall thickness will affect the performance of the pile, with buckling being the main concern. This is not considered in the following analyses, but should be studied together with the analyses done in this thesis when considering a wall thickness reduction, as it may lead to a high probability of buckling.

Since the thickness of the monopile at the mudline is decreased, the thickness of the rest of monopile above the mudline should be adjusted accordingly. As it would be neither convenient nor realistic to construct a monopile with a sudden drop in wall thickness from 0.06 m to 0.05 m or 0.04 m at the mudline, it was decided to set the whole substructure wall thickness equal to the foundation wall thickness. The tower dimensions above the TP were unchanged. The new pile properties were implemented in PILES, and the resulting stiffness coefficients for the three models are presented in table 7.3.

Table 7.3: Stiffness coefficients from PILES for different pile wall thickness.

Pile wall thickness	k_{uu} (N/m)	$k_{u\theta}$ (N/rad)	$k_{\theta\theta}$ (Nm/rad)
$t_w = 0.06$ m	2.84×10^9	-1.56×10^{10}	1.93×10^{11}
$t_w = 0.05$ m	2.74×10^9	-1.43×10^{10}	1.68×10^{11}
$t_w = 0.04$ m	2.61×10^9	-1.28×10^{10}	1.43×10^{11}

The improved AF properties were calculated from the stiffness values in table 7.3, keeping I constant and setting $L_2 = 5$ m, as before. The calculated improved AF properties are presented in table 7.4.

Table 7.4: Improved AF properties corresponding to piles with different wall thicknesses.

Pile wall thickness	AF beam	L (m)	d (m)	t_w (m)	I (m ⁴)	E (N/m ²)	G (N/m ²)
$t_w = 0.06$ m	1	19.88	6.00	0.06	5.089	1.743×10^{12}	6.702×10^{11}
	2	5.00	6.00	0.06	5.089	1.388×10^{11}	5.339×10^{10}
$t_w = 0.05$ m	1	19.23	6.00	0.05	4.241	1.886×10^{12}	7.254×10^{11}
	2	5.00	6.00	0.05	4.241	1.419×10^{11}	5.459×10^{10}
$t_w = 0.04$ m	1	18.98	6.00	0.04	3.396	2.239×10^{12}	8.612×10^{11}
	2	5.00	6.00	0.04	3.396	1.479×10^{11}	5.687×10^{10}

These properties were implemented in the SubDyn input file, and FAST simulations were run. The SubDyn input file for the model with $t_w = 0.05$ m is presented in Appendix F. The time series from 30 to 90 seconds of mudline moment and tower top displacement are plotted in figure 7.3 and 7.4.

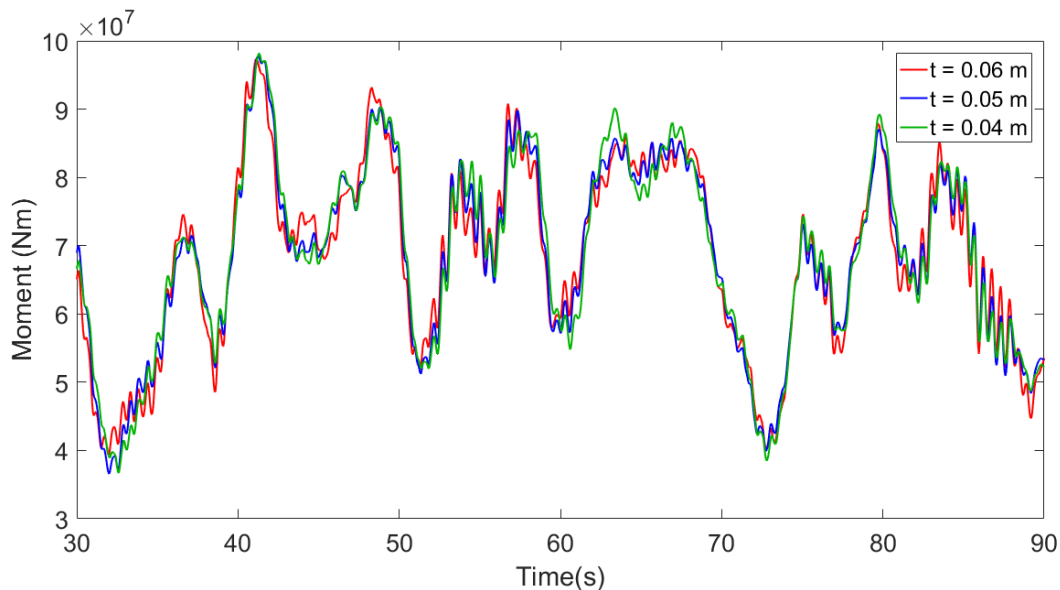


Figure 7.3: Fore-aft mudline moment for the models with different wall thickness.

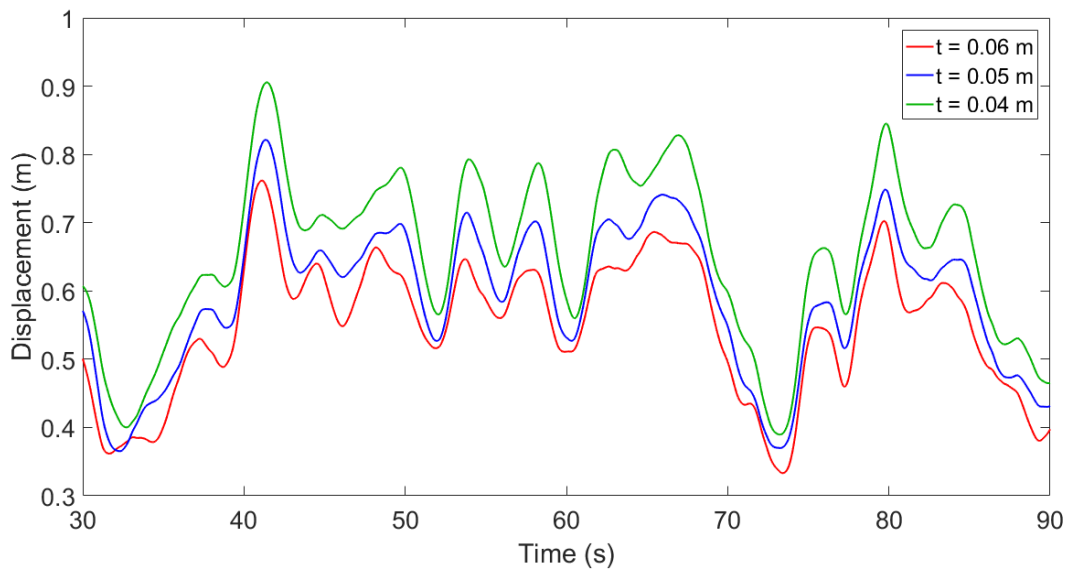


Figure 7.4: Tower top fore-aft displacement the models with different pile wall thickness.

The plots show small differences in mudline bending moment and in tower top displacement. Even though the differences in moment are not very large, it represents a great difference in bending stress, due to the reduction of I . This is seen from the flexure formula:

$$\sigma_b = \frac{M}{I}y \quad (7.3)$$

where M is the bending moment occurring in a cross section with outer radius y . The maximum values for the tower top displacement and mudline bending moment from the simulations above are listed in table 7.5, along with the maximum bending stresses at the mudline, calculated from equation 7.3. The percentage differences between the reduced thickness models compared to the regular monopile are also presented.

Table 7.5: Maximum response values from FAST simulations of the models with different pile wall thickness.

Wall thickness	Tower top displacement		Mudline moment		Mudline stress	
	Max value (m)	%	Max value (MNm)	%	Max value (MPa)	%
$t_w = 0.06$ m	0.813	0.0	115.8	0.0	68.4	0.0
$t_w = 0.05$ m	0.901	+10.8	116.7	+0.8	82.6	+20.8
$t_w = 0.04$ m	1.013	+24.6	120.0	+3.6	106.0	+55.0

Table 7.5 underlines how large effect reduced wall thickness has on the bending stress in the structure. This will definitely have a high impact on the fatigue damage of the structure, a topic that will be studied in chapter 9. Figure 7.5 shows PSDs of the smaller wall thickness model compared to the original model, which underlines the softer behaviour.

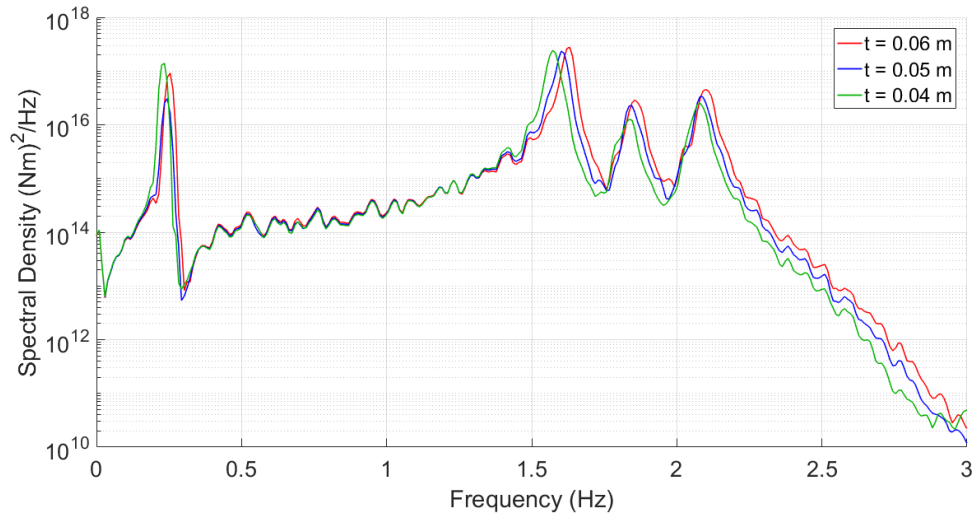


Figure 7.5: PSD from mudline fore-aft bending moment for the models with different wall thickness.

8 Suction Caisson Foundations

Modelling of a new foundation type is introduced in this chapter, with the purpose of comparing the dynamic response and fatigue life of different foundation concepts and dimensions. Even though the monopile is the most common foundation type, other alternative foundation concepts are currently being developed, the main ones introduced in section 2.3. As the turbine sizes and water depths increase, production and installation of large-diameter monopiles becomes more challenging and requires heavy installation vessels and equipment. The suction caisson, also called *suction bucket* or *monopod*, is a newer alternative originally developed for the foundation of offshore oil platforms. It has the advantages of being easy to install and remove, is suitable for deeper water depths up to 55 meters, and requires less steel than a comparable monopile.

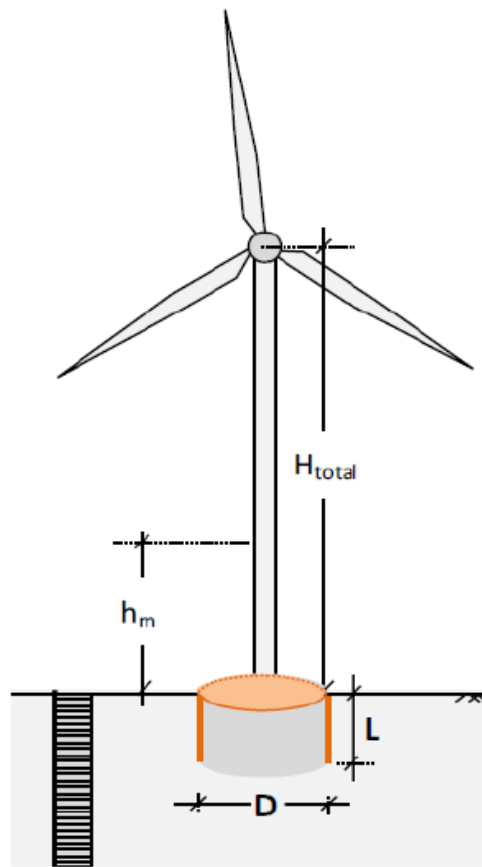


Figure 8.1: Illustration of an OWT with caisson foundation.

The suction caisson is a cylindrical skirted foundation, attached to the base of the monopile and partially inserted into the seabed. It consists of a circular top plate whose capacity is enhanced by peripheral embedded skirts which confine the internal soil, see figure 8.2. The caisson is driven into the seabed by means of self-weight and by pumping out the water trapped inside it. The induced pressure difference creates suction, attracting the bucket lid downwards into the soil like a plug (Kourkoulis et al., 2014). After installation it behaves as a skirted gravity foundation that utilizes the friction between the skirts and the soil, as well as the mass contained within the bucket to remain stable. In deep waters, three or four smaller caissons may be favourable for supporting one OWT, called tripod and quadripod. This thesis will focus on a one caisson foundation.

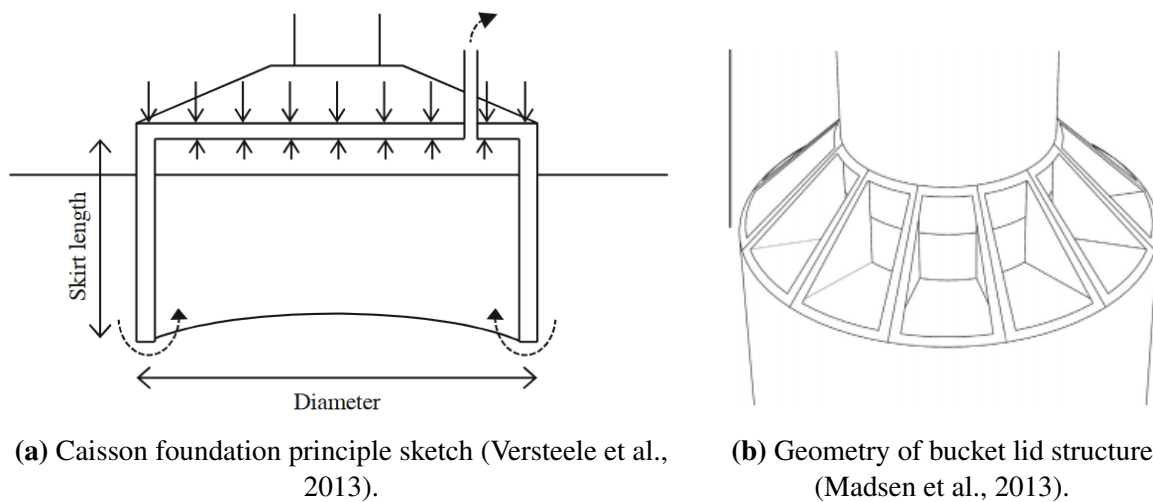


Figure 8.2: Caisson foundation geometry.

The first prototype of the monopod was installed in 2002 in Fredrikshavn, supporting a 3MW Vestas V90 turbine in 4 meters water depth. To further demonstrate that the monopod foundation could be successfully installed offshore, prototypes supporting meteorological masts have been installed at the Horns Rev 2 offshore project (2009) and the Dogger Bank project (2013). The Fredrikshavn and Horns Rev 2 caisson had a diameter of 12 meters, a skirt length of 6 meters and a weight of 165 tonnes, while the Dogger Bank caisson had a diameter of 15 meters and a skirt length of 7.5 meters (Nielsen, 2014), (Nielsen, 2013).

8.1 Sensitivity Analyses of Caisson Foundations

In this section, simplified models of caisson foundations with different dimensions supporting the NREL 5MW will be implemented in FAST. As discussed earlier, a reduction in foundation dimensions will be highly favourable in cost reducing the offshore wind industry. Therefore, sensitivity analyses consisting of varying the diameter and depth of the caisson will be presented.

In order to model the caisson foundations, the same approach was used as for the monopile; First, the soil-foundation properties were presented by a stiffness matrix at the mudline, obtained from a geotechnical software, followed by representing this flexibility through the improved AF method.

The same soil profile as in chapter 5 and 6 was used. Instead of using the software *PILES*, which was created for cylindrical piles, a program called *G123* (Tassoulas, 1981) was used to obtain the mudline stiffness matrix of the soil-bucket system. The required inputs to *G123* are the radius of the caisson, mass density ρ , shear modulus G , Poisson's ratio ν and damping of both the soil layers and the foundation. *G123* assumes the foundation to be a solid shallow footing, implying that the input properties have to be set to include the soil confined by the bucket skirts. Ideally, a FE model of the caisson should be made to obtain the representative properties. However, previous analyses of caisson foundations show that they turn out to be very stiff, almost perfectly rigid, due to the internal stiffeners and incompressible soil in the compartments (Kaynia, 2017). With that in mind, the shear modulus G of the caisson was set as 1000 times larger than the shear modulus of the upper soil layer surrounding it, namely 4.26×10^7 and 4.26×10^{10} . The density of the bucket was set to 2500 kg/m^3 .

It was assumed that the caisson foundation is directly and rigidly connected to the substructure of the NREL 5MW at the mudline. That is, possible stiffeners between the caisson and the monopile were not considered, implying the loads experienced at the mudline will be directly transferred to the pile with the same dimensions as the original monopile. The rest of the OWT above the foundation was kept exactly the same as the original model.

Since the caisson foundation industry is still in its early phase, there are no indicative numbers on the dimensions of a monopod designed for a large turbine like the NREL 5MW. Also, the properties of the caisson highly depends on the seabed conditions on the site. Researchers claim that diameters of up to 16-18 meters would be required for a 8MW turbine in 55 metre waters (Hill, 2015).

As a starting point, in order to compare the caisson foundation to the previous modelled monopile foundation models, it is convenient to obtain a reference model that exhibit similar response as the standard monopile. Hence, analyses of caissons with different dimensions were run in G123 to find a size that lead to a mudline stiffness approximate to the monopile. A caisson foundation with diameter $D_c = 10$ m and depth $L_c = 5$ m turned out to be a suitable reference model, which is emphasized in figure 8.3. Two caissons with the dimensions of the monopod prototypes described in the previous section, namely $12\text{ m} \times 6\text{ m}$ and $15\text{ m} \times 7.5\text{ m}$, were also modelled. The mudline stiffness coefficients for the caisson models, calculated from G123, are listed in table 7.1.

Table 8.1: Stiffness coefficients from G123 for different caisson dimensions.

Caisson dimensions	k_{uu} (N/m)	$k_{u\theta}$ (N/rad)	$k_{\theta\theta}$ (Nm/rad)
$15 \times 7.5\text{ m}$	5.54×10^9	-2.96×10^{10}	5.05×10^{11}
$12\text{ m} \times 6\text{ m}$	4.08×10^9	-1.77×10^{10}	2.46×10^{11}
$10\text{ m} \times 5\text{ m}$	3.17×10^9	-1.14×10^{10}	1.35×10^{11}

The improved AF properties were calculated using equations 6.3, 6.4 and 6.5, as before. The results are presented in table 8.2. The SubDyn input file for the $12\text{ m} \times 6\text{ m}$ caisson foundation model is given in Appendix G.

Table 8.2: Improved AF properties of caisson models with different dimensions.

Caisson dimensions	AF beam	L (m)	d (m)	t_w (m)	I (m ⁴)	E (N/m ²)	G (N/m ²)
$15\text{ m} \times 1.5\text{ m}$	1	33.70	6.00	0.06	5.089	1.563×10^{13}	6.012×10^{12}
	2	5.00	6.00	0.06	5.089	3.995×10^{11}	1.536×10^{11}
$12\text{ m} \times 6\text{ m}$	1	32.40	6.00	0.06	5.089	1.096×10^{13}	4.215×10^{12}
	2	5.00	6.00	0.06	5.089	1.844×10^{11}	7.091×10^{10}
$10\text{ m} \times 5\text{ m}$	1	36.87	6.00	0.06	5.089	1.301×10^{13}	5.002×10^{12}
	2	5.00	6.00	0.06	5.089	9.746×10^{10}	3.748×10^{10}

630 seconds FAST analyses were run for the different models, with $H_s = 6$ m, $T_p = 10$ s, $U = 12$ s and $TI = 14\%$. The water depth was kept at 20 m in order to compare the results to the monopile models. Like the monopile, the monopod will experience large moment and horizontal loads, particularly at the mudline. Figure 8.3 shows a time window of the mudline fore-aft bending moments for models of the NREL 5MW supported by monocaissons with different dimensions,

compared to both the monopile and the fixed base model. Figure 8.4 shows the corresponding tower top fore-aft displacement.

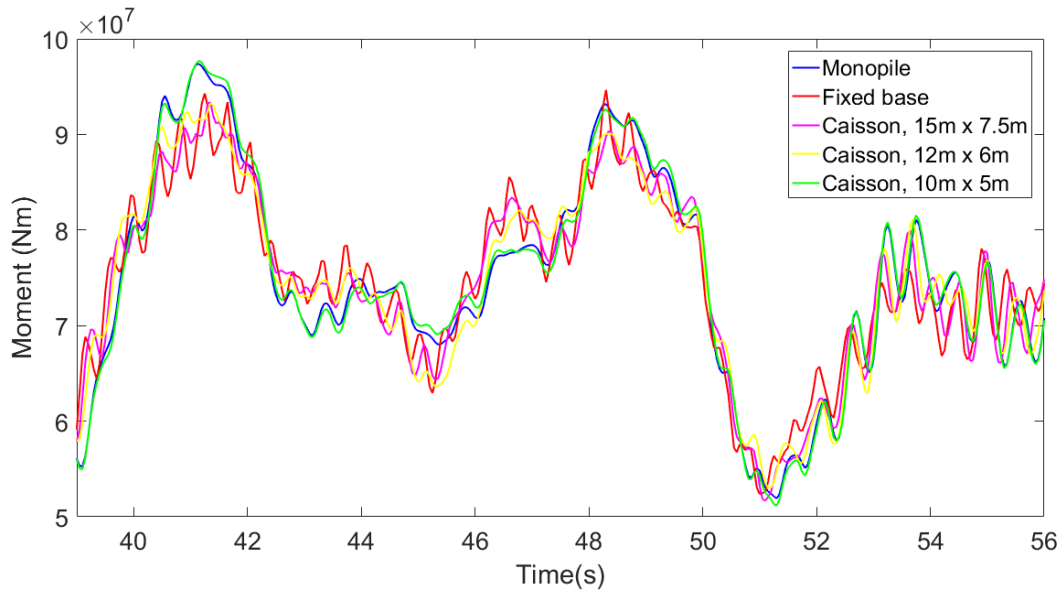


Figure 8.3: Time window of mudline fore-aft bending moment for different caisson dimensions, compared to the regular monopile and the fixed base model.

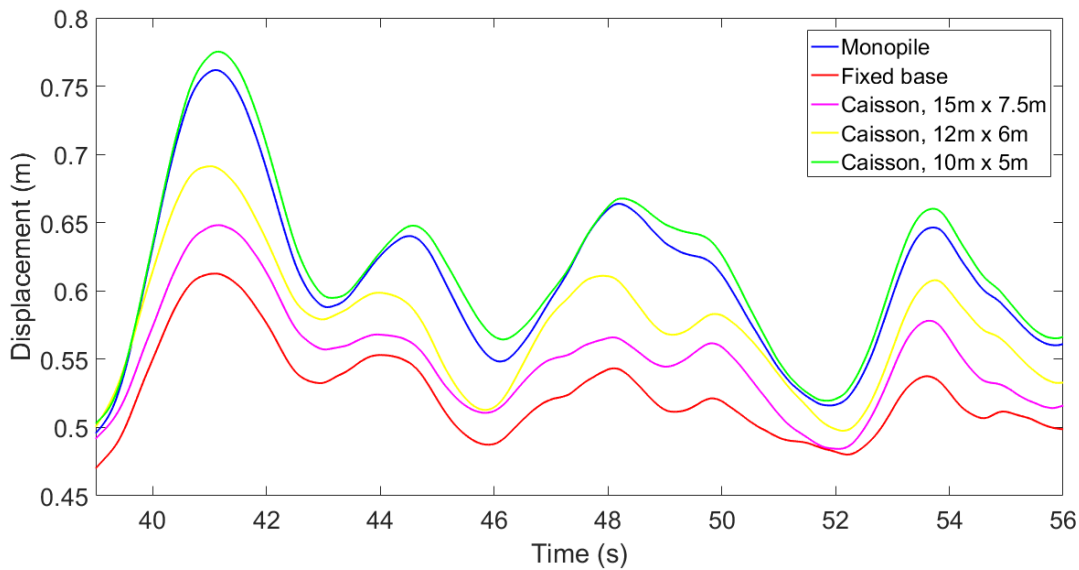


Figure 8.4: Time window of tower top fore-aft displacement for different caisson dimensions, compared to the regular monopile and the fixed base model.

As was discussed in chapter 7, the sensitivity analyses made in this thesis do not consider all aspects of dimension reduction, like capacity and buckling. The bucket is a thin shell structure with a large aspect ratio between diameter and wall thickness, meaning that buckling is a critical issue during installation (Madsen et al., 2013). In addition, the soil capacity and plastic deformations of the soil are not taken into account. Nevertheless, the results from this chapter are still useful to compare the dynamic response and, in the next chapter, the relative fatigue life of the different foundation models.

To get a greater picture of the effect of dimension changes, three models with dimensions 12 m × 5 m, 8 m × 5 m and 8 m × 4 m were also simulated. These are only used for obtaining response values for sensitivity purposes, and are not given attention for the rest of the thesis. It is highly unlikely that a caisson with a small diameter of 8 m will have the capacity of supporting a large monopile with diameter of 6 m without overturning or sinking into the seabed. The mean and maximum values for the mudline moments, mudline shear force and tower top displacement for FAST simulations of models with different caisson dimensions, along with the regular monopile and the fixed base model, are listed in table 8.3.

Table 8.3: Maximum and mean values of mudline moment, mudline shear force and tower top displacement from 10 minutes FAST simulations of different caisson dimensions.

Caisson Dimensions	Mudline fore-aft moment (MNm)		Mudline fore-aft shear force (MN)		Tower-top fore-aft displacement (m)	
	Max	Mean	Max	Mean	Max	Mean
15 m x 7.5 m	118.10	67.47	3.683	0.596	0.688	0.486
12 m x 6 m	115.50	67.53	3.652	0.596	0.744	0.511
12 m x 5 m	113.80	67.57	3.634	0.596	0.767	0.520
10 m x 5 m	115.70	67.65	3.615	0.596	0.822	0.548
8 m x 5 m	119.10	67.78	3.566	0.596	0.957	0.600
8 m x 4 m	119.40	67.90	3.632	0.596	1.035	0.640
Monopile	115.80	67.62	3.616	0.596	0.813	0.540
Fixed base	114.50	67.39	3.632	0.598	0.644	0.462

The results for the tower top displacement show that reductions in caisson dimensions yield larger displacements, as expected. However, the mudline shear force and mudline moment do not exhibit the same clear trend. The mean value of the shear force is similar for all the models, while the maximum shear force decrease for decreased dimensions except for the smallest caisson. The

mean value of the fore-aft mudline moment increase slightly with reduced caisson dimensions, which is expected based on the previous analyses of foundation models with reduced stiffness. However, the maximum moment of the three largest caissons decrease with decreased dimensions, but increase for the three smallest caissons. There is no straightforward explanation to why the maximum moments do not follow the same trend as the mean values for the largest caissons. However, an explanation to the overall trend of increasing moments for the smaller dimensions is that as the foundation dimensions decrease, the natural frequencies of the structure decrease, especially for higher modes, moving closer to resonance. As mentioned earlier, the smallest cases are only chosen for sensitivity purposes and will not be given further attention.

PSDs of the three main caisson models were obtained and are plotted in figure 8.5. The PSD show the expected reductions in natural frequencies for reduced caisson dimensions, especially for the higher modes.

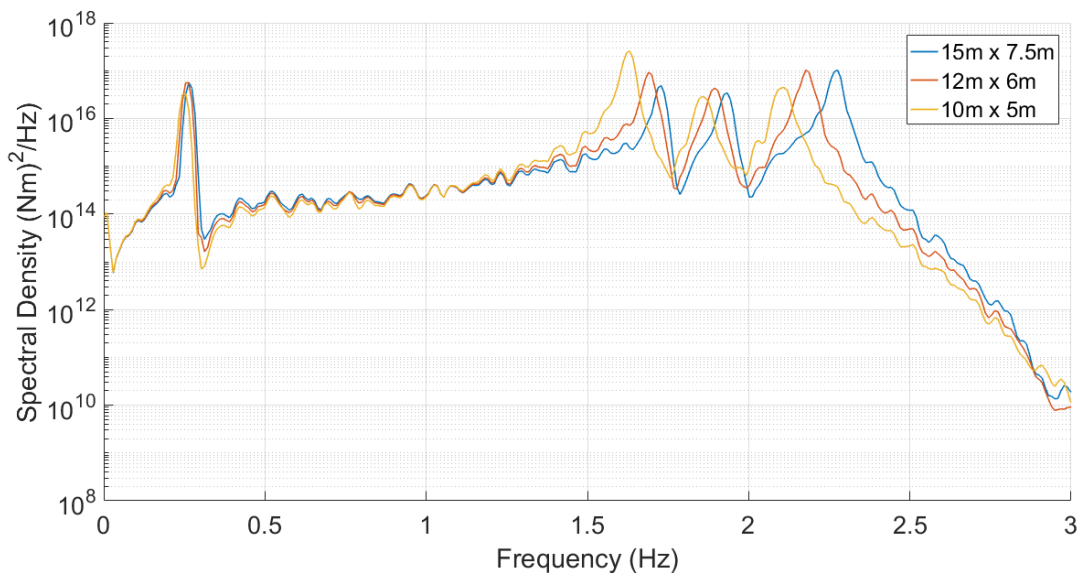


Figure 8.5: PSD from mudline fore-aft bending moment for models with different caisson dimensions.

Based on the simulation results in this chapter, and considering the chosen assumptions and simplifications, it can be concluded that a monopile with length 36 m and diameter 6 m supporting the NREL 5MW gives almost the exact same dynamic response in FAST as a caisson with diameter 10 m and depth 5 m in 20 m water depth. However, further analyses regarding capacity would have to be performed to make a valid conclusion on required caisson dimensions to replace the monopile.

9 Fatigue Analyses

Thus far, the only parameters used to compare the different foundation models have been FAST output time series. To gain insight on how these output loads affect the lifetime of the OWT, fatigue analyses of the different foundation models are carried out in this chapter, using the MATLAB-based tool *MLife*. *MLife* is developed by NREL, is mainly created to post-process FAST outputs, and computes statistical information and fatigue estimates for one or more time-series. *MLife* calculates damage rates and *damage equivalent loads* (DELs), as well as the accumulated lifetime damage and the time until failure. In this thesis, *MLife* will be used to investigate the difference in fatigue life and DELs between the foundation models presented earlier in this thesis. First, the load conditions for FAST simulations that will be the basis of the fatigue analyses will be presented in section 9.1, then *MLife* theory will be presented in section 9.2, followed by descriptions of the relevant *MLife* inputs in section 9.3. Finally, the results from the *MLife* analyses will be presented and discussed in section 9.4.

9.1 Load Conditions and FAST Simulations

Lifetime damage and fatigue life are highly dependent on the load conditions the OWT is exposed to. In IEC 61499.3 (NEK IEC 61400-3, 2009) a large number of design load cases (DLCs) to consider when doing fatigue and ultimate load analyses are listed. The DLCs cover the most significant conditions an OWT may experience, including normal operating conditions, extreme conditions, start-up and shutdown events, fault situations and parked or idling states. The load cases in 61400-3 make it possible to perform fatigue analyses without possessing climate data from the considered site. However, to get a realistic presentation of a typical offshore wind site, the wind and wave conditions from the well known *Project UpWind*, presented in Fischer et al. (2010), are used in this thesis. These site conditions were also used for the fatigue analyses performed by Aasen et al. (2016). Fischer et al. (2010) describe an offshore wind site located in the Dutch North Sea, called *K13*, which is a typical shallow site suitable for monopile foundations. Climate data has been measured on this site for 22 years, and is described with scatter diagrams including mean wind speed at hub height, significant wave height and peak spectral period. These values match well with scatter diagrams of the North Sea climate from Det Norske Veritas (2010), and will therefore be used in the proceeding analyses. The measurement data is lumped into 17 different

load cases (LCs) with different wind and wave combinations and probability of occurrence. The load cases from the *K13* site are presented in table 9.1.

Table 9.1: Load cases from Fischer et al. (2010).

Load case	U (m/s)	TI (%)	Hs (m)	Tp (m)	f (%)
1	2	29.2	1.07	6.03	0.06071
2	4	20.4	1.10	5.88	0.08911
3	6	17.5	1.18	5.76	0.14048
4	8	16.0	1.31	5.67	0.13923
5	10	15.2	1.48	5.74	0.14654
6	12	14.6	1.70	5.88	0.14272
7	14	14.2	1.91	6.07	0.08381
8	16	13.9	2.19	6.37	0.08316
9	18	13.6	2.47	6.71	0.04186
10	20	13.4	2.76	6.99	0.03480
11	22	13.3	3.09	7.40	0.01534
12	24	13.1	3.42	7.80	0.00974
13	26	12.0	3.76	8.14	0.00510
14	28	11.9	4.17	8.49	0.00202
15	30	11.8	4.46	8.86	0.00096
16	32	11.8	4.79	9.12	0.00050
17	34-42	11.7	4.90	9.43	0.00019

U is the mean wind speed at hub height, and $f(\%)$ is the frequency of occurrence of the load case. The wind speed of the 17th load case is set to the mean value, $U = 38$ m/s.

LC2-LC12 from 9.1, where the mean wind is between cut-in (3 m/s) and cut-out (25 m/s) speed, represents *DLC 1.2 Power production* from NEK IEC 61400-3 (2009), while LC1, with wind below cut-in speed, and LC13-LC17, with wind above cut-out speed, apply to *DLC 6.4 Parked (standing still or idling)*. It is assumed that the turbine is operating at all times during the design lifetime when the wind speed is between cut-in and cut-out speed, so LC1 and LC13-LC17 are the only cases where the rotor is idling. The DLCs representing start-up, shut down and other fault events are not included. This decision was made based on two reasons. Firstly, generating and simulating all the DLCs recommended in NEK IEC 61400-3 (2009) including all the possible fault

events for every wind speed for every foundation model would be very time consuming. Secondly, because the main aim of this thesis is to compare foundation models, exciting the different models with the range of environmental loads presented above will give sufficient results for that purpose.

Wind fields for the 17 load cases were generated by TurbSim, using the Kaimal spectral model and the power law wind profile, as in the previous chapters. The hydrodynamic loads were generated by HydroDyn, using a JONSWAP spectrum. When the wind speed is higher than the rated wind speed of 11.4 m/s, the initial blade pitch angles increase with wind speed due to the turbine's blade-pitch controller. These angles were changed in the ElastoDyn file for each load case. The blade pitch angles up to cut-out wind speeds are presented in table 7-1 in Jonkman et al. (2009).

Jonkman (2013a), Jonkman et al. (2016a) and Jonkman (2014) describe the changes required in FAST for modelling an idling or parked rotor. For these non-operating cases, LC1 and LC13-LC17, the rotor speed was set to 0, the generator was turned off, and the blade pitch angles were set to 90° to make them pitched out of the wind.

As recommended by NEK IEC 61400-3 (2009), for every foundation model considered, 10 minute simulations of each load case were run in FAST. The FAST output time series of the mudline bending moment in the fore-aft direction will be used for the fatigue analysis.

Figure 9.1 shows mudline moment time series of a selection of the load cases for the regular monopile modelled with the improved AF method. As stated in Jonkman (2007), the highest loads are expected to occur at the rated (11.4 m/s) and the cut-out wind speeds. Figure 9.1 shows that the highest moments occur in LC6, which has a wind speed of 12 m/s, close to the rated speed. However, the largest moment ranges occur at the highest environmental loads plotted, LC15 and LC17. In addition to these containing the strongest winds and highest waves, the rotor is idling, which means that the aerodynamic damping is highly reduced, leading to high load amplitudes at the mudline.

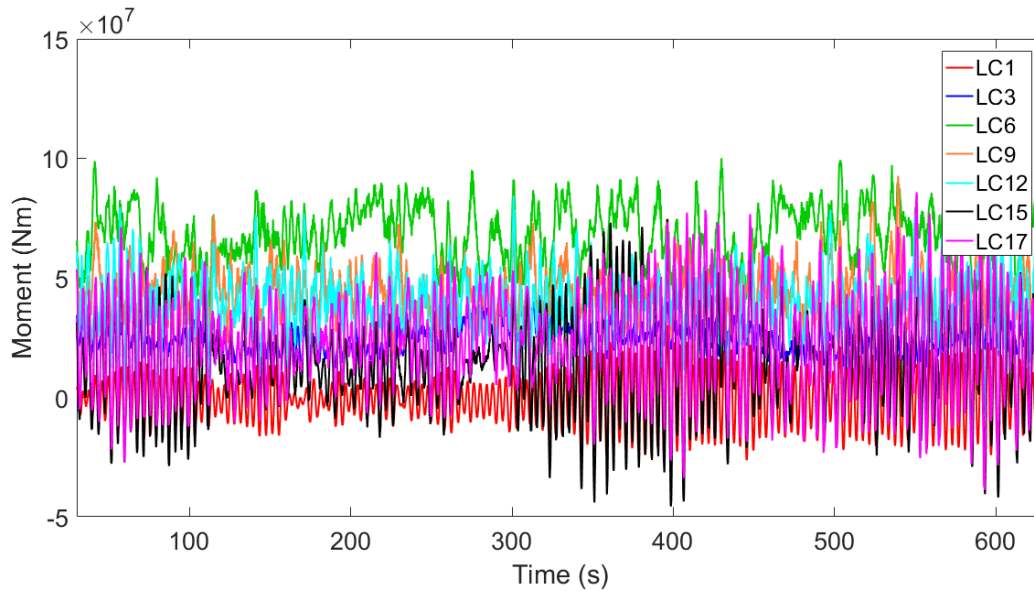


Figure 9.1: Mudline for-aft bending moment for selected load cases of the monopile.

A shorter time window of the mudline moments is shown in figure 9.2. It is clear that LC1, LC15 and LC17 represent an idling rotor, while the operational natural frequencies are present in LC3, LC6, LC9 and LC12, causing high frequency moment oscillations.

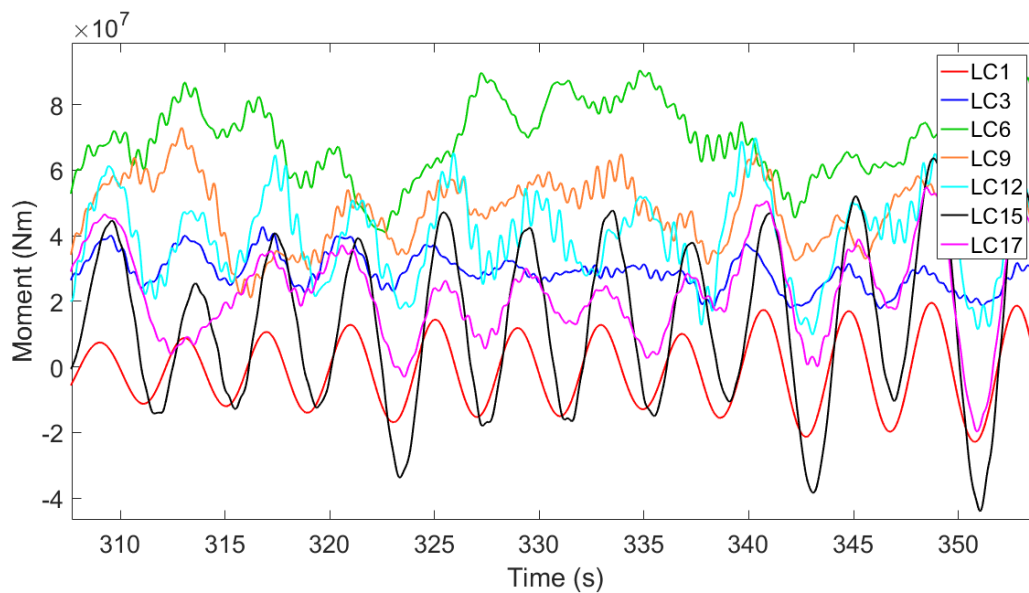


Figure 9.2: Details of mudline for-aft bending moment for selected load cases for the improved AF model monopile.

9.2 MLife Theory

In this section, the theory and equations behind the relevant MLife calculations will be presented.

MLife uses Rainflow Cycle-Counting (RCC) on the load time series' to obtain load ranges, which is common practice in fatigue analysis recommended by Det Norske Veritas (2014). RCC breaks the loads from the time series into cycles by matching pairs of similar half-cycles (Hayman and Buhl, 2012a). The load half cycles are counted by rotating the time series 90 degrees and imagining rain flowing off a building with multiple roofs, illustrated in figure 9.3. The rainflow stops when it encounters a larger maximum or minimum, which means that a half cycle is identified. Half cycle pairs are combined and binned in blocks with a certain load mean and range.

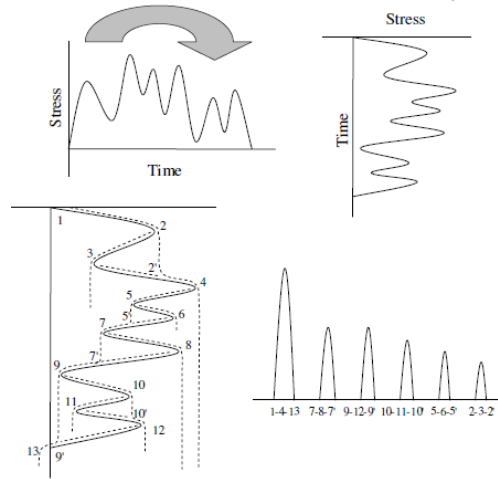


Figure 9.3: Rainflow cycle-counting illustration (der Tempel, 2006).

One or more load time series are used by MLife to calculate the lifetime damage of the wind turbine. To explain the basic theory behind the MLife calculations, only one time series is considered to begin with. As mentioned in section 2.6, the total damage at a given location subject to a fluctuating load is given by the Palmgren-Miner rule:

$$D = \sum_i \frac{n_i}{N_i(L_i^{RF})} \quad (9.1)$$

where D is the accumulated fatigue damage, n_i is the number of load cycles in block i , N_i is the number of cycles before failure for load block i , and L_i^{RF} is the cycle's load range about a fixed load-mean value.

The relationship between load range and cycles to failure, called the S-N curve, is modeled in MLife by

$$N_i = \left(\frac{L^{ult} - |L^{MF}|}{\left(\frac{1}{2}L_i^{RF}\right)} \right)^m \quad (9.2)$$

where L^{ult} is the ultimate design load of the component considered, L^{MF} is the fixed load-mean and m is the Wöhler exponent, which is dependent on the structural detail considered.

Equation 9.1 and 9.2 assume that the load cycles occur over a fixed load mean, while in reality the load mean vary for every cycle. Therefore, a correction called Goodman correction must be applied to the load ranges:

$$L_i^{RF} = L_i^R \left(\frac{L^{ult} - |L^{MF}|}{L^{ult} - |L_i^M|} \right) \quad (9.3)$$

where L_i^R is the i^{th} cycle's range about a load mean of L_i^M .

As mentioned in section 2.6, the design lifetime T^{Life} of an offshore wind turbine is 20 years. The lifetime fatigue damage is normally estimated using a number of short time-series, whose load cycles are extrapolated over the design lifetime. In order to extrapolate the load cycles, MLife models the wind with a Weibull distribution, divided into wind speed bins with a corresponding probability of occurrence. From this, a cycle count extrapolation factor f_j^{Life} is obtained for the wind speed of time series j , and is multiplied with the cycle count n_{ji} , to determine the number of load cycles from load block i for time series j that will occur over the OWT lifetime:

$$n_{ji}^{Life} = f_j^{Life} n_{ji} \quad (9.4)$$

The total lifetime damage for all load cycles and time-series is then

$$D^{Life} = \sum_j \sum_i \frac{n_{ji}^{Life}}{N_{ji}} \quad (9.5)$$

where N_{ji} is the number of cycles to failure for block i in time series j .

Failure occurs when $D^{Life} \geq 1$, implying that the time until failure is the ratio of the design

lifetime over the accumulated damage:

$$T^{Fail} = \frac{T^{Life}}{D^{Life}} \quad (9.6)$$

In addition to lifetime damage and time until failure, damage equivalent loads (DELs) are useful to characterize fatigue for wind turbines. MLife calculates both short-time DELs based on single time series, and lifetime DELs based on the entire set of time-series. A DEL is a fluctuating load with constant amplitude and constant frequency, prescribed by the MLife user, causing the equivalent damage as the stochastic loads from the time series, such that

$$D_j^{ST} = \sum_i \frac{n_{ji}}{N_{ji}} = \frac{n_j^{STeq}}{N_j^{eq}} \quad (9.7)$$

where D_j^{ST} is the short term damage from time series j . n_j^{STeq} is the total equivalent number of load cycles for time series j ,

$$n_j^{STeq} = f^{eq} T_j \quad (9.8)$$

where f^{eq} is the DEL frequency and T_j is the elapsed time of time series j . N_j^{eq} is the equivalent number of cycles until failure for time series j ,

$$N_j^{eq} = \left(\frac{L^{ult} - |L^{MF}|}{(\frac{1}{2} DEL_j^{ST})} \right)^m \quad (9.9)$$

where DEL_j^{ST} is the DEL for time-series j about a fixed mean. Solving equation 9.9 yields

$$DEL_j^{ST} = \left(\frac{\sum_i (n_{ji} (L_{ji}^{RF})^m)}{n_j^{STeq}} \right)^{\frac{1}{m}} \quad (9.10)$$

MLife produces a lifetime DEL which includes the fatigue cycles from all the input time series. The lifetime DEL about a fixed load mean value is calculated with the following equation:

$$DEL^{Life} = \left(\frac{\sum_i \sum_j (n_{ji}^{Life} (L_{ji}^{RF})^m)}{n^{Life,eq}} \right)^{\frac{1}{m}} \quad (9.11)$$

where the lifetime equivalent number of cycles is defined as

$$n^{Life,eq} = \sum_j f_j^{Life} n_j^{STeq} \quad (9.12)$$

where f_j^{Life} is the lifetime cycle count extrapolation factor.

9.3 MLife Analyses

All the fatigue analyses were based on mudline fore-aft bending moment time series from the FAST analyses of the 17 load cases from table 9.1 for each foundation model. The MLife user must specify the scale- and shape factors of the Weibull distribution of the wind, which are dependant on site, as well as cut-in, cut-out and maximum wind speed to include in the analysis. In addition, a number of other parameters need to be specified in the MLife input file: The design lifetime, the DEL frequency, the Wöhler exponent m to be used in the S-N curve, the load range binning values, the fixed-mean load and the ultimate design load L^{ult} (Hayman and Buhl, 2012b). The ultimate load is the highest load that the cross section of the studied component can withstand before failure. Ideally, the ultimate load would be based on a finite element analysis (FEA) of the component, or on data specified for the NREL 5MW. However, as no FE model or data are available, two methods that can be used to obtain the ultimate load are described below.

In Matha (2009) and in NWTC (2017) it is stated that the ultimate load can be obtained by multiplying the extreme loads of the land-based NREL 5MW turbine occurring at normal operation with a so-called *ultimate load factor* (ULF). In Jonkman (2007) over 2500 different load cases were run in FAST for the land-based 5MW OWT. Table 6-2 in that report lists extreme events for the mudline moments of the land-based turbine under normal operating conditions, weighted using *partial safety factors* (PSFs), as recommended by Det Norske Veritas (2014). PSFs take account of uncertainties and variability in loads, materials and analysis methods, and a typical value of PSF for an ultimate load is 1.35. The maximum mudline moment experienced by the land-based turbine in Jonkman (2007) is 153 MNm. Hence, the ultimate design load is:

$$L^{ult} = L^{max} \times ULF = 153 \text{ MNm} \times ULF \quad (9.13)$$

Unfortunately, there is no recommended practice for what value to choose for the ULF, and it can be anything from 1.25 to 20. After trying different values, it was evident that the chosen ULF highly affects the fatigue life results. Hence, it was decided to use another approach to obtain L^{ult} , where the ultimate tensile strength σ^{ult} of the studied cross section was used as a reference for failure, and the corresponding ultimate load was calculated using the flexure formula introduced in section 7.2, equation 7.3.

Typical values of the ultimate strength for normal strength steel are listed in Det Norske Veritas (2012) as 400 – 520 MPa. The ultimate strength of the steel used for the NREL 5MW substructure is assumed by the author to be 440 MPa, and the value of the ultimate load was calculated as

$$L^{ult} = M^{ult} = \frac{\sigma^{ult}}{y} I = 7.46 \times 10^8 \text{ Nm} \quad (9.14)$$

Comparing this result to the first approach explained above gives $ULF = 4.88$.

Det Norske Veritas (2014) states that the Wöhler exponent, m , for steel can be either 3, 4 or 5, dependant on the steel type, the environment around the component and the number of cycles to failure. The OWT monopile at mudline fits into the structural detail type F3 from Det Norske Veritas (2014), situated in seawater with cathodic protection, and N is in the high cycle region, so $m = 5$ was chosen to be the suitable choice for this analysis. Moreover, the load bin width was set to 100 Nm, and the fixed-mean load was set to AM , telling MLife to compute the fixed mean using the aggregate mean across all input files. The input files were sorted in standard operating conditions and idling conditions, as these are weighted differently by MLife. As mentioned in section 9.1, it was assumed that the turbine is operating at all times during the design lifetime when the wind speed is between cut-in and cut-out speeds. The Weibull scale- and shape factors for the $K12$ site are specified in Fischer et al. (2010) as $\lambda_W=11.31$ m/s and $k_W=1.97$.

MLife fatigue analyses were run for the following foundation models:

- The NREL 5MW fixed base reference model
- Monopile foundation models: The monopile with regular dimensions, the 16 m pile and the models with reduced pile wall thickness

- Caisson foundation models: 12 m × 6 m model, 15 m × 7.5 m model, and 10 m × 5 m model

All these models have the same cross-sectional properties at the mudline, and hence the same ultimate load, except for the models with reduced wall thickness. L^{ult} for the model with $t_w = 0.04$ m is reduced by 1/3, and L^{ult} for the model with $t_w = 0.05$ m is reduced by 1/6, based on equation 7.2 and equation 9.14. It is important to calculate the ultimate load based on cross sectional dimensions, because this is the only input parameter saying anything about the cross section considered.

An overview of the steps of the method for fatigue analyses is illustrated in figure 9.4, from load generation in TurbSim and HydroDyn to calculating lifetime damage and DELs in MLife. The MLife input file for the regular monopile can be found in Appendix H. The results of the analyses are presented and compared in the following section.

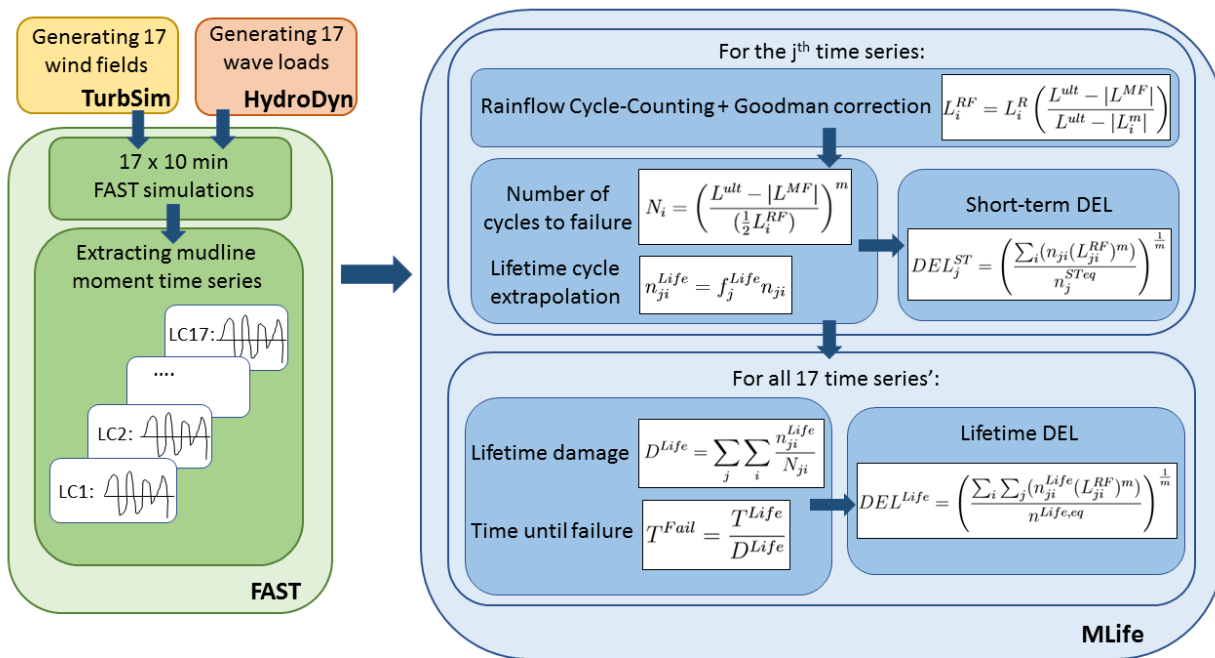


Figure 9.4: Steps of the fatigue analyses

9.4 Results

Table 9.2 lists the results of the MLife analyses for the different foundation models. The DELs are reported as range values, or peak-to-peak values, with fixed mean values calculated by MLife. fluctuating with a frequency of 1 Hz. As mentioned in section 9.2, the oscillation frequency of the DELs are prescribed by the MLife user, and highly affects the load values. In these analyses, the DEL frequency is set to 1 Hz.

Table 9.2: Results from MLife fatigue analyses.

Model	Lifetime damage (-)	Time until failure (years)	Lifetime DEL (MNm)
Fixed base	0.700	28.57	23.1
Monopile	0.898	22.26	24.3
Monopile, L=16m	0.901	22.20	24.3
Monopile, $t_w=0.05\text{m}$	2.360	8.47	24.3
Monopile, $t_w=0.04\text{m}$	8.270	2.42	24.5
Caisson, 15m x 7.5m	0.701	28.54	23.1
Caisson, 12m x 6m	0.775	25.81	23.6
Caisson, 10m x 5m	0.891	22.45	24.3

First considering the differences between the fixed base model and the monopile, table 9.2 shows a significant difference in fatigue life for the two. Even though the differences in mudline moments from section 6.1 are not very large, 1.1% increase in maximum moment and 6.5 % increase in standard deviation, the differences are large enough to highly affect the fatigue life. The time until failure, or fatigue life, is reduced by 22.1% when a flexible foundation is introduced. Furthermore, the monopile with a shorter length of 16 m show almost no difference in fatigue life compared to the original monopile, which underlines the conclusions drawn in section 7.1.

Moving on to the reduced thickness monopiles, table 9.2 shows how important a reduction in wall thickness is for the fatigue life, due to the higher bending stresses, as explained in chapter 7. The fatigue life of the model with $t_w = 0.05\text{ m}$ is reduced to 8.47 years, a reduction of 61.9%, and the model with $t_w = 0.04\text{ m}$ has a short fatigue life of 2.42 years, a reduction of 89.1% Hence, it can be concluded that an OWT with a monopile wall thickness of 0.05 m or 0.04 m will not, by far, live through its expected lifetime of 20 years.

The model with a $10\text{ m} \times 5\text{ m}$ caisson foundation gives similar MLife results as the monopile, while the $12\text{ m} \times 6\text{ m}$ caisson has an accumulated fatigue life between the fixed base and the regular monopile, which is expected based on the mudline moment plots in figure 8.3 and the maximum moment values from table 8.3. The largest caisson gives MLife results very close to the fixed base model, implying that OWTs with caissons of that size can be treated as rigidly connected to the seabed. However, as mentioned earlier, capacity and plastic deformations of the soil are not taken into account.

The short term DELs for each input time series are shown in figure 9.5 for the analyzed foundation models.

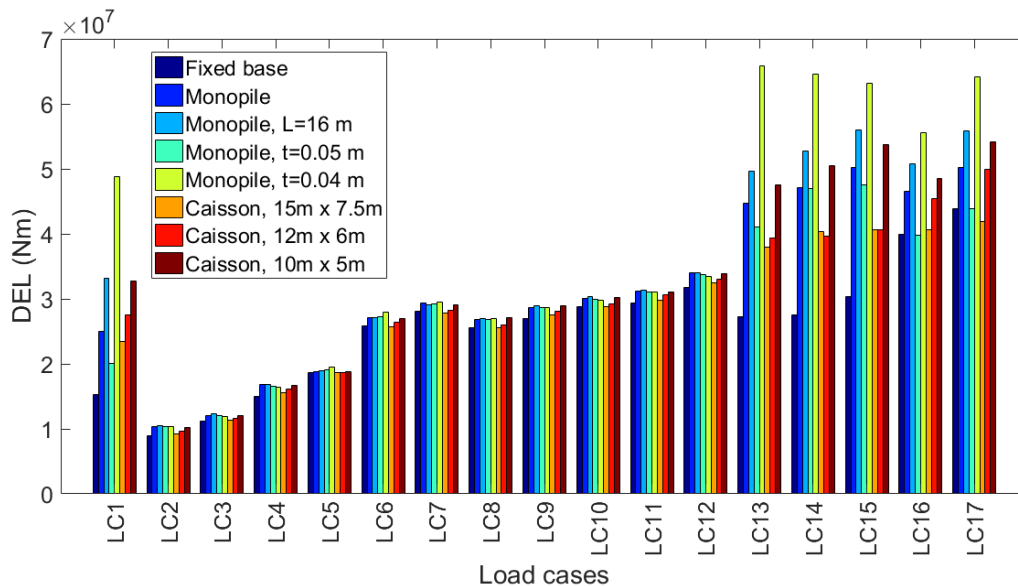


Figure 9.5: Short term DEL for the different load cases.

Figure 9.5 show that the highest DELs, and also the largest deviation between the models, occur for LC13-LC17, as expected, due to the high moment amplitudes of these cases. The high DELs for LC1 may seem counter intuitive, as the wind and wave loads are low for this case. However, as was shown in figure 9.1, when the rotor is idling and the aerodynamic damping is reduced, the tower is free to oscillate at its first natural frequency, which gives high moment amplitudes despite small maximum values. The largest DELs occur for the model with the smallest wall thickness. The reason why this increase is not present in the lifetime DEL from table 9.2 is the short lifetime the DELs are assumed to act on the structure.

Figure 9.6 shows the relative DELs, weighted with the load cases' probability of occurrence from

table 9.1. The load case with the highest DEL, and hence the load case contributing the most to the lifetime damage is LC6, due to the combination of the wind speed being close to the turbine's rated wind speed and the high probability of occurrence. The high probability of occurrence of LC1 leads to a large contribution from this case as well, particularly for the monopile with $t_w = 0.04$ m. Note that the DELs are loads and not stresses, implying that similar DELs give significantly larger fatigue damage for the reduced wall thickness models.

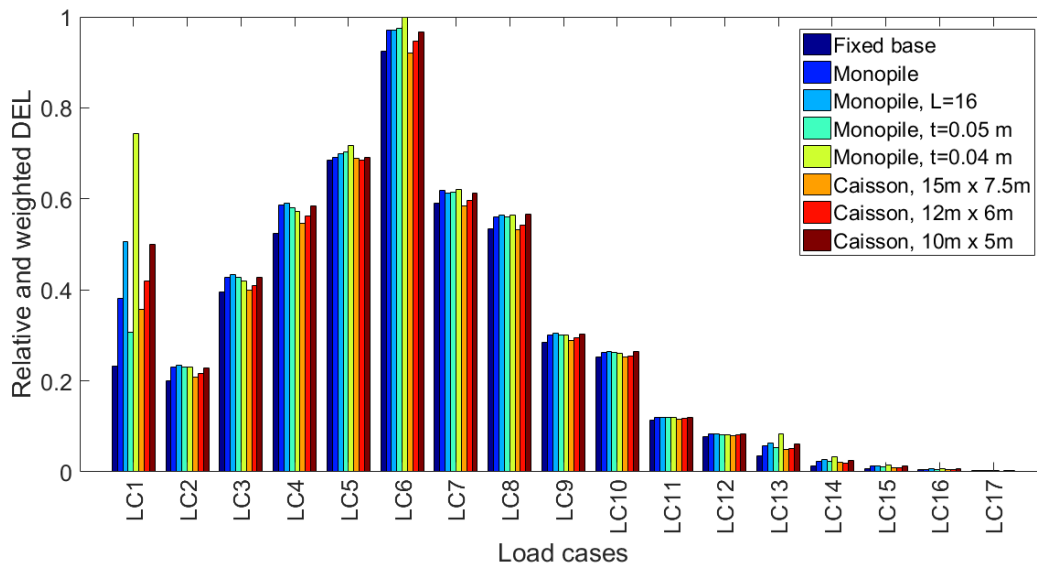


Figure 9.6: Relative short term DEL for the different load cases, weighted with probability of occurrence

From these results, it can be concluded that in general, mean winds below cut-in speed and around rated wind speed contribute the most to fatigue damage of an offshore wind turbine. The difference in DELs between different foundation models are moderate for an operating turbine, but large for mean winds below cut-in and above cut-out speeds when the turbine is idling and damping is low.

10 Conclusions and Recommendations for Further Work

Modelling capabilities of OWT foundations are in general not well developed in most wind turbine simulation codes. In FAST, the wind turbine model is assumed to be fixed at the mudline, implying that the effect of the foundation flexibility on the structural dynamic response is not considered. This may lead to wrong predictions of structural response and fatigue damage. The first objective of this thesis was to study the effect of including flexibility of the foundation in FAST. This was done through the apparent fixity method, first with a simplified approach, followed by the development of a more exact approach. The second objective was to perform sensitivity analyses of monopile foundations with different dimensions and suction caisson foundations with different dimensions with respect to dynamic response and fatigue damage.

10.1 Conclusions

Based on the analyses carried out in this thesis, the following conclusions can be drawn:

- Neglecting the effect of the foundation in the OWT model, like the fixed base default model in FAST, when running simulations gives inaccurate and underestimated results for the structural dynamic response and fatigue damage. A significant reduction in fatigue life of 22.1% was present for the flexible foundation model compared to the fixed base model.
- The method chosen for modelling the OWT foundation is important to obtain a correct representation of the structural dynamic response. The effect of the off-diagonal terms in the soil-foundation stiffness matrix at the mudline plays an important part when modelling the foundation flexibility. Disregarding the off-diagonal terms in the simplified apparent fixity method in chapter 5 gave a foundation model that was too soft, and lead to over-predictions of the loads and displacements in the substructure. Including the off-diagonal terms of the stiffness matrix, done in the improved AF method in chapter 6, lead to a stiffer foundation model and gave a significant difference in structural response compared to the simplified

method.

- Reductions of the monopile subsoil length have almost no effect on the FAST results, due to minimal changes in soil-pile stiffness coefficients from the soil-profile considered. A reduction from 36 m to 26 m lead to no noticeable difference, and the length had to be reduced to 16 m for a small difference to be present.
- A small reduction of the monopile wall thickness leads to a moderate increase in bending moments, but a large increase in fatigue damage, and hence a large reduction in fatigue life. Designing the NREL 5MW with a wall thickness smaller than 0.06 m will probably lead to failure, either by fatigue or possibly by buckling.
- A suction caisson foundation with a diameter of 10 m and a depth of 5 m gives similar dynamic response and fatigue life as the regular monopile with length 36 m and diameter 6 m with the assumptions made and modelling methods used in this thesis.
- Capacity analyses of the soil-foundation system would have to be carried out in addition to the analyses presented in this thesis in order to conclude on possibilities of dimension reduction, both regarding pile wall thickness, pile length and caisson size. Buckling is especially of concern for the monopile models with reduced wall thickness and for the caisson models.
- The fatigue damage calculations in MLife are highly dependent on input parameters, especially the Wöhler exponent and the ultimate load. For the NREL 5MW there are no recommended values to use for the ultimate load when a FE model is not available, and research on the topic provide a wide range of alternatives. This has to be taken under consideration when evaluating the values of the resulting fatigue damage and when comparing the results to previous research. Without knowing the exact values to choose for the input parameters, the MLife fatigue analysis will produce results suitable for comparing models, as demonstrated in this thesis, but may not give exact values of the fatigue life for the component considered. Hence, running all the DLCs recommended by NEK IEC 61400-3 (2009) will still not give exact results for fatigue damage when lacking information on the prescribed MLife input parameters.
- There is no need to update the assumed mode shape input in FAST for the different foundations models considered in this thesis. The boundary conditions change with the different foundation modelling methods and foundation dimensions, but after studying the effect of changing the mode shapes it was clear that it does not affect the simulation output.

10.2 Recommendations for Further Work

The work done in this thesis has made the author aware of the complexity of offshore wind turbine foundation analyses. There are many aspects to consider when studying OWT foundations, especially if the aim is to make the design more cost-effective. In this section, recommendations for possible extensions of the work done in this thesis will be presented.

- Carry out throughout fatigue analyses of the foundation models with all the DLCs recommended by NEK IEC 61400-3 (2009), including start-up, shut down and fault events. The purpose of this would be to study whether the relative differences between the foundation models change when these DLCs are included.
- Run more than one TurbSim simulation for each wind speed in the fatigue analyses, changing the seed, i.e. the phases for the wind velocity time series. The purpose of this is to take care of the randomness and deviations from the mean wind due to simulation of turbulence. Jason Jonkman suggests in NWTC (2017) to run more simulations with different seeds per wind-speed bin to make sure the fatigue results are seed independent.
- Make a FE model of the NREL 5MW monopile. This has mainly two purposes. The first one would be to obtain the ultimate design load to use for the MLife fatigue analyses in order to get exact results for the fatigue damage and lifetime. In addition, the FE model should be made in a software capable of modelling the true nonlinear behaviour of the soil. This would be highly favorable in order to validate the improved AF method developed in this thesis and to study the effect of assuming linear behaviour of the soil.
- Make a FE model of the caisson foundation to obtain its exact properties and behaviour. This model should be used to perform a comprehensive non-linear buckling analysis, as well as validating the simplified modelling method used in this thesis.
- Continue the sensitivity analyses of both the monopile and the caisson foundations with geotechnical capacity analyses to get a complete picture of the behaviour of the soil-foundation system. Since the structural response is highly dependant on soil type, it would be convenient to study the SSI of softer and stiffer soil profiles. Combining capacity analyses with the results from this thesis may lead to conclusions on the possibilities of foundation dimension reduction. Such a study would also result in guidelines to the suitability of different foundation types in different soils with regards to elasticity, strength and layering.

Bibliography

- Aasen, S., Page, A. M., Skau, K. S., and Nygaard, T. A. (2016). Effect of the Foundation Modelling on the Fatigue Lifetime of a Monopile-based Offshore Wind Turbine.
- Andersen, L. V., Vahdatirad, M. J., Sichani, M. T., and Sørensen, J. D. (2012). Natural frequencies of wind turbines on monopile foundations in clayey soils - A probabilistic approach. *Computers and Geotechnics*, 43:1–11.
- Bendat, J. S., P. A. G. (2011). *Random Data: Analysis and Measurement Procedures*. Wiley, Hoboken, fourth edition.
- Bir, G. (2007). User's Guide to BModes (Software for Computing Rotating Beam Coupled Modes). Manual, National Renewable Energy Laboratory.
- Bloomberg New Energy Finance (2017a). Global Trends in Renewable Energy Investment 2017. Report, Frankfurt School of Finance and Management.
- Bloomberg New Energy Finance (2017b). Offshore Wind Farms Offer Subsidy-Free Power for First Time.
- Bush, E., Agarwal, P., and Manuel, L. (2008). The influence of foundation modeling assumptions on long-term load prediction for offshore wind turbines. In *ASME 27th International Conference on Offshore and Arctic Engineering*. OMA2008-57893.
- Bush, E. and Manuel, L. (2009). Foundation Models for Offshore Wind Turbines. *47th AIAA Aerospace Sciences Meeting*.
- Carswell, W., Johansson, J., Løvholt, F., Arwade, S. R., Madshus, C., Degroot, D. J., and Myers, A. T. (2015). Foundation damping and the dynamics of offshore wind turbine monopiles. *Renewable Energy*.
- Damiani, R., Jonkman, J., and Hayman, G. (2015). SubDyn User's Guide and Theory Manual. Manual, National Renewable Energy Laboratory.
- der Tempel, J. V. (2006). *Design of Support Structures for Offshore Wind Turbines*. Phd, Technische Universiteit Delft.

- Det Norske Veritas (2010). DNV-RP-C205. Environmental Conditions and Environmental Loads.
- Det Norske Veritas (2012). DNV-OS-B101 - Metallic Materials. Standard.
- Det Norske Veritas (2014). DNV-OS-J101 Design of Offshore Wind Turbine Structures. Standard.
- Faltinsen, O. M. O. M. (1990). *Sea Loads on Ships and Offshore Structures*. Cambridge University Press.
- Fischer, T., de Vries, W., and Schmidt, B. (2010). Upwind Design Basis (WP4: Offshore Foundations and Support Structures). *Project Upwind*.
- Global Wind Energy Council (2016). Global Wind Report 2015. Report.
- Global Wind Energy Council (2017). Global Wind Statistics 2016. Report.
- Halfpenny, A. (1998). *Dynamic analysis of both on and offshore wind turbines in the frequency domain*. Phd, University College London.
- Hayman, G. J. and Buhl, M. (2012a). MLife Theory Manual for Version 1.00. Technical report, National Renewable Energy Laboratory.
- Hayman, G. J. and Buhl, M. (2012b). MLife User ' s Guide for Version 1.00. Manual, National Renewable Energy Laboratory.
- Hill, D. (2015). The Foundations of the Industry: The Next Generation.
- Jonkman, B. and Jonkman, J. (2016). FAST v8.16.00a-bjj. Manual, National Renewable Energy Laboratory.
- Jonkman, B. J. and Kilcher, L. (2012). TurbSim User's Guide: Version 1.06.00. Manual, National Renewable Energy Laboratory.
- Jonkman, J. (2013a). Overview of the ElastoDyn Structural-Dynamics Module. Manual, National Renewable Energy Laboratory.
- Jonkman, J. (2013b). The New Modularization Framework for the FAST Wind Turbine CAE Tool Preprint. National Renewable Energy Laboratory.
- Jonkman, J. (2014). Overview of the ServoDyn Control & Electrical-Drive Module. Manual, National Renewable Energy Laboratory.

- Jonkman, J. (2015). FAST: A Developer-Community Environment for Wind Turbine Multi-Physics Engineering Modeling. *NAWEA 2015 Symposium*.
- Jonkman, J., Butterfield, S., Musial, W., and Scott, G. (2009). Definition of a 5-MW reference wind turbine for offshore system development. Technical report, National Renewable Energy Laboratory.
- Jonkman, J. M. (2007). Dynamics Modeling and Loads Analysis of an Offshore Floating Wind Turbine. Technical report, National Renewable Energy Laboratory.
- Jonkman, J. M. (2017). Personal Communication.
- Jonkman, J. M. and Buhl, M. L. (2005). FAST User's Guide. Manual, National Renewable Energy Laboratory.
- Jonkman, J. M., Hayman, G. J., Jonkman, B. J., and Damiani, R. R. (2016a). AeroDyn v15 User's Guide and Theory Manual. Manual, National Renewable Energy Laboratory.
- Jonkman, J. M. and Musial, W. (2010). IEA Wind Task 23, Offshore Wind Technology and Deployment. *Subtask 2, The Offshore Code Comparison Collaboration (OC3)*.
- Jonkman, J. M., Robertson, A. N., and Hayman, G. J. (2016b). HydroDyn User's Guide and Theory Manual. Manual, National Renewable Energy Laboratory.
- Kallehave, D., Byrne, B. W., LeBlanc Thilsted, C., Mikkelsen, K. K., de Vries, W., and Frandsen, S. (2015). Optimization of monopiles for offshore wind turbines. *Philosophical Transactions of the Royal Society A: Mathematical, Physical and Engineering Sciences*.
- Kaynia, A. (1982). Dynamic stiffness and seismic response of pile groups. Technical report, MIT, Cambridge.
- Kaynia, A. M. (2017). personal communication.
- Kourkoulis, R., Lekakakis, P., Gelagoti, F., and Kaynia, A. (2014). Suction caisson foundations for offshore wind turbines subjected to wave and earthquake loading: effect of soil-foundation interface. *Géotechnique*, 64(3):171–185.
- Kramer, S. L. (1996). *Geotechnical Earthquake Engineering*. Prentice Hall.
- Krathe, V. L. and Kaynia, A. (2016). Implementation of a non-linear foundation model for soil-structure interaction analysis of offshore wind turbines in FAST. *Wind Energy*.

- Lombardi, D., Bhattacharya, S., and Muir Wood, D. (2013). Dynamic soil-structure interaction of monopile supported wind turbines in cohesive soil. *Soil Dynamics and Earthquake Engineering*, 49:165–180.
- Lynn, P. A. (2012). *Onshore and Offshore Wind Energy: An Introduction*. John Wiley & Sons, Ltd, Chichester, UK.
- Madsen, S., Andersen, L., and Ibsen, L. (2013). Numerical buckling analysis of large suction caissons for wind turbines on deep water. *Engineering Structures*, 57:443–452.
- Matha, D. (2009). Model Development and Loads Analysis of a Wind Turbine on a Floating Offshore Tension Leg Platform. Technical report, University of Colorado - Boulder.
- Moriarty, P. J. and Hansen, A. C. (2005). AeroDyn Theory Manual.
- National Renewable Energy Laboratory (2016). NWTC Information Portal (FAST v8).
- NEK IEC 61400-3 (2009). Wind Turbines - Part 3: Design requirements for offshore wind turbines. Standard, Norwegian Electrotechnical Publication.
- Newland, D. E. (2005). *An Introduction to Random Vibrations, Spectral & Wavelet Analysis*. Dover Publications, Inc., Mineola, New York, third edition.
- Nielsen, H. L. (2013). Universal Foundation Suction Bucket. A solution in support for offshore wind. Technical Report April, Fred. Olsen United.
- Nielsen, S. (2014). Case: Aalborg University - Universal Foundation. Technical report, Universal Foundation.
- NWTC (2017). NWTC Forums - NWTC Information Portal.
- Passon, P. (2006). Derivation and Description of the Soil-Pile-Interaction Models. Technical report, University of Stuttgart.
- Passon, P. and Kühn, M. (2005). State-of-the-art and development needs of simulation codes for offshore wind turbines. Paper, Endowed Chair of Wind Energy (SWE), University of Stuttgart.
- Schaffarczyk, A. (2014). *Understanding Wind Power Technology: Theory, Deployment and Optimisation*. John Wiley & Sons, Ltd.
- Strømme, E. (2010). *Theory of Bridge Aerodynamics*. Springer Berlin Heidelberg, 2nd edition.

- Tassoulas, J. (1981). Elements for numerical analysis of wave motion in layered media. Technical report, MIT, Cambridge.
- The Scottish Government (2006). Planning for Micro Renewables Annex to PAN 45 Renewable Energy Technologies.
- Versteede, H., Ny, C. S. A., Stuyts, B., and Cathie, D. (2013). Cyclic loading of caisson supported offshore wind structures in sand. In *18th International Conference on Soil Mechanics and Geotechnical Engineering*, pages 2411–2414, Paris.
- Welch, P. (1967). The use of fast Fourier transform for the estimation of power spectra: A method based on time averaging over short, modified periodograms. *IEEE Transactions on Audio and Electroacoustics*, 15(2).
- Wind Europe (2017). The European offshore wind industry - Key trends and statistics 2016. Report.
- Zaaijer, M. B. (2006). Foundation modelling to assess dynamic behaviour of offshore wind turbines. *Applied Ocean Research*, 28(1):45–57.

A FAST Input Files for the NREL 5MW OWT

A.1 FAST Main Input File

```
Test19
----- FAST v8.16.* INPUT FILE -----
FAST Certification Test #19: NREL 5.0 MW Baseline Wind Turbine with OC3 Monopile RF Configuration, for use in offshore analysis
----- SIMULATION CONTROL -----
False      Echo          - Echo input data to <RootName>.ech (flag)
"FATAL"    AbortLevel - Error level when simulation should abort (string) {"WARNING", "SEVERE", "FATAL"}
          630 TMax        - Total run time (s)
          0.005 DT         - Recommended module time step (s)
          2 InterpOrder - Interpolation order for input/output time history (-) {1=linear, 2=quadratic}
          0 NumCrctn     - Number of correction iterations (-) {0=explicit calculation, i.e., no corrections}
          99999 DT_UJac  - Time between calls to get Jacobians (s)
          1E+06 UJacScfFact - Scaling factor used in Jacobians (-)
----- FEATURE SWITCHES AND FLAGS -----
          1 CompElast   - Compute structural dynamics (switch) {1=ElastoDyn; 2=ElastoDyn + BeamDyn for blades}
          1 CompInflow  - Compute inflow wind velocities (switch) {0=still air; 1=InflowWind; 2=external from OpenFOAM}
          2 CompAero    - Compute aerodynamic loads (switch) {0=None; 1=AeroDyn v14; 2=AeroDyn v15}
          1 CompServo   - Compute control and electrical-drive dynamics (switch) {0=None; 1=ServoDyn}
          1 CompHydro   - Compute hydrodynamic loads (switch) {0=None; 1=HydroDyn}
          1 CompSub     - Compute sub-structural dynamics (switch) {0=None; 1=SubDyn}
          0 CompMooring - Compute mooring system (switch) {0=None; 1=MAP++; 2=FEAMooring; 3=MoorDyn; 4=OrcaFlex}
          0 CompIce     - Compute ice loads (switch) {0=None; 1=IceFloe; 2=IceDyn}
----- INPUT FILES -----
"5MW_Baseline/NRELOffshBrBslne5MW_OC3Monopile_ElastoDyn.dat" EDFFile - Name of file containing ElastoDyn input parameters (quoted string)
"5MW_Baseline/NRELOffshBrBslne5MW_BeamDyn.dat" BDBldFile(1) - Name of file containing BeamDyn input parameters for blade 1 (quoted string)
"5MW_Baseline/NRELOffshBrBslne5MW_BeamDyn.dat" BDBldFile(2) - Name of file containing BeamDyn input parameters for blade 2 (quoted string)
"5MW_Baseline/NRELOffshBrBslne5MW_BeamDyn.dat" BDBldFile(3) - Name of file containing BeamDyn input parameters for blade 3 (quoted string)
"5MW_Baseline/NRELOffshBrBslne5MW_InflowWind_12mps.dat" InflowFile - Name of file containing inflow wind input parameters (quoted string)
"5MW_Baseline/NRELOffshBrBslne5MW_OC3Monopile_AeroDyn15.dat" AeroFile - Name of file containing aerodynamic input parameters (quoted string)
"5MW_Baseline/NRELOffshBrBslne5MW_OC3Monopile_ServoDyn.dat" ServoFile - Name of file containing control and electrical-drive input parameters (quoted string)
"5MW_Baseline/NRELOffshBrBslne5MW_OC3Monopile_HydroDyn.dat" HydroFile - Name of file containing hydrodynamic input parameters (quoted string)
"5MW_Baseline/NRELOffshBrBslne5MW_OC3Monopile_SubDyn.dat" SubFile - Name of file containing sub-structural input parameters (quoted string)
"unused" MooringFile - Name of file containing mooring system input parameters (quoted string)
"unused" IceFile - Name of file containing ice input parameters (quoted string)
----- OUTPUT -----
True      SumPrint     - Print summary data to "<RootName>.sum" (flag)
          1 SttsTime    - Amount of time between screen status messages (s)
          99999 ChkptTime - Amount of time between creating checkpoint files for potential restart (s)
          0.05 DT_Out   - Time step for tabular output (s) (or "default")
          30 TStart    - Time to begin tabular output (s)
          3 OutFileFmt - Format for tabular (time-marching) output file (switch) {1: text file [<RootName>.out], 2: binary file [<RootName>.outb], 3: both}
True      TabDelim    - Use tab delimiters in text tabular output file? (flag) {uses spaces if false}
"ES10.3E2" OutFmt     - Format used for text tabular output, excluding the time channel. Resulting field should be 10 characters. (quoted string)
----- LINEARIZATION -----
False     Linearize   - Linearization analysis (flag)
          2 NLinTimes  - Number of times to linearize (-) [>=1] [unused if Linearize=False]
          30, 60 LinTimes - List of times at which to linearize (s) [1 to NLinTimes] [unused if Linearize=False]
          1 LinInputs - Inputs included in linearization (switch) {0=none; 1=standard; 2=all module inputs (debug)} [unused if Linearize=False]
          1 LinOutputs - Outputs included in linearization (switch) {0=none; 1=from OutList(s); 2=all module outputs (debug)} [unused if Linearize=False]
False     LinOutJac   - Include full Jacobians in linearization output (for debug) (flag) [unused if Linearize=False; used only if LinInputs=LinOutputs=2]
False     LinOutMod   - Write module-level linearization output files in addition to output for full system? (flag) [unused if Linearize=False]
----- VISUALIZATION -----
          0 WrVTK      - VTK visualization data output: (switch) {0=none; 1=initialization data only; 2=animation}
          3 VTK_type   - Type of VTK visualization data: (switch) {1=surfaces; 2=basic meshes (lines/points); 3=all meshes (debug)} [unused if WrVTK=0]
false     VTK_fields  - Write mesh fields to VTK data files? (flag) {true/false} [unused if WrVTK=0]
          15 VTK_fps    - Frame rate for VTK output (frames per second){will use closest integer multiple of DT} [used only if WrVTK=2]
```

A.2 ElastoDyn Input File

```

----- NRELOffshrBsline5MW_OC3Monopile_ElastoDyn -----
----- ELASTODYN v1.03.* INPUT FILE -----
NREL 5.0 MW Baseline Wind Turbine for Use in Offshore Analysis. Properties from Dutch Offshore Wind Energy Converter (DOWEC)
6MW Pre-Design (10046_009.pdf) and REpower 5M 5MW (5m_uk.pdf);
----- SIMULATION CONTROL -----
False      Echo          - Echo input data to "<RootName>.ech" (flag)
           3 Method      - Integration method: {1: RK4, 2: AB4, or 3: ABM4} (-)
"default"   DT             - Integration time step (s)
----- ENVIRONMENTAL CONDITION -----
           9.80665 Gravity - Gravitational acceleration (m/s^2)
----- DEGREES OF FREEDOM -----
True       FlapDOF1    - First flapwise blade mode DOF (flag)
True       FlapDOF2    - Second flapwise blade mode DOF (flag)
True       EdgeDOF     - First edgewise blade mode DOF (flag)
False      TeetDOF     - Rotor-teeter DOF (flag) [unused for 3 blades]
True       DrTrDOF     - Drivetrain rotational-flexibility DOF (flag)
True       GenDOF      - Generator DOF (flag)
True       YawDOF      - Yaw DOF (flag)
True       TwFADOF1    - First fore-aft tower bending-mode DOF (flag)
True       TwFADOF2    - Second fore-aft tower bending-mode DOF (flag)
True       TwSSDOF1    - First side-to-side tower bending-mode DOF (flag)
True       TwSSDOF2    - Second side-to-side tower bending-mode DOF (flag)
True       PtfmSgDOF   - Platform horizontal surge translation DOF (flag)
True       PtfmSwDOF   - Platform horizontal sway translation DOF (flag)
True       PtfmHVDOF   - Platform vertical heave translation DOF (flag)
True       PtfmRDOF    - Platform roll tilt rotation DOF (flag)
True       PtfmPDOF    - Platform pitch tilt rotation DOF (flag)
True       PtfmYDOF    - Platform yaw rotation DOF (flag)
----- INITIAL CONDITIONS -----
           0 OoPDefl    - Initial out-of-plane blade-tip displacement (meters)
           0 IPDefl     - Initial in-plane blade-tip deflection (meters)
           0 BLPitch(1) - Blade 1 initial pitch (degrees)
           0 BLPitch(2) - Blade 2 initial pitch (degrees)
           0 BLPitch(3) - Blade 3 initial pitch (degrees) [unused for 2 blades]
           0 TeetDefl    - Initial or fixed teeter angle (degrees) [unused for 3 blades]
           0 Azimuth     - Initial azimuth angle for blade 1 (degrees)
           12.1 RotSpeed - Initial or fixed rotor speed (rpm)
           0 NacYaw      - Initial or fixed nacelle-yaw angle (degrees)
           0 TTDspFA     - Initial fore-aft tower-top displacement (meters)
           0 TTDspSS     - Initial side-to-side tower-top displacement (meters)
           0 PtfmSurge   - Initial or fixed horizontal surge translational displacement of platform (meters)
           0 PtfmSway    - Initial or fixed horizontal sway translational displacement of platform (meters)
           -0.0009 PtfmHeave - Initial or fixed vertical heave translational displacement of platform (meters)
           0 PtfmRoll    - Initial or fixed roll tilt rotational displacement of platform (degrees)
           0 PtfmPitch   - Initial or fixed pitch tilt rotational displacement of platform (degrees)
           0 PtfmYaw     - Initial or fixed yaw rotational displacement of platform (degrees)
----- TURBINE CONFIGURATION -----
           3 NumBl      - Number of blades (-)
           63 TipRad     - The distance from the rotor apex to the blade tip (meters)
           1.5 HubRad    - The distance from the rotor apex to the blade root (meters)
           -2.5 PreCone(1) - Blade 1 cone angle (degrees)
           -2.5 PreCone(2) - Blade 2 cone angle (degrees)
           -2.5 PreCone(3) - Blade 3 cone angle (degrees) [unused for 2 blades]
           0 HubCM       - Distance from rotor apex to hub mass [positive downwind] (meters)
           0 UndSling    - Undersling length [distance from teeter pin to the rotor apex] (meters) [unused for 3 blades]
           0 Delta3      - Delta-3 angle for teetering rotors (degrees) [unused for 3 blades]
           0 AzimB1Up    - Azimuth value to use for I/O when blade 1 points up (degrees)
           -5.0191 OverHang - Distance from yaw axis to rotor apex [3 blades] or teeter pin [2 blades] (meters)
           1.912 ShftGagl - Distance from rotor apex [3 blades] or teeter pin [2 blades] to shaft strain gages [positive for
upwind rotors] (meters)
           -5 ShftTilt   - Rotor shaft tilt angle (degrees)
           1.9 NacCMxn    - Downwind distance from the tower-top to the nacelle CM (meters)
           0 NacCMyn     - Lateral distance from the tower-top to the nacelle CM (meters)
           1.75 NacCMzn   - Vertical distance from the tower-top to the nacelle CM (meters)
           -3.09528 NcIMUxn - Downwind distance from the tower-top to the nacelle IMU (meters)
           0 NcIMUyn     - Lateral distance from the tower-top to the nacelle IMU (meters)
           2.23336 NcIMUzn - Vertical distance from the tower-top to the nacelle IMU (meters)
           1.96256 Twr2Shft - Vertical distance from the tower-top to the rotor shaft (meters)
           87.6 TowerHt   - Height of tower above ground level [onshore] or MSL [offshore] (meters)
           10 TowerBsHt  - Height of tower base above ground level [onshore] or MSL [offshore] (meters)
           0 PtfmCMxt    - Downwind distance from the ground level [onshore] or MSL [offshore] to the platform CM (meters)
           0 PtfmCMyt    - Lateral distance from the ground level [onshore] or MSL [offshore] to the platform CM (meters)
           10 PtfmCMzt   - Vertical distance from the ground level [onshore] or MSL [offshore] to the platform CM (meters)
           10 PtfmRefzt  - Vertical distance from the ground level [onshore] or MSL [offshore] to the platform reference
point (meters)
----- MASS AND INERTIA -----
           0 TipMass(1)  - Tip-brake mass, blade 1 (kg)
           0 TipMass(2)  - Tip-brake mass, blade 2 (kg)
           0 TipMass(3)  - Tip-brake mass, blade 3 (kg) [unused for 2 blades]
           56780 HubMass  - Hub mass (kg)
           115926 HubIner - Hub inertia about rotor axis [3 blades] or teeter axis [2 blades] (kg m^2)
           534.116 GenIner - Generator inertia about HSS (kg m^2)
           240000 NacMass  - Nacelle mass (kg)
           2.60789E+06 NacYIner - Nacelle inertia about yaw axis (kg m^2)

```

```

                                NRELOffshBrBsline5MW_OC3Monopile_ElastoDyn
0   YawBrMass - Yaw bearing mass (kg)
0   PtfmMass  - Platform mass (kg)
0   PtfmRIner - Platform inertia for roll tilt rotation about the platform CM (kg m^2)
0   PtfmPIner - Platform inertia for pitch tilt rotation about the platform CM (kg m^2)
1.534E+06 PtfmYIner - Platform inertia for yaw rotation about the platform CM (kg m^2)
----- BLADE -----
17  BldNodes  - Number of blade nodes (per blade) used for analysis (-)
"NRELOffshBrBsline5MW_Blade.dat"  BldFile(1) - Name of file containing properties for blade 1 (quoted string)
"NRELOffshBrBsline5MW_Blade.dat"  BldFile(2) - Name of file containing properties for blade 2 (quoted string)
"NRELOffshBrBsline5MW_Blade.dat"  BldFile(3) - Name of file containing properties for blade 3 (quoted string) [unused for 2
blades]
----- ROTOR-TEETER -----
0   TeetMod   - Rotor-teeter spring/damper model {0: none, 1: standard, 2: user-defined from routine UserTeet}
(switch) [unused for 3 blades]
0   TeetDmpP  - Rotor-teeter damper position (degrees) [used only for 2 blades and when TeetMod=1]
0   TeetDmp   - Rotor-teeter damping constant (N-m/(rad/s)) [used only for 2 blades and when TeetMod=1]
0   TeetCDmp  - Rotor-teeter rate-independent Coulomb-damping moment (N-m) [used only for 2 blades and when
TeetMod=1]
0   TeetSStP  - Rotor-teeter soft-stop position (degrees) [used only for 2 blades and when TeetMod=1]
0   TeetHStP  - Rotor-teeter hard-stop position (degrees) [used only for 2 blades and when TeetMod=1]
0   TeetSSSp  - Rotor-teeter soft-stop linear-spring constant (N-m/rad) [used only for 2 blades and when
TeetMod=1]
0   TeetHSSp  - Rotor-teeter hard-stop linear-spring constant (N-m/rad) [used only for 2 blades and when
TeetMod=1]
----- DRIVETRAIN -----
100 GBoxEff   - Gearbox efficiency (%)
97  GBRatio   - Gearbox ratio (-)
8.67637E+08 DTTorSpr - Drivetrain torsional spring (N-m/rad)
6.215E+06  DTTorDmp - Drivetrain torsional damper (N-m/(rad/s))
----- FURLING -----
False  Furling - Read in additional model properties for furling turbine (flag) [must currently be FALSE]
"unused" FurlFile - Name of file containing furling properties (quoted string) [unused when Furling=False]
----- TOWER -----
20  TwrNodes - Number of tower nodes used for analysis (-)
"NRELOffshBrBsline5MW_OC3Monopile_ElastoDyn_Tower.dat" TwrFile - Name of file containing tower properties (quoted
string)
----- OUTPUT -----
True  SumPrint - Print summary data to "<RootName>.sum" (flag)
1  OutFile   - Switch to determine where output will be placed: {1: in module output file only; 2: in glue code
output file only; 3: both} (currently unused)
True  TabDelim - Use tab delimiters in text tabular output file? (flag) (currently unused)
"ES10.3E2" OutFmt - Format used for text tabular output (except time). Resulting field should be 10 characters.
(quoted string) (currently unused)
0  TStart    - Time to begin tabular output (s) (currently unused)
1  DecFact   - Decimation factor for tabular output {1: output every time step} (-) (currently unused)
1  NTwGages  - Number of tower nodes that have strain gages for output [0 to 9] (-)
20 TwrGagNd  - List of tower nodes that have strain gages [1 to TwrNodes] (-) [unused if NTwGages=0]
3  NBlGages  - Number of blade nodes that have strain gages for output [0 to 9] (-)
5, 9, 13 BldGagNd - List of blade nodes that have strain gages [1 to BldNodes] (-) [unused
if NBlGages=0]
OutList - The next line(s) contains a list of output parameters. See OutListParameters.xlsx for a listing
of available output channels, (-)
"OoPDefl1, IPDefl1, TwstDefl1" - Blade 1 out-of-plane and in-plane deflections and tip twist
"BldPitch1" - Blade 1 pitch angle
"Azimuth" - Blade 1 azimuth angle
"RotSpeed, GenSpeed" - Low-speed shaft and high-speed shaft speeds
"TwHt1TPxi, TwHt1TPyi, TTDspTwst" - Tower fore-aft and side-to-side displacements and top twist
"PtfmSurge, PtfmSway" - Platform horizontal surge displacement
"PtfmRoll, PtfmPitch" - Platform rotational displacements
"Spn2MLxb1, Spn2MLyb1" - Blade 1 local edgewise and flapwise bending moments at span station 2 (approx. 50% span)
"RootFxc1, RootFyc1, RootFzc1" - Out-of-plane shear, in-plane shear, and axial forces at the root of blade 1
"RootMxc1, RootMyc1, RootMzc1" - In-plane bending, out-of-plane bending, and pitching moments at the root of blade 1
"RotTorq, LSSGagMya, LSSGagMza" - Rotor torque and low-speed shaft 0- and 90-bending moments at the main bearing
"YawBrFxp, YawBrFyp, YawBrFzp" - Fore-aft shear, side-to-side shear, and vertical forces at the top of the tower (not
rotating with nacelle yaw)
"YawBrMxp, YawBrMyp, YawBrMzp" - Side-to-side bending, fore-aft bending, and yaw moments at the top of the tower (not
rotating with nacelle yaw)
END of input file (the word "END" must appear in the first 3 columns of this last OutList line)
-----

```

A.3 ElastoDyn Tower File

```

NRELOffshrbaseline5MW_OC3Monopile_ElastoDyn_Tower
----- ELASTODYN V1.00.* TOWER INPUT FILE -----
NREL 5.0 MW offshore baseline monopile tower for flexible monopile modeled in SubDyn.
----- TOWER PARAMETERS -----
    11  NTwInpSt  - Number of input stations to specify tower geometry
    1.0  TwrFADmp(1) - Tower 1st fore-aft mode structural damping ratio (%)
    1.0  TwrFADmp(2) - Tower 2nd fore-aft mode structural damping ratio (%)
    1.0  TwrSSDmp(1) - Tower 1st side-to-side mode structural damping ratio (%)
    1.0  TwrSSDmp(2) - Tower 2nd side-to-side mode structural damping ratio (%)
----- TOWER ADJUSTMUNT FACTORS -----
    1.0  FASTunr(1) - Tower fore-aft modal stiffness tuner, 1st mode (-)
    1.0  FASTunr(2) - Tower fore-aft modal stiffness tuner, 2nd mode (-)
    1.0  SSSStunr(1) - Tower side-to-side stiffness tuner, 1st mode (-)
    1.0  SSSStunr(2) - Tower side-to-side stiffness tuner, 2nd mode (-)
    1.0  AdjTwMa  - Factor to adjust tower mass density (-)
    1.0  AdjFAST  - Factor to adjust tower fore-aft stiffness (-)
    1.0  AdjSSSt  - Factor to adjust tower side-to-side stiffness (-)
----- DISTRIBUTED TOWER PROPERTIES -----
HtFract      TMassDen      TwFASTif      TwSSStif
(-)           (kg/m)           (Nm^2)        (Nm^2)
0.0           4.3065100E+03   4.7449000E+11 4.7449000E+11
1.0E-01      4.0304400E+03   4.1308000E+11 4.1308000E+11
2.0E-01      3.7634500E+03   3.5783000E+11 3.5783000E+11
3.0E-01      3.5055200E+03   3.0830000E+11 3.0830000E+11
4.0E-01      3.2566600E+03   2.6408000E+11 2.6408000E+11
5.0E-01      3.0168600E+03   2.2480000E+11 2.2480000E+11
6.0E-01      2.7861300E+03   1.9006000E+11 1.9006000E+11
7.0E-01      2.5644600E+03   1.5949000E+11 1.5949000E+11
8.0E-01      2.3518700E+03   1.3277000E+11 1.3277000E+11
9.0E-01      2.1483400E+03   1.0954000E+11 1.0954000E+11
1.0E+00      1.9538700E+03   8.9490000E+10 8.9490000E+10
----- TOWER FORE-AFT MODE SHAPES -----
    0.9877  TwFAM1Sh(2) - Mode 1, coefficient of x^2 term
    0.1608  TwFAM1Sh(3) -           , coefficient of x^3 term
   -0.1884  TwFAM1Sh(4) -           , coefficient of x^4 term
    0.1508  TwFAM1Sh(5) -           , coefficient of x^5 term
   -0.1108  TwFAM1Sh(6) -           , coefficient of x^6 term
   -1.0297  TwFAM2Sh(2) - Mode 2, coefficient of x^2 term
    1.4443  TwFAM2Sh(3) -           , coefficient of x^3 term
    0.8883  TwFAM2Sh(4) -           , coefficient of x^4 term
   -0.1276  TwFAM2Sh(5) -           , coefficient of x^5 term
   -0.1752  TwFAM2Sh(6) -           , coefficient of x^6 term
----- TOWER SIDE-TO-SIDE MODE SHAPES -----
    0.9792  TwSSM1Sh(2) - Mode 1, coefficient of x^2 term
    0.1618  TwSSM1Sh(3) -           , coefficient of x^3 term
   -0.1797  TwSSM1Sh(4) -           , coefficient of x^4 term
    0.1453  TwSSM1Sh(5) -           , coefficient of x^5 term
   -0.1065  TwSSM1Sh(6) -           , coefficient of x^6 term
   -1.2253  TwSSM2Sh(2) - Mode 2, coefficient of x^2 term
    1.3297  TwSSM2Sh(3) -           , coefficient of x^3 term
    1.0340  TwSSM2Sh(4) -           , coefficient of x^4 term
   -0.1508  TwSSM2Sh(5) -           , coefficient of x^5 term
    0.0123  TwSSM2Sh(6) -           , coefficient of x^6 term

```

A.4 SubDyn Input File

```

NRELOffshrbaseline5MW_OC3Monopile_SubDyn
----- SubDyn v1.01.x MultiMember Support Structure Input File -----
OC3 Monopile configuration (pile only).
----- SIMULATION CONTROL -----
False      Echo          - Echo input data to "<rootname>.SD.ech" (flag)
"DEFAULT"  SDdeltaT             - Local Integration Step. If "default", the glue-code integration step will be used.
3          IntMethod    - Integration Method [1/2/3/4 = RK4/AB4/ABM4/AM2].
True       SttcSolve    - Solve dynamics about static equilibrium point
----- FEA and CRAIG-BAMPTON PARAMETERS -----
3          FEMMod      - FEM switch: element model in the FEM. [1= Euler-Bernoulli(E-B); 2=Tapered E-B (unavailable);
3= 2-node Timoshenko; 4= 2-node tapered Timoshenko (unavailable)]
3          NDiv        - Number of sub-elements per member
True       CBMod       - [T/F] If True perform C-B reduction, else full FEM dofs will be retained. If True, select
Nmodes to retain in C-B reduced system.
0          Nmodes      - Number of internal modes to retain (ignored if CBMod=False). If Nmodes=0 --> Guyan Reduction.
1          JDampings   - Damping Ratios for each retained mode (% of critical) If Nmodes>0, list Nmodes structural
damping ratios for each retained mode (% of critical), or a single damping ratio to be applied to all retained modes. (last
entered value will be used for all remaining modes).
---- STRUCTURE JOINTS: joints connect structure members (~Hydrodyn Input File)---
4          NJoints    - Number of joints (-)
JointID   JointXss      JointYss      JointZss [Coordinates of Member joints in SS-Coordinate
System]
(-)       (m)          (m)          (m)
1         0.00000      0.00000      -20.00010
2         0.00000      0.00000      -10.00000
3         0.00000      0.00000      0.00000
4         0.00000      0.00000      10.00000
----- BASE REACTION JOINTS: 1/0 for Locked/Free DOF @ each Reaction Node -----
1          NReact     - Number of Joints with reaction forces; be sure to remove all rigid motion DOFs of the
structure (else det([K])=0)]
RJointID  RctTDXss      RctTDYss      RctTDZss      RctRDXss      RctRDYss      RctRDZss      [Global Coordinate System]
(-)       (flag)      (flag)      (flag)      (flag)      (flag)      (flag)
1         1         1         1         1         1         1         ""
----- INTERFACE JOINTS: 1/0 for Locked (to the TP)/Free DOF @each Interface Joint (only Locked-to-TP implemented thus far
(=rigid TP)) -----
1          NInterf    - Number of interface joints locked to the Transition Piece (TP): be sure to remove all rigid
motion dofs
IJointID  ItfTDXss      ItfTDYss      ItfTDZss      ItfRDXss      ItfRDYss      ItfRDZss      [Global Coordinate System]
(-)       (flag)      (flag)      (flag)      (flag)      (flag)      (flag)
4         1         1         1         1         1         1
----- MEMBERS -----
3          NMembers   - Number of frame members
MemberID  MJointID1     MJointID2     MPropSetID1   MPropSetID2   COSMID
(-)       (-)          (-)          (-)          (-)          (-)
1         1         2         1         1
2         2         3         1         1
3         3         4         1         1
----- MEMBER X-SECTION PROPERTY data 1/2 [isotropic material for now: use this table for circular-tubular
elements] -----
4          NPropSets  - Number of structurally unique x-sections (i.e. how many groups of X-sectional properties are
utilized throughout all of the members)
PropSetID YoungE        ShearG        MatDens        XsecD        XsecT
(-)       (N/m2)       (N/m2)       (kg/m3)       (m)          (m)
1         2.10000e+11 8.08000e+10 8500.00       6.000000    0.060000
2         2.10000e+11 8.08000e+10 8500.00       6.000000    0.027000
3         2.10000e+11 8.08000e+10 8500.00       3.870000    0.019000
4         2.10000e+14 8.08000e+14 1.00          1.000000    0.010000
----- MEMBER X-SECTION PROPERTY data 2/2 [isotropic material for now: use this table if any section other than
circular, however provide COSM(i,j) below] -----
0          NXPPropSets - Number of structurally unique non-circular x-sections (if 0 the following table is ignored)
PropSetID YoungE        ShearG        MatDens        XsecA        XsecAsx        XsecAsy        XsecJyy        XsecJxx
XsecJyy   XsecJ0
(-)       (N/m2)       (N/m2)       (kg/m3)       (m2)          (m2)          (m2)          (m4)          (m4)
(m4)
----- MEMBER COSINE MATRICES COSM(i,j) -----
0          NCOSMs    - Number of unique cosine matrices (i.e., of unique member alignments including principal axis
rotations); ignored if NXPPropSets=0 or 9999 in any element below
COSMID    COSM11     COSM12     COSM13     COSM21     COSM22     COSM23     COSM31     COSM32     COSM33
(-)       (-)       (-)       (-)       (-)       (-)       (-)       (-)       (-)       (-)
----- JOINT ADDITIONAL CONCENTRATED MASSES -----
0          NCmass    - Number of joints with concentrated masses; Global Coordinate System
CMJointID JMass      JMXX      JMYX      JMZZ
(-)       (kg)      (kg*m^2) (kg*m^2) (kg*m^2)
----- OUTPUT: SUMMARY & OUTFILE -----
True      SSSum      - Output a Summary File (flag).It contains: matrices K,M and C-B reduced M_BB, M-BM, K_BB,
K_MM(OMG^2), PHI_R, PHI_L. It can also contain COSMs if requested.
False     OutCOSM    - Output cosine matrices with the selected output member forces (flag)
False     OutAll     - [T/F] Output all members' end forces
2         OutSwTch  - [1/2/3] Output requested channels to: 1=<rootname>.SD.out; 2=<rootname>.out (generated by
FAST); 3=both files.
True      TabDelim   - Generate a tab-delimited output in the <rootname>.SD.out file
1         OutDec    - Decimation of output in the <rootname>.SD.out file
"ES11.4e2" OutFmt     - Output format for numerical results in the <rootname>.SD.out file
"A11"     OutSFmt    - Output format for header strings in the <rootname>.SD.out file

```

```

----- MEMBER OUTPUT LIST -----
      2  NMOutputs  - Number of members whose forces/displacements/velocities/accelerations will be output (-) [Must
be <= 9].
MemberID  NOutCnt  NodeCnt [NOutCnt=how many nodes to get output for [< 10]; NodeCnt are local ordinal numbers from the
start of the member, and must be >=1 and <= NDiv+1] If NMOutputs=0 leave blank as well.
  (-)      (-)      (-)
    2         1         1
    3         1         1
----- SSOuList: The next line(s) contains a list of output parameters that will be output in
<rootname>.SD.out or <rootname>.out. -----
"M2N1MKxe, M2N1MKye" - The local side-to-side and fore-aft bending moments at node 1 of member 3 (located at
0 m, i.e. MSL).
"M1N1MKxe, M1N1MKye" - The local side-to-side and fore-aft bending moments at node 1 of member 2 (located at
-10 m, i.e. half way between MSL and mudline).
"-ReactFXss, -ReactFYss, -ReactFZss" - Base reactions: fore-aft shear, side-to-side shear and vertical forces at the mudline.
"-ReactMXss, -ReactMYss, -ReactMZss" - Base reactions: side-to-side, fore-aft and yaw moments at the mudline.
END of output channels and end of file. (the word "END" must appear in the first 3 columns of this line)

```

A.5 ServoDyn Input File

```

----- NRELOffshrbSline5MW_OC3Monopile_ServoDyn -----
----- SERVODYN v1.05.* INPUT FILE -----
NREL 5.0 MW Baseline Wind Turbine for Use in Offshore Analysis. Properties from Dutch Offshore Wind Energy Converter (DOWEC)
6MW Pre-Design (10046_009.pdf) and REpower 5M 5MW (5m_uk.pdf);
----- SIMULATION CONTROL -----
False      Echo          - Echo input data to <RootName>.ech (flag)
"default"  DT              - Communication interval for controllers (s) (or "default")
----- PITCH CONTROL -----
5          PCMode      - Pitch control mode {0: none, 3: user-defined from routine PitchCntrl, 4: user-defined from
Simulink/Labview, 5: user-defined from Bladed-style DLL} (switch)
0          TPCOn       - Time to enable active pitch control (s) [unused when PCMode=0]
9999.9    TPitManS(1) - Time to start override pitch maneuver for blade 1 and end standard pitch control (s)
9999.9    TPitManS(2) - Time to start override pitch maneuver for blade 2 and end standard pitch control (s)
9999.9    TPitManS(3) - Time to start override pitch maneuver for blade 3 and end standard pitch control (s) [unused for
2 blades]
2          PitManRat(1) - Pitch rate at which override pitch maneuver heads toward final pitch angle for blade 1 (deg/s)
2          PitManRat(2) - Pitch rate at which override pitch maneuver heads toward final pitch angle for blade 2 (deg/s)
2          PitManRat(3) - Pitch rate at which override pitch maneuver heads toward final pitch angle for blade 3 (deg/s)
[unused for 2 blades]
0          BlPitchF(1) - Blade 1 final pitch for pitch maneuvers (degrees)
0          BlPitchF(2) - Blade 2 final pitch for pitch maneuvers (degrees)
0          BlPitchF(3) - Blade 3 final pitch for pitch maneuvers (degrees) [unused for 2 blades]
----- GENERATOR AND TORQUE CONTROL -----
5          VSContrl    - Variable-speed control mode {0: none, 1: simple VS, 3: user-defined from routine UserVSCont, 4:
user-defined from Simulink/Labview, 5: user-defined from Bladed-style DLL} (switch)
2          GenModel    - Generator model {1: simple, 2: Thevenin, 3: user-defined from routine UserGen} (switch) [used
only when VSContrl=0]
94.4      GenEff       - Generator efficiency [ignored by the Thevenin and user-defined generator models] (%)
True      GenTiStr    - Method to start the generator {T: timed using TimGenOn, F: generator speed using SpdGenOn}
(flag)
True      GenTiStp    - Method to stop the generator {T: timed using TimGenOf, F: when generator power = 0} (flag)
9999.9    SpdGenOn    - Generator speed to turn on the generator for a startup (HSS speed) (rpm) [used only when
GenTiStr=False]
0          TimGenOn    - Time to turn on the generator for a startup (s) [used only when GenTiStr=True]
9999.9    TimGenOf    - Time to turn off the generator (s) [used only when GenTiStp=True]
----- SIMPLE VARIABLE-SPEED TORQUE CONTROL -----
9999.9    VS_RtGnSp   - Rated generator speed for simple variable-speed generator control (HSS side) (rpm) [used only
when VSContrl=1]
9999.9    VS_RtTq     - Rated generator torque/constant generator torque in Region 3 for simple variable-speed generator
control (HSS side) (N-m) [used only when VSContrl=1]
9999.9    VS_Rgn2K    - Generator torque constant in Region 2 for simple variable-speed generator control (HSS side)
(N-m/rpm^2) [used only when VSContrl=1]
9999.9    VS_SlPc     - Rated generator slip percentage in Region 2 1/2 for simple variable-speed generator control (%)
[used only when VSContrl=1]
----- SIMPLE INDUCTION GENERATOR -----
9999.9    SIG_SlPc    - Rated generator slip percentage (%) [used only when VSContrl=0 and GenModel=1]
9999.9    SIG_SySp    - Synchronous (zero-torque) generator speed (rpm) [used only when VSContrl=0 and GenModel=1]
9999.9    SIG_RtTq    - Rated torque (N-m) [used only when VSContrl=0 and GenModel=1]
9999.9    SIG_PORT    - Pull-out ratio (Tpullout/Trated) (-) [used only when VSContrl=0 and GenModel=1]
----- THEVENIN-EQUIVALENT INDUCTION GENERATOR -----
9999.9    TEC_Freq    - Line frequency [50 or 60] (Hz) [used only when VSContrl=0 and GenModel=2]
9998      TEC_NPol    - Number of poles [even integer > 0] (-) [used only when VSContrl=0 and GenModel=2]
9999.9    TEC_SRes    - Stator resistance (ohms) [used only when VSContrl=0 and GenModel=2]
9999.9    TEC_RRes    - Rotor resistance (ohms) [used only when VSContrl=0 and GenModel=2]
9999.9    TEC_VLL     - Line-to-line RMS voltage (volts) [used only when VSContrl=0 and GenModel=2]
9999.9    TEC_SLR     - Stator leakage reactance (ohms) [used only when VSContrl=0 and GenModel=2]
9999.9    TEC_RLR     - Rotor leakage reactance (ohms) [used only when VSContrl=0 and GenModel=2]
9999.9    TEC_MR      - Magnetizing reactance (ohms) [used only when VSContrl=0 and GenModel=2]
----- HIGH-SPEED SHAFT BRAKE -----
0          HSSBrMode  - HSS brake model {0: none, 1: simple, 3: user-defined from routine UserHSSBr, 4: user-defined
from Simulink/Labview, 5: user-defined from Bladed-style DLL} (switch)
9999.9    THSSBrDp    - Time to initiate deployment of the HSS brake (s)
0.6       HSSBrDT     - Time for HSS-brake to reach full deployment once initiated (sec) [used only when HSSBrMode=1]
28116.2   HSSBrTqF    - Fully deployed HSS-brake torque (N-m)
----- NACELLE-YAW CONTROL -----
0          YCMode     - Yaw control mode {0: none, 3: user-defined from routine UserYawCont, 4: user-defined from
Simulink/Labview, 5: user-defined from Bladed-style DLL} (switch)
9999.9    TYCon       - Time to enable active yaw control (s) [unused when YCMode=0]
0          YawNeut    - Neutral yaw position--yaw spring force is zero at this yaw (degrees)
9.02832E+09 YawSpr     - Nacelle-yaw spring constant (N-m/rad)
1.916E+07 YawDamp       - Nacelle-yaw damping constant (N-m/(rad/s))
9999.9    TYawManS    - Time to start override yaw maneuver and end standard yaw control (s)
2          YawManRat  - Yaw maneuver rate (in absolute value) (deg/s)
0          NacYawF    - Final yaw angle for override yaw maneuvers (degrees)
----- TUNED MASS DAMPER -----
False     CompNTMD    - Compute nacelle tuned mass damper {true/false} (flag)
"unused"  NTMDfFile     - Name of the file for nacelle tuned mass damper (quoted string) [unused when CompNTMD is false]
False     CompTTMD    - Compute tower tuned mass damper {true/false} (flag)
"unused"  TTMDfFile     - Name of the file for tower tuned mass damper (quoted string) [unused when CompTTMD is false]
----- BLADED INTERFACE ----- [used only with Bladed Interface]
"ServoData/DISCON_win32.dll" DLL_FileName - Name/location of the dynamic library {dll [Windows] or .so [Linux]} in the
Bladed-DLL format (-) [used only with Bladed Interface]
"DISCON.IN" DLL_InFile - Name of input file sent to the DLL (-) [used only with Bladed Interface]
"DISCON"   DLL_ProcName - Name of procedure in DLL to be called (-) [case sensitive; used only with DLL Interface]

```

```

                                NRELOffshrBsline5MW_OC3Monopile_ServoDyn
"default"    DLL_DT      - Communication interval for dynamic library (s) (or "default") [used only with Bladed Interface]
false       DLL_Ramp    - Whether a linear ramp should be used between DLL_DT time steps [introduces time shift when true]
(flag) [used only with Bladed Interface]
9999.9      BPCutoff    - Cutoff frequency for low-pass filter on blade pitch from DLL (Hz) [used only with Bladed
Interface]
0           NacYaw_North - Reference yaw angle of the nacelle when the upwind end points due North (deg) [used only with
Bladed Interface]
0           Ptch_Cntrl  - Record 28: Use individual pitch control {0: collective pitch; 1: individual pitch control}
( (switch) [used only with Bladed Interface]
0           Ptch_SetPnt - Record 5: Below-rated pitch angle set-point (deg) [used only with Bladed Interface]
0           Ptch_Min    - Record 6: Minimum pitch angle (deg) [used only with Bladed Interface]
0           Ptch_Max    - Record 7: Maximum pitch angle (deg) [used only with Bladed Interface]
0           PtchRate_Min - Record 8: Minimum pitch rate (most negative value allowed) (deg/s) [used only with Bladed
Interface]
0           PtchRate_Max - Record 9: Maximum pitch rate (deg/s) [used only with Bladed Interface]
0           Gain_OM     - Record 16: Optimal mode gain (Nm/(rad/s)^2) [used only with Bladed Interface]
0           GenSpd_MinOM - Record 17: Minimum generator speed (rpm) [used only with Bladed Interface]
0           GenSpd_MaxOM - Record 18: Optimal mode maximum speed (rpm) [used only with Bladed Interface]
0           GenSpd_Dem   - Record 19: Demanded generator speed above rated (rpm) [used only with Bladed Interface]
0           GenTrq_Dem   - Record 22: Demanded generator torque above rated (Nm) [used only with Bladed Interface]
0           GenPwr_Dem   - Record 13: Demanded power (W) [used only with Bladed Interface]
----- BLADED INTERFACE TORQUE-SPEED LOOK-UP TABLE -----
0           DLL_NumTrq  - Record 26: No. of points in torque-speed look-up table {0 = none and use the optimal mode
parameters; nonzero = ignore the optimal mode PARAMETERS by setting Record 16 to 0.0} (-) [used only with Bladed Interface]
GenSpd_TLU  GenTrq_TLU
(rpm)       (Nm)
----- OUTPUT -----
True        SumPrint    - Print summary data to <RootName>.sum (flag) (currently unused)
1           OutFile     - Switch to determine where output will be placed: {1: in module output file only; 2: in glue code
output file only; 3: both} (currently unused)
True        TabDelim    - Use tab delimiters in text tabular output file? (flag) (currently unused)
"ES10.3E2"  OutFmt      - Format used for text tabular output (except time). Resulting field should be 10 characters.
(quoted string) (currently unused)
30         TStart      - Time to begin tabular output (s) (currently unused)
           OutList     - The next line(s) contains a list of output parameters. See OutListParameters.xlsx for a listing
of available output channels, (-)
"GenPwr"   - Electrical generator power and torque
"GenTq"    - Electrical generator power and torque
END of input file (the word "END" must appear in the first 3 columns of this last OutList line)
-----

```


A.6 InflowWind File

```

----- InflowWind v3.01.* INPUT FILE -----
NRELOffshrBslime5MW_InflowWind_12mps
12 m/s turbulent winds on 31x31 FF grid and tower for FAST CertTests #18, #19, #21, #22, #23, and #24
-----
False      Echo      - Echo input data to <RootName>.ech (flag)
          3  WindType  - switch for wind file type (1=steady; 2=uniform; 3=binary TurbSim FF; 4=binary Bladed-style FF;
5=HAWC format; 6=User defined)
          0  PropagationDir - Direction of wind propagation (meteorological rotation from aligned with X (positive rotates
towards -Y) -- degrees)
          1  NWindVel   - Number of points to output the wind velocity (0 to 9)
          0  WindVxIList - List of coordinates in the inertial X direction (m)
          0  WindVyIList - List of coordinates in the inertial Y direction (m)
          90 WindVzIList - List of coordinates in the inertial Z direction (m)
===== Parameters for Steady Wind Conditions [used only for WindType = 1] =====
          0  HWindSpeed - Horizontal windspeed (m/s)
          90 RefHt     - Reference height for horizontal wind speed (m)
          0.2 PLExp    - Power law exponent (-)
===== Parameters for Uniform wind file [used only for WindType = 2] =====
"Wind/90m_12mps_twr.bts"  FileName - Filename of time series data for uniform wind field. (-)
          90 RefHt     - Reference height for horizontal wind speed (m)
          125.88 RefLength - Reference length for linear horizontal and vertical sheer (-)
===== Parameters for Binary TurbSim Full-Field files [used only for WindType = 3] =====
"Wind/90m_12mps_twr630.bts"  FileName - Name of the Full field wind file to use (.bts)
===== Parameters for Binary Bladed-style Full-Field files [used only for WindType = 4] =====
"Wind/90m_12mps_twr"  FileNameRoot - Rootname of the full-field wind file to use (.wnd, .sum)
False      TowerFile - Have tower file (.twr) (flag)
===== Parameters for HAWC-format binary files [Only used with WindType = 5] =====
"wasp\Output\basic_5u.bin"  FileName_u - name of the file containing the u-component fluctuating wind (.bin)
"wasp\Output\basic_5v.bin"  FileName_v - name of the file containing the v-component fluctuating wind (.bin)
"wasp\Output\basic_5w.bin"  FileName_w - name of the file containing the w-component fluctuating wind (.bin)
          64 nx       - number of grids in the x direction (in the 3 files above) (-)
          32 ny       - number of grids in the y direction (in the 3 files above) (-)
          32 nz       - number of grids in the z direction (in the 3 files above) (-)
          16 dx       - distance (in meters) between points in the x direction (m)
          3  dy       - distance (in meters) between points in the y direction (m)
          3  dz       - distance (in meters) between points in the z direction (m)
          90 RefHt    - reference height; the height (in meters) of the vertical center of the grid (m)
----- Scaling parameters for turbulence -----
          1  ScaleMethod - Turbulence scaling method [0 = none, 1 = direct scaling, 2 = calculate scaling factor based
on a desired standard deviation]
          1  SFx       - Turbulence scaling factor for the x direction (-) [ScaleMethod=1]
          1  SFy       - Turbulence scaling factor for the y direction (-) [ScaleMethod=1]
          1  SFz       - Turbulence scaling factor for the z direction (-) [ScaleMethod=1]
          12 SigmaFx   - Turbulence standard deviation to calculate scaling from in x direction (m/s)
[ScaleMethod=2]
          8  SigmaFy   - Turbulence standard deviation to calculate scaling from in y direction (m/s)
[ScaleMethod=2]
          2  SigmaFz   - Turbulence standard deviation to calculate scaling from in z direction (m/s)
[ScaleMethod=2]
----- Mean wind profile parameters (added to HAWC-format files) -----
          5  URef      - Mean u-component wind speed at the reference height (m/s)
          2  WindProfile - Wind profile type (0=constant;1=logarithmic;2=power law)
          0.2 PLExp    - Power law exponent (-) (used for PL wind profile type only)
          0.03 Z0      - Surface roughness length (m) (used for LG wind profile type only)
===== OUTPUT =====
False      SumPrint   - Print summary data to <RootName>.IfW.sum (flag)
          OutList    - The next line(s) contains a list of output parameters. See OutListParameters.xlsx for a listing
of available output channels, (-)
"Wind1VelX" X-direction wind velocity at point WindList(1)
"Wind1VelY" Y-direction wind velocity at point WindList(1)
"Wind1VelZ" Z-direction wind velocity at point WindList(1)
END of input file (the word "END" must appear in the first 3 columns of this last OutList line)
-----

```

A.7 AeroDyn Input File

```

----- AERODYN v15.03.* INPUT FILE -----
NREL 5.0 MW offshore baseline aerodynamic input properties, with OC3 Monopile tower
===== General Options =====
False      Echo          - Echo the input to "<rootname>.AD.ech"? (flag)
"default"  DTAero             - Time interval for aerodynamic calculations {or "default"} (s)
1          WakeMod      - Type of wake/induction model (switch) {0=none, 1=BEMT}
2          AFAeroMod    - Type of blade airfoil aerodynamics model (switch) {1=steady model, 2=Beddoes-Leishman
unsteady model}
1          TwrPotent    - Type tower influence on wind based on potential flow around the tower (switch) {0=none,
1=baseline potential flow, 2=potential flow with Bak correction}
False     TwrShadow     - Calculate tower influence on wind based on downstream tower shadow? (flag)
True      TwrAero       - Calculate tower aerodynamic loads? (flag)
False     FrozenWake    - Assume frozen wake during linearization? (flag) [used only when WakeMod=1 and when
linearizing]
===== Environmental Conditions =====
1.225     AirDens       - Air density (kg/m^3)
1.464E-05 KinVisc      - Kinematic air viscosity (m^2/s)
335      SpdSound      - Speed of sound (m/s)
===== Blade-Element/Momentum Theory Options ===== [used only when
WakeMod=1]
2          SkewMod      - Type of skewed-wake correction model (switch) {1=uncoupled, 2=Pitt/Peters, 3=coupled}
[used only when WakeMod=1]
True      TipLoss      - Use the Prandtl tip-loss model? (flag) [used only when WakeMod=1]
True      HubLoss      - Use the Prandtl hub-loss model? (flag) [used only when WakeMod=1]
true      TanInd       - Include tangential induction in BEMT calculations? (flag) [used only when WakeMod=1]
False     AIDrag       - Include the drag term in the axial-induction calculation? (flag) [used only when
WakeMod=1]
False     TIDrag       - Include the drag term in the tangential-induction calculation? (flag) [used only when
WakeMod=1 and TanInd=TRUE]
"default" IndToler     - Convergence tolerance for BEMT nonlinear solve residual equation {or "default"} (-) [used
only when WakeMod=1]
100      MaxIter       - Maximum number of iteration steps (-) [used only when WakeMod=1]
===== Beddoes-Leishman Unsteady Airfoil Aerodynamics Options ===== [used only when
AFAeroMod=2]
3          UAMod        - Unsteady Aero Model Switch (switch) {1=Baseline model (Original), 2=Gonzalez's variant
(changes in Cn,Cc,Cm), 3=Minemna/Pierce variant (changes in Cc and Cm)} [used only when AFAeroMod=2]
True      FLookup      - Flag to indicate whether a lookup for f' will be calculated (TRUE) or whether best-fit
exponential equations will be used (FALSE); if FALSE S1-S4 must be provided in airfoil input files (flag) [used only when
AFAeroMod=2]
===== Airfoil Information =====
1          InCol_Alfa   - The column in the airfoil tables that contains the angle of attack (-)
2          InCol_Cl     - The column in the airfoil tables that contains the lift coefficient (-)
3          InCol_Cd     - The column in the airfoil tables that contains the drag coefficient (-)
4          InCol_Cm     - The column in the airfoil tables that contains the pitching-moment coefficient; use zero
if there is no Cm column (-)
0          InCol_Cpmin  - The column in the airfoil tables that contains the Cpmin coefficient; use zero if there is
no Cpmin column (-)
8          NumAFfiles   - Number of airfoil files used (-)
"Airfoils/Cylinder1.dat" AFNames - Airfoil file names (NumAFfiles lines) (quoted strings)
"Airfoils/Cylinder2.dat"
"Airfoils/DU40_A17.dat"
"Airfoils/DU35_A17.dat"
"Airfoils/DU30_A17.dat"
"Airfoils/DU25_A17.dat"
"Airfoils/DU21_A17.dat"
"Airfoils/NACA64_A17.dat"
===== Rotor/Blade Properties =====
True      UseBlCm      - Include aerodynamic pitching moment in calculations? (flag)
"NRELOffshBrBslne5MW_AeroDyn_blade.dat" ADB1File(1) - Name of file containing distributed aerodynamic properties
for Blade #1 (-)
"NRELOffshBrBslne5MW_AeroDyn_blade.dat" ADB1File(2) - Name of file containing distributed aerodynamic properties
for Blade #2 (-) [unused if NumBl < 2]
"NRELOffshBrBslne5MW_AeroDyn_blade.dat" ADB1File(3) - Name of file containing distributed aerodynamic properties
for Blade #3 (-) [unused if NumBl < 3]
===== Tower Influence and Aerodynamics ===== [used only when
TwrPotent/=0, TwrShadow=True, or TwrAero=True]
11        NumTwrNds    - Number of tower nodes used in the analysis (-) [used only when TwrPotent/=0,
TwrShadow=True, or TwrAero=True]
TwrElev   TwrDiam      TwrCd
(m)       (m)         (-)
1.000000E+01 6.000000E+00 1.000000E+00
1.776000E+01 5.787000E+00 1.000000E+00
2.552000E+01 5.574000E+00 1.000000E+00
3.328000E+01 5.361000E+00 1.000000E+00
4.104000E+01 5.148000E+00 1.000000E+00
4.880000E+01 4.935000E+00 1.000000E+00
5.656000E+01 4.722000E+00 1.000000E+00
6.432000E+01 4.509000E+00 1.000000E+00
7.208000E+01 4.296000E+00 1.000000E+00
7.984000E+01 4.083000E+00 1.000000E+00
8.760000E+01 3.870000E+00 1.000000E+00
===== Outputs =====
True      SumPrint     - Generate a summary file listing input options and interpolated properties to

```

```

                                NRELOffshrBsline5MW_OC3Monopile_AeroDyn15
"<rootname>.AD.sum"? (flag)
    0  NB1Outs      - Number of blade node outputs [0 - 9] (-)
    2, 9, 16, 4, 5, 7, 11, 13, 14  B1OutNd
- Blade nodes whose values will be output (-)
    0  NTwOuts     - Number of tower node outputs [0 - 9] (-)
    1, 2, 3, 4, 5  TwOutNd      - Tower nodes whose values will be output
(-)
    OutList      - The next line(s) contains a list of output parameters. See OutListParameters.xlsx
for a listing of available output channels, (-)
"RtAeroFhx, RtAeroFyh, RtAeroFzh"
"RtAeroMhx, RtAeroMyh, RtAeroMzh"
END of input file (the word "END" must appear in the first 3 columns of this last OutList line)
-----

```

A.8 HydroDyn Input File

```

                                NRELOffshBsrBslne5MW_OC3Monopile_HydroDyn
Pro----- HydroDyn v2.03.* Input File -----
NREL 5.0 MW offshore baseline floating platform input properties for the OC3 Monopile.
False      Echo          - Echo the input file data (flag)
----- ENVIRONMENTAL CONDITIONS -----
      1027  WtrDens      - Water density (kg/m^3)
      20    WtrDpth      - Water depth (meters)
      0     MSL2SWL      - Offset between still-water level and mean sea level (meters) [positive upward; unused when
WaveMod = 6; must be zero if PotMod=1 or 2]
----- WAVES -----
      2     WaveMod      - Incident wave kinematics model {0: none=still water, 1: regular (periodic), 1P#: regular
with user-specified phase, 2: JONSWAP/Pierson-Moskowitz spectrum (irregular), 3: White noise spectrum (irregular), 4:
user-defined spectrum from routine UserWaveSpctrm (irregular), 5: Externally generated wave-elevation time series, 6:
Externally generated full wave-kinematics time series [option 6 is invalid for PotMod=0]} (switch)
      0     WaveStMod      - Model for stretching incident wave kinematics to instantaneous free surface {0: none=no
stretching, 1: vertical stretching, 2: extrapolation stretching, 3: Wheeler stretching} (switch) [unused when WaveMod=0 or
when PotMod=0]
      3630  WaveTMax      - Analysis time for incident wave calculations (sec) [unused when WaveMod=0; determines
WaveDOmega=2Pi/WaveTMax in the IFFT]
      0.25  WaveDT        - Time step for incident wave calculations (sec) [unused when WaveMod=0; 0.1<=WaveDT<=1.0
recommended; determines WaveOmegaMax=Pi/WaveDT in the IFFT]
      6     WaveHs        - Significant wave height of incident waves (meters) [used only when WaveMod=1, 2, or 3]
      10    WaveTp        - Peak-spectral period of incident waves (sec) [used only when WaveMod=1 or 2]
"DEFAULT" WavePkShp      - Peak-shape parameter of incident wave spectrum (-) or DEFAULT (string) [used only when
WaveMod=2; use 1.0 for Pierson-Moskowitz]
      0.15708 WvLowCOff    - Low cut-off frequency or lower frequency limit of the wave spectrum beyond which the wave
spectrum is zeroed (rad/s) [unused when WaveMod=0, 1, or 6]
      3.2    WvHiCOff     - High cut-off frequency or upper frequency limit of the wave spectrum beyond which the wave
spectrum is zeroed (rad/s) [unused when WaveMod=0, 1, or 6]
      0     WaveDir      - Incident wave propagation heading direction (degrees) [unused when
WaveMod=0 or 6]
      0     WaveDirMod    - Directional spreading function {0: none, 1: COS2S} (-) [only used
when WaveMod=2,3, or 4]
      1     WaveDirSpread - Wave direction spreading coefficient ( > 0 ) (-) [only used
when WaveMod=2,3, or 4 and WaveDirMod=1]
      1     WaveNDir      - Number of wave directions (-) [only used
when WaveMod=2,3, or 4 and WaveDirMod=1; odd number only]
      90    WaveDirRange  - Range of wave directions (full range: WaveDir +/- 1/2*WaveDirRange) (degrees) [only used
when WaveMod=2,3, or 4 and WaveDirMod=1]
      123456789 WaveSeed(1) - First random seed of incident waves [-2147483648 to 2147483647] (-) [unused when
WaveMod=0, 5, or 6]
      1011121314 WaveSeed(2) - Second random seed of incident waves [-2147483648 to 2147483647] (-) [unused when
WaveMod=0, 5, or 6]
TRUE     WaveNDamp      - Flag for normally distributed amplitudes (flag) [only used
when WaveMod=2, 3, or 4]
""       WvKinFile      - Root name of externally generated wave data file(s) (quoted string) [used only
when WaveMod=5 or 6]
      1     NWaveElev     - Number of points where the incident wave elevations can be computed (-) [maximum of 9
output locations]
      0     WaveElevxi    - List of xi-coordinates for points where the incident wave elevations can be output (meters)
[NWaveElev points, separated by commas or white space; unused if NWaveElev = 0]
      0     WaveElevyi    - List of yi-coordinates for points where the incident wave elevations can be output (meters)
[NWaveElev points, separated by commas or white space; unused if NWaveElev = 0]
----- 2ND-ORDER WAVES ----- [unused with WaveMod=0 or 6]
True     WvDiffQTF      - Full difference-frequency 2nd-order wave kinematics (flag)
True     WvSumQTF       - Full summation-frequency 2nd-order wave kinematics (flag)
      0     WvLowCOFFD    - Low frequency cutoff used in the difference-frequencies (rad/s) [Only used with a
difference-frequency method]
      3.04292 WvHiCOFFD   - High frequency cutoff used in the difference-frequencies (rad/s) [Only used with a
difference-frequency method]
      0.314159 WvLowCOFFS - Low frequency cutoff used in the summation-frequencies (rad/s) [Only used with a
summation-frequency method]
      3.2    WvHiCOFFS   - High frequency cutoff used in the summation-frequencies (rad/s) [Only used with a
summation-frequency method]
----- CURRENT ----- [unused with WaveMod=6]
      0     CurrMod      - Current profile model {0: none=no current, 1: standard, 2: user-defined from routine
UserCurrent} (switch)
      0     CurrSSV0     - Sub-surface current velocity at still water level (m/s) [used only when CurrMod=1]
"DEFAULT" CurrSSDir     - Sub-surface current heading direction (degrees) or DEFAULT (string) [used only when
CurrMod=1]
      20    CurrNSRef     - Near-surface current reference depth (meters) [used only when CurrMod=1]
      0     CurrNSV0     - Near-surface current velocity at still water level (m/s) [used only when CurrMod=1]
      0     CurrNSDir    - Near-surface current heading direction (degrees) [used only when CurrMod=1]
      0     CurrDIV      - Depth-independent current velocity (m/s) [used only when CurrMod=1]
      0     CurrDIDir    - Depth-independent current heading direction (degrees) [used only when CurrMod=1]
----- FLOATING PLATFORM ----- [unused with WaveMod=6]
      0     PotMod      - Potential-flow model {0: none=no potential flow, 1: frequency-to-time-domain transforms
based on WAMIT output, 2: fluid-impulse theory (FIT)} (switch)
"unused" PotFile        - Root name of potential-flow model data; WAMIT output files containing the linear,
nondimensionalized, hydrostatic restoring matrix (.hst), frequency-dependent hydrodynamic added mass matrix and damping
matrix (.1), and frequency- and direction-dependent wave excitation force vector per unit wave amplitude (.3) (quoted string)
[MAKE SURE THE FREQUENCIES INHERENT IN THESE WAMIT FILES SPAN THE PHYSICALLY-SIGNIFICANT RANGE OF FREQUENCIES FOR THE GIVEN
PLATFORM; THEY MUST CONTAIN THE ZERO- AND INFINITE-FREQUENCY LIMITS!]
      1     WAMITULEN    - Characteristic body length scale used to redimensionalize WAMIT output (meters) [only used

```

NREOffshrbaseline5MW_OC3Monopile_HydroDyn

```

when PotMod=1]
0 PtfmVol0 - Displaced volume of water when the platform is in its undisplaced position (m^3) [only used
when PotMod=1; USE THE SAME VALUE COMPUTED BY WAMIT AS OUTPUT IN THE .OUT FILE!]
0 PtfmCOBxt - The xt offset of the center of buoyancy (COB) from the platform reference point (meters)
[only used when PotMod=1]
0 PtfmCOByt - The yt offset of the center of buoyancy (COB) from the platform reference point (meters)
[only used when PotMod=1]
1 RdtnMod - Radiation memory-effect model {0: no memory-effect calculation, 1: convolution, 2:
state-space} (switch) [only used when PotMod=1; STATE-SPACE REQUIRES *.ss INPUT FILE]
60 RdtnTMax - Analysis time for wave radiation kernel calculations (sec) [only used when PotMod=1;
determines RdtnDOmega=Pi/RdtnTMax in the cosine transform; MAKE SURE THIS IS LONG ENOUGH FOR THE RADIATION IMPULSE RESPONSE
FUNCTIONS TO DECAY TO NEAR-ZERO FOR THE GIVEN PLATFORM!]
0.005 RdtnDT - Time step for wave radiation kernel calculations (sec) [only used when PotMod=1;
DT<=RdtnDT<=0.1 recommended; determines RdtnOmegaMax=Pi/RdtnDT in the cosine transform]
----- 2ND-ORDER FLOATING PLATFORM FORCES ----- [unused with WaveMod=0 or 6, or PotMod=0 or
2]
0 MnDrift - Mean-drift 2nd-order forces computed {0: None; [7, 8,
9, 10, 11, or 12]: WAMIT file to use} [Only one of MnDrift, NewmanApp, or DiffQTF can be non-zero]
0 NewmanApp - Mean- and slow-drift 2nd-order forces computed with Newman's approximation {0: None; [7, 8,
9, 10, 11, or 12]: WAMIT file to use} [Only one of MnDrift, NewmanApp, or DiffQTF can be non-zero. Used only when
WaveDirMod=0]
0 DiffQTF - Full difference-frequency 2nd-order forces computed with full QTF {0: None; [10,
11, or 12]: WAMIT file to use} [Only one of MnDrift, NewmanApp, or DiffQTF can be non-zero]
0 SumQTF - Full summation -frequency 2nd-order forces computed with full QTF {0: None; [10,
11, or 12]: WAMIT file to use}
----- FLOATING PLATFORM FORCE FLAGS ----- [unused with WaveMod=6]
TRUE PtfmSgF - Platform horizontal surge translation force (flag) or DEFAULT
TRUE PtfmSwF - Platform horizontal sway translation force (flag) or DEFAULT
TRUE PtfmHVF - Platform vertical heave translation force (flag) or DEFAULT
TRUE PtfmRF - Platform roll tilt rotation force (flag) or DEFAULT
TRUE PtfmPF - Platform pitch tilt rotation force (flag) or DEFAULT
TRUE PtfmYF - Platform yaw rotation force (flag) or DEFAULT
----- PLATFORM ADDITIONAL STIFFNESS AND DAMPING -----
0 0 0 0 0 0 AddF0 - Additional preload (N, N-m)
0 0 0 0 0 0 AddCLin - Additional linear stiffness
(N/m, N/rad, N-m/m, N-m/rad)
0 0 0 0 0 0
0 0 0 0 0 0
0 0 0 0 0 0
0 0 0 0 0 0
0 0 0 0 0 0 AddBLin - Additional linear
damping(N/(m/s), N/(rad/s), N-m/(m/s), N-m/(rad/s))
0 0 0 0 0 0
0 0 1462500 0 0 0
0 0 0 0 0 0
0 0 0 0 0 0
0 0 0 0 0 0
0 0 0 0 0 0 AddBQuad - Additional quadratic
drag(N/(m/s)^2, N/(rad/s)^2, N-m(m/s)^2, N-m/(rad/s)^2)
0 0 0 0 0 0
0 0 0 0 0 0
0 0 0 0 0 0
0 0 0 0 0 0
----- AXIAL COEFFICIENTS -----
1 NAXcoef - Number of axial coefficients (-)
AxCoefID AxCd AxCa AxCp
(-) (-) (-) (-)
1 0.00 0.00 1.00
----- MEMBER JOINTS -----
2 NJoints - Number of joints (-) [must be exactly 0 or at least 2]
JointID Jointxi Jointyi Jointzi JointAxID JointOvr1p [JointOvr1p= 0: do nothing at joint, 1: eliminate
overlaps by calculating super member]
(-) (m) (m) (m) (-) (switch)
1 0.00000 0.00000 -20.00010 1 0
2 0.00000 0.00000 10.00000 1 0
----- MEMBER CROSS-SECTION PROPERTIES -----
1 NPropSets - Number of member property sets (-)
PropSetID PropD PropThck
(-) (m) (m)
1 6.00000 0.06000
----- SIMPLE HYDRODYNAMIC COEFFICIENTS (model 1) -----
SimplCd SimplCdMG SimplCa SimplCaMG SimplCp SimplCpMG SimplAxCa SimplAxCaMG SimplAxCp SimplAxCpMG
(-) (-) (-) (-) (-) (-) (-) (-) (-) (-)
1.00 1.00 1.00 1.00 1.00 1.00 1.00 1.00 1.00 1.00
----- DEPTH-BASED HYDRODYNAMIC COEFFICIENTS (model 2) -----
0 NCoeffDpth - Number of depth-dependent coefficients (-)
Dpth DpthCd DpthCdMG DpthCa DpthCaMG DpthCp DpthCpMG DpthAxCa DpthAxCaMG DpthAxCp DpthAxCpMG
(m) (-) (-) (-) (-) (-) (-) (-) (-) (-)
----- MEMBER-BASED HYDRODYNAMIC COEFFICIENTS (model 3) -----
0 NCoeffMembers - Number of member-based coefficients (-)
MemberID MemberCd1 MemberCd2 MemberCdMG1 MemberCdMG2 MemberCa1 MemberCa2 MemberCaMG1 MemberCaMG2

```

```

NRELOffshBsrBsline5MW_OC3Monopile_HydroDyn
MemberCp1      MemberCp2      MemberCpMG1    MemberCpMG2    MemberAxCa1    MemberAxCa2    MemberAxCaMG1  MemberAxCaMG2  MemberAxCp1
MemberAxCp2    MemberAxCpMG1  MemberAxCpMG2
(-)            (-)            (-)            (-)            (-)            (-)            (-)            (-)            (-)
(-)            (-)            (-)            (-)            (-)            (-)            (-)            (-)            (-)
(-)            (-)            (-)
----- MEMBERS -----
1      NMembers      - Number of members (-)
MemberID  MJointID1  MJointID2  MPropSetID1  MPropSetID2  MDivSize  MCoefMod  PropPot  [MCoefMod=1: use simple coeff table,
2: use depth-based coeff table, 3: use member-based coeff table] [ PropPot/=0 if member is modeled with potential-flow
theory]
(-)      (-)      (-)      (-)      (-)      (m)      (switch)  (flag)
1         1         2         1         1         0.5000    1         FALSE
----- FILLED MEMBERS -----
0      NFillGroups  - Number of filled member groups (-) [If FillDens = DEFAULT, then FillDens = WtrDens;
FillFSLoc is related to MSL2SWL]
FillNumM  FillMList      FillFSLoc      FillDens
(-)      (-)            (m)            (kg/m^3)
----- MARINE GROWTH -----
0      NMGDepths    - Number of marine-growth depths specified (-)
MGDpth    MGTThk      MGDens
(m)      (m)      (kg/m^3)
----- MEMBER OUTPUT LIST -----
0      NMOutputs    - Number of member outputs (-) [must be < 10]
MemberID  NOutLoc      NodeLocs [NOutLoc < 10; node locations are normalized distance from the start of the member, and must
be >=0 and <= 1] [unused if NMOutputs=0]
(-)      (-)      (-)
----- JOINT OUTPUT LIST -----
0      NJOutputs    - Number of joint outputs [Must be < 10]
0      JOutLst      - List of JointIDs which are to be output (-)[unused if NJOutputs=0]
----- OUTPUT -----
True      HDSum      - Output a summary file [flag]
False     OutAll     - Output all user-specified member and joint loads (only at each member end, not interior
locations) [flag]
2      OutSwitch  - Output requested channels to: [1=Hydrodyn.out, 2=GlueCode.out, 3=both files]
"ES11.4e2"  OutFmt    - Output format for numerical results (quoted string) [not checked for validity!]
"A11"      OutSFmt   - Output format for header strings (quoted string) [not checked for validity!]
----- OUTPUT CHANNELS -----
"Wave1Elev" - Wave elevation at the WAMIT reference point (0,0)
END of output channels and end of file. (the word "END" must appear in the first 3 columns of this line)

```

B TurbSim Input File

90m_12mps_twr

TurbSim Input File.

```
-----Runtime Options-----
13428      RandSeed1      - First random seed (-2147483648 to 2147483647)
RanLux     RandSeed2      - Second random seed (-2147483648 to 2147483647) for intrinsic pRNG, or an alternative pRNG:
"RanLux" or "RNSNLW"
False     WrBHHTP      - Output hub-height turbulence parameters in binary form? (Generates RootName.bin)
False     WrFHHTP      - Output hub-height turbulence parameters in formatted form? (Generates RootName.dat)
False     WrADHH      - Output hub-height time-series data in AeroDyn form? (Generates RootName.hh)
True      WrADFF      - Output full-field time-series data in TurbSim/AeroDyn form? (Generates RootName.bts)
False     WrBLFF      - Output full-field time-series data in BLADED/AeroDyn form? (Generates RootName.bts)
True      WrADTWR      - Output tower time-series data? (Generates RootName.twr)
False     WrFMTFF      - Output full-field time-series data in formatted (readable) form? (Generates RootName.u,
RootName.v, RootName.w)
False     WrACT      - Output coherent turbulence time steps in AeroDyn form? (Generates RootName.cts)
True      Clockwise   - Clockwise rotation looking downwind? (used only for full-field binary files - not necessary
for AeroDyn)
0         ScaleIEC    - Scale IEC turbulence models to exact target standard deviation? [0=no additional scaling;
1=use hub scale uniformly; 2=use individual scales]

-----Turbine/Model Specifications-----
31        NumGrid_Z      - Vertical grid-point matrix dimension
31        NumGrid_Y      - Horizontal grid-point matrix dimension
0.05     TimeStep      - Time step [seconds]
630.0    AnalysisTime  - Length of analysis time series [seconds]
630.0    UsableTime   - Usable length of output time series [seconds] (program will add GridWidth/MeanHHWS seconds)
[bjj: was 630]
90.0     HubHt        - Hub height [m] (should be > 0.5*GridHeight)
145.0    GridHeight    - Grid height [m]
145.0    GridWidth    - Grid width [m] (should be >= 2*(RotorRadius+ShaftLength))
0        VFlowAng     - Vertical mean flow (uptilt) angle [degrees]
0        HFlowAng     - Horizontal mean flow (skew) angle [degrees]

-----Meteorological Boundary Conditions-----
IECKAI    TurbModel      - Turbulence model ("IECKAI"=Kaimal, "IECVKM"=von Karman, "GP_LLJ", "NWTUP", "SMOOTH",
"WF_UPW", "WF_07D", "WF_14D", or "NONE")
"1-ed3"   IECstandard  - Number of IEC 61400-x standard (x=1,2, or 3 with optional 61400-1 edition number (i.e.
"1-Ed2") )
"B"       IECturbc    - IEC turbulence characteristic ("A", "B", "C" or the turbulence intensity in percent)
("KHTST" option with NWTUP, not used for other models)
NTM       IECwindType  - IEC turbulence type ("NTM"=normal, "xETM"=extreme turbulence, "xEWM1"=extreme 1-year wind,
"xEWM50"=extreme 50-year wind, where x=wind turbine class 1, 2, or 3)
default   ETMc        - IEC Extreme turbulence model "c" parameter [m/s]
PL        WindProfileType - Wind profile type ("JET"=Low-level jet, "LOG"=Logarithmic, "PL"=Power law, or "default", or
"USR"=User-defined)
90.       RefHt       - Height of the reference wind speed [m]
12.0     URef         - Mean (total) wind speed at the reference height [m/s]
default   ZJetMax     - Jet height [m] (used only for JET wind profile, valid 70-490 m)
default   PLExp       - Power law exponent [-] (or "default")
default   Z0         - Surface roughness length [m] (or "default")

-----Non-IEC Meteorological Boundary Conditions-----
default   Latitude    - Site latitude [degrees] (or "default")
0.05     RICH_NO      - Gradient Richardson number
default   UStar       - Friction or shear velocity [m/s] (or "default")
default   ZI         - Mixing layer depth [m] (or "default")
default   PC_UW       - Hub mean u'w' Reynolds stress [(m/s)^2] (or "default")
default   PC_UV       - Hub mean u'v' Reynolds stress [(m/s)^2] (or "default")
default   PC_VW       - Hub mean v'w' Reynolds stress [(m/s)^2] (or "default")
default   IncDec1     - u-component coherence parameters (e.g. "10.0 0.3e-3" in quotes) (or "default")
default   IncDec2     - v-component coherence parameters (e.g. "10.0 0.3e-3" in quotes) (or "default")
default   IncDec3     - w-component coherence parameters (e.g. "10.0 0.3e-3" in quotes) (or "default")
default   CohExp      - Coherence exponent (or "default")

-----Coherent Turbulence Scaling Parameters-----
"M:\coh_events\eventdata" CTEventPath - Name of the path where event data files are located
"Random"  CTEventFile   - Type of event files ("random", "les" or "dns")
true      Randomize   - Randomize disturbance scale and location? (true/false)
1.0       DistScal   - Disturbance scale (ratio of dataset height to rotor disk).
0.5       CTLy       - Fractional location of tower centerline from right (looking downwind) to left side of the
dataset.
0.5       CTLz       - Fractional location of hub height from the bottom of the dataset.
10.0     CTStartTime  - Minimum start time for coherent structures in RootName.cts [seconds]

=====
NOTE: Do not add or remove any lines in this file!
=====
```

C Input Files for the Simplified AF Model

The input files that are changed when implementing the foundation is presented here, and the changes made are highlighted with yellow.

C.1 SubDyn Input file

```

NRELOffshrbSline5MW_OC3Monopile_SubDyn_SimplifiedAF
----- SubDyn v1.01.x MultiMember Support Structure Input File -----
OC3 Monopile configuration (pile only).
----- SIMULATION CONTROL -----
False      Echo      - Echo input data to "<rootname>.SD.ech" (flag)
"DEFAULT"  SDDeltaT - Local Integration Step. If "default", the glue-code integration step will be used.
3          IntMethod - Integration Method [1/2/3/4 = RK4/AB4/ABM4/AM2].
True       SttcSolve - Solve dynamics about static equilibrium point
----- FEA and CRAIG-BAMPTON PARAMETERS -----
3          FEMMod   - FEM switch: element model in the FEM. [1= Euler-Bernoulli(E-B); 2=Tapered E-B (unavailable);
3= 2-node Timoshenko; 4= 2-node tapered Timoshenko (unavailable)]
3          NDiv     - Number of sub-elements per member
True       CBMod    - [T/F] If True perform C-B reduction, else full FEM dofs will be retained. If True, select
Nmodes to retain in C-B reduced system.
0          Nmodes   - Number of internal modes to retain (ignored if CBMod=False). If Nmodes=0 --> Guyan Reduction.
1          JDampings - Damping Ratios for each retained mode (% of critical) If Nmodes>0, list Nmodes structural
damping ratios for each retained mode (% of critical), or a single damping ratio to be applied to all retained modes. (last
entered value will be used for all remaining modes).
---- STRUCTURE JOINTS: joints connect structure members (~Hydrodyn Input File)---
5          NJoints  - Number of joints (-)
JointID    JointXss      JointYss      JointZss [Coordinates of Member joints in SS-Coordinate
System]
(-)        (m)          (m)          (m)
5          0.00000    0.00000     -34.27840
1          0.00000    0.00000     -20.00010
2          0.00000    0.00000     -10.00000
3          0.00000    0.00000     0.00000
4          0.00000    0.00000     10.00000
----- BASE REACTION JOINTS: 1/0 for Locked/Free DOF @ each Reaction Node -----
1          NReact   - Number of Joints with reaction forces; be sure to remove all rigid motion DOFs of the
structure (else det([K])=[0])
RJointID  RctTDXss  RctTDYss  RctTDZss  RctRDXss  RctRDYss  RctRDZss [Global Coordinate System]
(-)       (flag)   (flag)   (flag)   (flag)   (flag)   (flag)
5         1       1       1       1       1       1 ""
----- INTERFACE JOINTS: 1/0 for Locked (to the TP)/Free DOF @each Interface Joint (only Locked-to-TP implemented thus far
(=rigid TP)) -----
1          NInterf  - Number of interface joints locked to the Transition Piece (TP): be sure to remove all rigid
motion dofs
IJointID  ItfTDXss  ItfTDYss  ItfTDZss  ItfRDXss  ItfRDYss  ItfRDZss [Global Coordinate System]
(-)       (flag)   (flag)   (flag)   (flag)   (flag)   (flag)
4         1       1       1       1       1       1
----- MEMBERS -----
4          NMembers - Number of frame members
MemberID  MJointID1 MJointID2 MPropSetID1 MPropSetID2 COSMID
(-)       (-)      (-)      (-)      (-)      (-)
1         1       2       1       1
2         2       3       1       1
3         3       4       1       1
4         5       1       5       5
----- MEMBER X-SECTION PROPERTY data 1/2 [isotropic material for now: use this table for circular-tubular
elements] -----
5          NPropSets - Number of structurally unique x-sections (i.e. how many groups of X-sectional properties are
utilized throughout all of the members)
PropSetID YoungE      ShearG      MatDens      XsecD      XsecT
(-)       (N/m2)    (N/m2)    (kg/m3)    (m)        (m)
1         2.10000e+11 8.08000e+10 8500.00    6.000000    0.060000
2         2.10000e+11 8.08000e+10 8500.00    6.000000    0.027000
3         2.10000e+11 8.08000e+10 8500.00    3.870000    0.019000
4         2.10000e+14 8.08000e+14 1.00       1.000000    0.010000
5         1.35367e+11 5.20642e+10 8500.00    6.000000    0.060000
----- MEMBER X-SECTION PROPERTY data 2/2 [isotropic material for now: use this table if any section other than
circular, however provide COSM(i,j) below] -----
0          NXPropSets - Number of structurally unique non-circular x-sections (if 0 the following table is ignored)
PropSetID YoungE      ShearG      MatDens      XsecA      XsecAsx      XsecAsy      XsecJxx
XsecJyy      XsecJ0
(-)       (N/m2)    (N/m2)    (kg/m3)    (m2)        (m2)        (m2)        (m4)        (m4)
(m4)
----- MEMBER COSINE MATRICES COSM(i,j) -----
0          NCOSMs - Number of unique cosine matrices (i.e., of unique member alignments including principal axis
rotations); ignored if NXPropSets=0 or 9999 in any element below
COSMID    COSM11    COSM12    COSM13    COSM21    COSM22    COSM23    COSM31    COSM32    COSM33
(-)       (-)      (-)      (-)      (-)      (-)      (-)      (-)      (-)      (-)

```



```

NRELOffshrBsline5MM_OC3Monopile_SubDyn_SimplifiedAF
----- JOINT ADDITIONAL CONCENTRATED MASSES -----
CMJointID      0  NCMass      - Number of joints with concentrated masses; Global Coordinate System
                JMass       JMXX       JMYX       JMZZ
                (kg)        (kg*m^2)   (kg*m^2)   (kg*m^2)
----- OUTPUT: SUMMARY & OUTFILE -----
True           SSSum       - Output a Summary File (flag).It contains: matrices K,M and C-B reduced M_BB, M-BM, K_BB,
K_MM(OMG^2), PHI_R, PHI_L. It can also contain COSMS if requested.
False          OutCOSM     - Output cosine matrices with the selected output member forces (flag)
False          OutAll      - [T/F] Output all members' end forces
3             OutSwitch  - [1/2/3] Output requested channels to: 1=<rootname>.SD.out; 2=<rootname>.out (generated by
FAST); 3=both files.
True           TabDelim   - Generate a tab-delimited output in the <rootname>.SD.out file
1             OutDec     - Decimation of output in the <rootname>.SD.out file
"ES11.4e2"    OutFmt     - Output format for numerical results in the <rootname>.SD.out file
"A11"        OutSFmt    - Output format for header strings in the <rootname>.SD.out file
----- MEMBER OUTPUT LIST -----
2             NMOutputs  - Number of members whose forces/displacements/velocities/accelerations will be output (-) [Must
be <= 9].
MemberID      NOutCnt    NodeCnt [NOutCnt=how many nodes to get output for [< 10]; NodeCnt are local ordinal numbers from the
start of the member, and must be >=1 and <= NDiv+1] If NMOutputs=0 leave blank as well.
(-)           (-)       (-)
2             1         1
3             1         1
----- SSOutList: The next line(s) contains a list of output parameters that will be output in
<rootname>.SD.out or <rootname>.out. -----
"M2N1MKxe, M2N1MKye" - The local side-to-side and fore-aft bending moments at node 1 of member 3 (located at
0 m, i.e. MSL).
"M1N1MKxe, M1N1MKye" - The local side-to-side and fore-aft bending moments at node 1 of member 2 (located at
-10 m, i.e. half way between MSL and mudline).
"-ReactFXss, -ReactFYss, -ReactFZss" - Base reactions: fore-aft shear, side-to-side shear and vertical forces at the mudline.
"-ReactMXss, -ReactMYss, -ReactMZss" - Base reactions: side-to-side, fore-aft and yaw moments at the mudline.
END of output channels and end of file. (the word "END" must appear in the first 3 columns of this line)

```

C.2 BModes Main Input File

```

Monopile_AF
===== BModes v3.00 Main Input File =====
NREL 5MW Tower

----- General parameters -----
true Echo Echo input file contents to *.echo file if true.
2 beam_type 1: blade, 2: tower (-)
0. romg: rotor speed, automatically set to zero for tower modal analysis (rpm)
1. romg_mult: rotor speed multiplicative factor (-)
87.6 radius: rotor tip radius measured along coned blade axis, OR tower height above ground level [onshore] or MSL
[offshore](m)
0. hub_rad: hub radius measured along coned blade axis OR tower rigid-base height (m)
0. precone: built-in precone angle, automatically set to zero for a tower (deg)
0. bl_thp: blade pitch setting, automatically set to zero for a tower (deg)
3 hub_conn: hub-to-blade or tower-base boundary condition [1: cantilevered; 2: free-free; 3: only axial and torsion
constraints] (-)
20 modepr: number of modes to be printed (-)
t TabDelim (true: tab-delimited output tables; false: space-delimited tables)
f mid_node_tw (true: output twist at mid-node of elements; false: no mid-node outputs)

----- Blade-tip or tower-top mass properties -----
3.500003109E+005 tip_mass blade-tip or tower-top mass (kg)
-0.4137754432 cm_loc tip-mass c.m. offset from the tower axis measured along x-tower axis (m)
1.9669893542 cm_axial tip-mass c.m. offset tower tip measures axially along the z axis (m)
4.370E7 ixx_tip blade lag mass moment of inertia about the tip-section x reference axis (kg-m^2)
2.353E7 iyy_tip blade flap mass moment of inertia about the tip-section y reference axis (kg-m^2)
2.542E7 izz_tip torsion mass moment of inertia about the tip-section z reference axis (kg-m^2)
0. ixy_tip cross product of inertia about x and y reference axes(kg-m^2)
1.169E6 izx_tip cross product of inertia about z and x reference axes(kg-m^2)
0. iyz_tip cross product of inertia about y and z reference axes(kg-m^2)

----- Distributed-property identifiers -----
1 id_mat: material_type [1: isotropic; non-isotropic composites option not yet available]
'Monopile_tower_secs_fromElastoDyn.dat' : sec_props_file name of beam section properties file (-)

Property scaling factors.....
1.0 sec_mass_mult: mass density multiplier (-)
1.0 flp_iner_mult: blade flap or tower f-a inertia multiplier (-)
1.0 lag_iner_mult: blade lag or tower s-s inertia multiplier (-)
1.0 flp_stff_mult: blade flap or tower f-a bending stiffness multiplier (-)
1.0 edge_stff_mult: blade lag or tower s-s bending stiffness multiplier (-)
1.0 tor_stff_mult: torsion stiffness multiplier (-)
1.0 axial_stff_mult: axial stiffness multiplier (-)
1.0 cg_offst_mult: cg offset multiplier (-)
1.0 sc_offst_mult: shear center multiplier (-)
1.0 tc_offst_mult: tension center multiplier (-)

----- Finite element discretization -----
61 nsel: no of blade or tower elements (-)
Distance of element boundary nodes from blade or flexible-tower root (normalized wrt blade or tower length), el_loc()
0 0.003481894 0.010445682 0.017409471 0.024373259 0.031337047 0.038300836 0.045264624
0.052228412 0.059192201 0.066155989 0.073119777 0.080083565 0.087047354 0.094011142 0.10097493
0.107938719 0.114902507 0.121866295 0.128830084 0.135793872 0.13990 0.149721448 0.156685237
0.163649025 0.170612813 0.177576602 0.18454039 0.191504178 0.198467967 0.205431755 0.212395543
0.219359331 0.22632312 0.233286908 0.240250696 0.247214485 0.250696379 0.320334262 0.37971
0.424791072 0.45961 0.486635 0.51366 0.54068 0.5677 0.594715 0.62173 0.64875 0.67577 0.70279 0.72981
0.75683 0.78385 0.81087 0.83789 0.864905 0.89192 0.91894 0.94596 0.97298 1.0

----- Properties of tower support subsystem (read only if beam_type is 2) -----
1 tow_support: additional tower support [0: no additional support; 1: floating-platform or monopile with or without
tension wires] (-)
-10.0 draft : depth of tower base from the ground or the MSL (mean sea level) (m)
0.0 cm_pform : distance of platform c.m. below the MSL (m)
0.0 mass_pform : platform mass (kg)
Platform mass inertia 3X3 matrix (i_matrix_pform):
0. 0. 0.
0. 0. 0.
0. 0. 0.
-10.0 ref_msl : distance of platform reference point below the MSL (m)
Platform-reference-point-referred hydrodynamic 6X6 matrix (hydro_M):
0.163267E+06 0.000000E+00 0.000000E+00 0.000000E+00 -0.105323E+07 0.000000E+00
0.000000E+00 0.163267E+06 0.000000E+00 0.105323E+07 0.000000E+00 0.000000E+00
0.000000E+00 0.000000E+00 0.160936E+06 0.000000E+00 0.000000E+00 0.000000E+00
0.000000E+00 0.105323E+07 0.000000E+00 0.917277E+07 0.000000E+00 0.000000E+00
-0.105323E+07 0.000000E+00 0.000000E+00 0.000000E+00 0.917278E+07 0.000000E+00
0.000000E+00 0.000000E+00 0.000000E+00 0.000000E+00 0.000000E+00 0.141992E+07
Platform-reference-point-referred hydrodynamic 6X6 stiffness matrix (hydro_K):
0.103015E+09 0.000000E+00 0.000000E+00 0.000000E+00 -0.251395E+10 0.000000E+00
0.000000E+00 0.103016E+09 0.000000E+00 0.251396E+10 0.000000E+00 0.000000E+00
0.000000E+00 0.000000E+00 0.450867E+10 0.000000E+00 0.000000E+00 0.000000E+00
0.000000E+00 0.251396E+10 0.000000E+00 0.812367E+11 0.000000E+00 0.000000E+00
-0.251396E+10 0.000000E+00 0.000000E+00 0.000000E+00 0.812366E+11 0.000000E+00
0.000000E+00 0.000000E+00 0.000000E+00 0.000000E+00 0.000000E+00 0.153012E+11
Mooring-system 6X6 stiffness matrix (mooring_K):

```

Monopile_AF

0.0 0.0 0.0 0.0 0.0 0.0
0.0 0.0 0.0 0.0 0.0 0.0
0.0 0.0 0.0 0.0 0.0 0.0
0.0 0.0 0.0 0.0 0.0 0.0
0.0 0.0 0.0 0.0 0.0 0.0
0.0 0.0 0.0 0.0 0.0 0.0

Distributed (hydrodynamic) added-mass per unit length along a flexible portion of the tower length:
0 n_secs_m_distr: number of sections at which added mass per unit length is specified (-)
0. 0. : z_distr_m [row array of size n_added_m_pts; section locations wrt the flexible tower base over which distributed mass is specified] (m)
0. 0. : distr_m [row array of size n_added_m_pts; added distributed masses per unit length] (kg/m)

Distributed elastic stiffness per unit length along a flexible portion of the tower length:
0 n_secs_k_distr: number of points at which distributed stiffness per unit length is specified (-)
0 1 2 3 4 5 6 7 8 9 10 11 12 13 14 15
16 17 18 19 20 21 22 23 24 25 26 27 28 29 30 31
32 33 34 35 36 : z_distr_k [row array of size n_added_m_pts; section locations wrt the flexible tower base over which distributed stiffness is specified] (m)
595318000.0 1165208000 1129400000 1095553000 1059931000 1024493000 989209000 953643000
918718000 883287000 847803000 812541000 777187000 741870000 706616000 671440000
636229000 600957000 565919000 530470000 495081000 459574000 425027000 390479000
280059000 254125000 227500000 200112000 171927000 143115000 114173000 80184000
52237000 35561000 20912000 900000 1156000 : distr_k [row array of size n_added_m_pts; distributed stiffness per unit length] (N/m^2)

Tension wires data
0 n_attachments: no of wire-attachment locations on tower [0: no tension wires] (-)
3 3 n_wires: no of wires attached at each location (must be 3 or higher) (-)
6 9 node_attach: node numbers of attachments location (node number must be more than 1 and less than nsel+2) (-)
0.e0 0.e0 wire_stfness: wire spring constant in each set (see users' manual) (N/m)
0. 0. th_wire: angle of tension wires (wrt the horizontal ground plane) at each attachment point (deg)

END of Main Input File Data *****

C.3 BModes Tower Section Properties

Monopile_tower_secs_fromElastoDyn

Tower section properties
 11 n_secs: number of tower sections at which properties are specified (-)

sec_loc	str_tw	tw_iner	mass_den	flp_iner	edge_iner	flp_stff	edge_stff	tor_stff	axial_stff	cg_offst	sc_offst
tc_offst	(deg)	(deg)	(kg/m)	(kg-m)	(kg-m)	(Nm^2)	(Nm^2)	(Nm^2)	(N)	(m)	(m)
0.00000	0.0	0.0	4306.51	0.0001	0.0001	474.49E9	474.49E9	365.133E15	106.396E15	0.0	0.0
0.10000	0.0	0.0	4030.44	0.0001	0.0001	413.08E9	413.08E9	317.878E15	99.576E15	0.0	0.0
0.20000	0.0	0.0	3763.45	0.0001	0.0001	357.83E9	357.83E9	275.356E15	92.979E15	0.0	0.0
0.30000	0.0	0.0	3505.52	0.0001	0.0001	308.30E9	308.30E9	237.242E15	86.607E15	0.0	0.0
0.40000	0.0	0.0	3256.66	0.0001	0.0001	264.08E9	264.08E9	203.220E15	80.459E15	0.0	0.0
0.50000	0.0	0.0	3016.86	0.0001	0.0001	224.80E9	224.80E9	172.987E15	74.534E15	0.0	0.0
0.60000	0.0	0.0	2786.13	0.0001	0.0001	190.06E9	190.06E9	146.252E15	68.834E15	0.0	0.0
0.70000	0.0	0.0	2564.46	0.0001	0.0001	159.49E9	159.49E9	122.735E15	63.357E15	0.0	0.0
0.80000	0.0	0.0	2351.87	0.0001	0.0001	132.77E9	132.77E9	102.167E15	58.105E15	0.0	0.0
0.90000	0.0	0.0	2148.34	0.0001	0.0001	109.54E9	109.54E9	84.291E15	53.077E15	0.0	0.0
1.00000	0.0	0.0	1953.87	0.0001	0.0001	89.49E9	89.49E9	68.863E15	48.272E15	0.0	0.0

**Note: If the above data represents TOWER properties, the following are overwritten:
 str_tw is set to zero
 tw_iner is set to zero
 cg_offst is set to zero
 sc_offst is set to zero
 tc_offst is set to zero
 edge_iner is set equal to flp_iner
 edge_stff is set equal to flp_stff

C.4 ElastoDyn Tower File

```

                                NRELOffshrBslne5MW_OC3Monopile_ElastoDyn_Tower_AF
----- ELASTODYN V1.00.* TOWER INPUT FILE -----
NREL 5.0 MW offshore baseline monopile tower for flexible monopile modeled in SubDyn.
----- TOWER PARAMETERS -----
    11  NTwInpSt  - Number of input stations to specify tower geometry
    1.0  TwrFADmp(1) - Tower 1st fore-aft mode structural damping ratio (%)
    1.0  TwrFADmp(2) - Tower 2nd fore-aft mode structural damping ratio (%)
    1.0  TwrSSDmp(1) - Tower 1st side-to-side mode structural damping ratio (%)
    1.0  TwrSSDmp(2) - Tower 2nd side-to-side mode structural damping ratio (%)
----- TOWER ADJUSTMUNT FACTORS -----
    1.0  FASTunr(1) - Tower fore-aft modal stiffness tuner, 1st mode (-)
    1.0  FASTunr(2) - Tower fore-aft modal stiffness tuner, 2nd mode (-)
    1.0  SSStunr(1) - Tower side-to-side stiffness tuner, 1st mode (-)
    1.0  SSStunr(2) - Tower side-to-side stiffness tuner, 2nd mode (-)
    1.0  AdjTwMa  - Factor to adjust tower mass density (-)
    1.0  AdjFAST  - Factor to adjust tower fore-aft stiffness (-)
    1.0  AdjSSSt  - Factor to adjust tower side-to-side stiffness (-)
----- DISTRIBUTED TOWER PROPERTIES -----
HtFract      TMassDen      TwFASTif      TwSSStif
(-)          (kg/m)          (Nm^2)        (Nm^2)
0.0          4.3065100E+03  4.7449000E+11 4.7449000E+11
1.0E-01     4.0304400E+03  4.1308000E+11 4.1308000E+11
2.0E-01     3.7634500E+03  3.5783000E+11 3.5783000E+11
3.0E-01     3.5055200E+03  3.0830000E+11 3.0830000E+11
4.0E-01     3.2566600E+03  2.6408000E+11 2.6408000E+11
5.0E-01     3.0168600E+03  2.2480000E+11 2.2480000E+11
6.0E-01     2.7861300E+03  1.9006000E+11 1.9006000E+11
7.0E-01     2.5644600E+03  1.5949000E+11 1.5949000E+11
8.0E-01     2.3518700E+03  1.3277000E+11 1.3277000E+11
9.0E-01     2.1483400E+03  1.0954000E+11 1.0954000E+11
1.0E+00     1.9538700E+03  8.9490000E+10 8.9490000E+10
----- TOWER FORE-AFT MODE SHAPES -----
    0.9940  TwFAM1Sh(2) - Mode 1, coefficient of x^2 term
    0.1505  TwFAM1Sh(3) -      , coefficient of x^3 term
   -0.1833  TwFAM1Sh(4) -      , coefficient of x^4 term
    0.1474  TwFAM1Sh(5) -      , coefficient of x^5 term
   -0.1086  TwFAM1Sh(6) -      , coefficient of x^6 term
    0.0630  TwFAM2Sh(2) - Mode 2, coefficient of x^2 term
    0.8824  TwFAM2Sh(3) -      , coefficient of x^3 term
    0.2132  TwFAM2Sh(4) -      , coefficient of x^4 term
   -0.0464  TwFAM2Sh(5) -      , coefficient of x^5 term
   -0.1122  TwFAM2Sh(6) -      , coefficient of x^6 term
----- TOWER SIDE-TO-SIDE MODE SHAPES -----
    0.3951  TwSSM1Sh(2) - Mode 1, coefficient of x^2 term
    1.7677  TwSSM1Sh(3) -      , coefficient of x^3 term
   -2.0120  TwSSM1Sh(4) -      , coefficient of x^4 term
    1.1996  TwSSM1Sh(5) -      , coefficient of x^5 term
   -0.3505  TwSSM1Sh(6) -      , coefficient of x^6 term
    4.0780  TwSSM2Sh(2) - Mode 2, coefficient of x^2 term
   31.1504  TwSSM2Sh(3) -      , coefficient of x^3 term
  -50.7793  TwSSM2Sh(4) -      , coefficient of x^4 term
   22.5284  TwSSM2Sh(5) -      , coefficient of x^5 term
  -5.9775  TwSSM2Sh(6) -      , coefficient of x^6 term

```

D Derivation of the Flexibility Relations for the Improved AF Method

The derivations of equations 6.3, 6.4 and 6.5 are presented here. To obtain δ_{uu} and $\delta_{\theta u}$ a force F with magnitude 1 is applied in DOF u . To obtain $\delta_{u\theta}$ and $\delta_{\theta\theta}$ a moment M with magnitude 1 is applied in DOF θ , see figure D.1. The displacements and rotations are found through stiffness relations for a cantilevered beam, listed in figure 6.2.

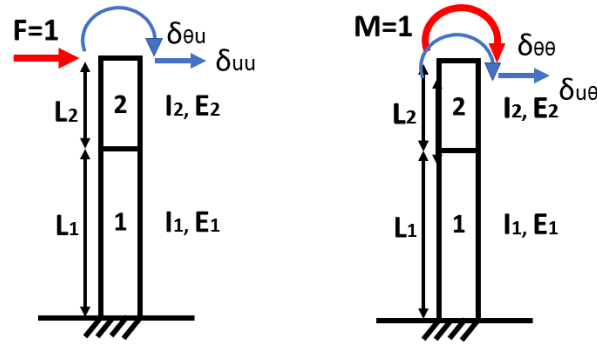


Figure D.1: Derivation of flexibility relations for the improved AF method

F leads to a force $F_1 = 1$ and a moment $M_1 = 1 \times L_2$ in beam 1. The horizontal displacement δ_{uu} caused by F is a result of displacement in beam 1, displacement in beam 2 and rotation of beam 1.

$$\delta_{uu} = u_1 + \theta_1 + u'_1 + \theta'_1 + u_2 \quad (\text{D.1})$$

where u_1 and θ_1 are the displacement and rotation of beam 1 caused by $F_1 = 1$:

$$u_1 = \frac{1 \times L_1^3}{3E_1I_1} \quad (\text{D.2})$$

$$\theta_1 = \frac{1 \times L_1^2}{2E_1I_1} \quad (\text{D.3})$$

u'_1 and θ'_1 are the displacement and rotation of beam 1 caused by $M_1 = 1 \times L_2$:

$$u'_1 = \frac{1 \times L_2L_1^2}{2E_1I_1} \quad (\text{D.4})$$

$$\theta'_1 = \frac{1 \times L_2 L_1}{E_1 I_1} \quad (\text{D.5})$$

u_2 is the displacement in beam 2 caused by $F = 1$,

$$u_2 = \frac{1 \times L_2^3}{3E_2 I_2} \quad (\text{D.6})$$

Equivalently, the rotation $\delta_{\theta u}$ caused by F is

$$\delta_{\theta u} = \theta_1 + \theta'_1 + \theta_2 \quad (\text{D.7})$$

where θ_2 is the rotation in beam 2 caused by F ,

$$\theta_2 = \frac{1 \times L_2^2}{2E_2 I_2} \quad (\text{D.8})$$

$\delta_{u\theta}$ is the displacement caused by the applied moment $M = 1$, and

$$\delta_{u\theta} = \delta_{\theta u} \quad (\text{D.9})$$

Finally, the total rotation in DOF θ caused by $M = 1$ is the combination of the rotation in beam 1 and the rotation in beam 2:

$$\delta_{\theta\theta} = \frac{1 \times L_1}{E_1 I_1} + \frac{1 \times L_2}{E_2 I_2} \quad (\text{D.10})$$

E SubDyn Input File for the Improved AF Model

The changes made compared to Appendix A.4 and C.1 are highlighted.

```

NRELOffshBslne5MW_OC3Monopile_SubDyn_ImprovedAF
----- SubDyn v1.01.x MultiMember Support Structure Input File -----
OC3 Monopile configuration (pile only).
----- SIMULATION CONTROL -----
False      Echo      - Echo input data to "<rootname>.SD.ech" (flag)
"DEFAULT"  SDDeltaT - Local Integration Step. If "default", the glue-code integration step will be used.
3          IntMethod - Integration Method [1/2/3/4 = RK4/AB4/ABM4/AM2].
True       SttcSolve - Solve dynamics about static equilibrium point
----- FEA and CRAIG-BAMPTON PARAMETERS -----
3          FEMMod    - FEM switch: element model in the FEM. [1= Euler-Bernoulli(E-B); 2=Tapered E-B (unavailable);
3= 2-node Timoshenko; 4= 2-node tapered Timoshenko (unavailable)]
3          NDiv      - Number of sub-elements per member
True       CBMod     - [T/F] If True perform C-B reduction, else full FEM dofs will be retained. If True, select
Nmodes to retain in C-B reduced system.
0          Nmodes    - Number of internal modes to retain (ignored if CBMod=False). If Nmodes=0 --> Guyan Reduction.
1          JDampings - Damping Ratios for each retained mode (% of critical) If Nmodes>0, list Nmodes structural
damping ratios for each retained mode (% of critical), or a single damping ratio to be applied to all retained modes. (last
entered value will be used for all remaining modes).
---- STRUCTURE JOINTS: joints connect structure members (~Hydrodyn Input File)---
6          NJoints   - Number of joints (-)
JointID    JointXss      JointYss      JointZss [Coordinates of Member joints in SS-Coordinate
System]
(-)        (m)          (m)          (m)
6          0.00000    0.00000    -44.88240
5          0.00000    0.00000    -25.00000
1          0.00000    0.00000    -20.00010
2          0.00000    0.00000    -10.00000
3          0.00000    0.00000     0.00000
4          0.00000    0.00000    10.00000
----- BASE REACTION JOINTS: 1/0 for Locked/Free DOF @ each Reaction Node -----
1          NReact    - Number of Joints with reaction forces; be sure to remove all rigid motion DOFs of the
structure (else det([K])=0)]
RJointID   RctTDXss  RctTDYss  RctTDZss  RctRDXss  RctRDYss  RctRDZss  [Global Coordinate System]
(-)        (flag)   (flag)   (flag)   (flag)   (flag)   (flag)
6          1       1       1       1       1       1
----- INTERFACE JOINTS: 1/0 for Locked (to the TP)/Free DOF @each Interface Joint (only Locked-to-TP implemented thus far
(=rigid TP)) -----
1          NInterf   - Number of interface joints locked to the Transition Piece (TP): be sure to remove all rigid
motion dofs
IJointID   ItfTDXss  ItfTDYss  ItfTDZss  ItfRDXss  ItfRDYss  ItfRDZss  [Global Coordinate System]
(-)        (flag)   (flag)   (flag)   (flag)   (flag)   (flag)
4          1       1       1       1       1       1
----- MEMBERS -----
5          NMembers  - Number of frame members
MemberID   MJointID1 MJointID2 MPropSetID1 MPropSetID2 COSMID
(-)        (-)        (-)        (-)        (-)        (-)
1          1       2       1       1
2          2       3       1       1
3          3       4       1       1
4          5       1       5       5
5          6       5       6       6
----- MEMBER X-SECTION PROPERTY data 1/2 [isotropic material for now: use this table for circular-tubular
elements] -----
6          NPropSets - Number of structurally unique x-sections (i.e. how many groups of X-sectional properties are
utilized throughout all of the members)
PropSetID  YoungE     ShearG     MatDens     XsecD     XsecT
(-)        (N/m2)    (N/m2)    (kg/m3)    (m)       (m)
1          2.10000e+11 8.08000e+10 8500.00    6.000000  0.060000
2          2.10000e+11 8.08000e+10 8500.00    6.000000  0.027000
3          2.10000e+11 8.08000e+10 8500.00    3.870000  0.019000
4          2.10000e+14 8.08000e+14 1.00       1.000000  0.010000
5          1.38820e+11  5.33923e+10 8500.00    6.000000  0.060000
6          1.74260e+12  6.70230e+11 8500.00    6.000000  0.060000
----- MEMBER X-SECTION PROPERTY data 2/2 [isotropic material for now: use this table if any section other than
circular, however provide COSM(i,j) below] -----
0          NXPropSets - Number of structurally unique non-circular x-sections (if 0 the following table is ignored)
PropSetID  YoungE     ShearG     MatDens     XsecA     XsecAsx   XsecAsy   XsecJxx
XsecJyy    XsecJ0
(-)        (N/m2)    (N/m2)    (kg/m3)    (m2)     (m2)     (m2)     (m4)     (m4)
(m4)
----- MEMBER COSINE MATRICES COSM(i,j) -----
0          NCOSMs    - Number of unique cosine matrices (i.e., of unique member alignments including principal axis
rotations); ignored if NXPropSets=0 or 9999 in any element below
COSMID     COSM11    COSM12    COSM13    COSM21    COSM22    COSM23    COSM31    COSM32    COSM33
(-)        (-)        (-)        (-)        (-)        (-)        (-)        (-)        (-)        (-)
----- JOINT ADDITIONAL CONCENTRATED MASSES -----
0          NCmass    - Number of joints with concentrated masses; Global Coordinate System
CMJointID  JMass     JMXX     JMYX     JMYX     JMYX     JMYX
(-)        (kg)     (kg*m^2) (kg*m^2) (kg*m^2) (kg*m^2) (kg*m^2)
----- OUTPUT: SUMMARY & OUTFILE -----
True       SSSum      - Output a Summary File (flag).It contains: matrices K,M and C-B reduced M_BB, M-BM, K_BB,
K_MM(OMG^2), PHI_R, PHI_L. It can also contain COSMs if requested.
False      OutCOSM    - Output cosine matrices with the selected output member forces (flag)
False      OutAll     - [T/F] Output all members' end forces

```



```

                                NRELOffshrbaseline5MW_OC3Monopile_SubDyn_ImprovedAF
3  OutSwitch - [1/2/3] Output requested channels to: 1=<rootname>.SD.out; 2=<rootname>.out (generated by
FAST); 3=both files.
True      TabDelim - Generate a tab-delimited output in the <rootname>.SD.out file
1  OutDec  - Decimation of output in the <rootname>.SD.out file
"ES11.4e2" OutFmt  - Output format for numerical results in the <rootname>.SD.out file
"A11"     OutSFmt - Output format for header strings in the <rootname>.SD.out file
----- MEMBER OUTPUT LIST -----
2  NMOutputs - Number of members whose forces/displacements/velocities/accelerations will be output (-) [Must
be <= 9].
MemberID  NOutCnt  NodeCnt [NOutCnt=how many nodes to get output for [< 10]; NodeCnt are local ordinal numbers from the
start of the member, and must be >=1 and <= NDiv+1] If NMOutputs=0 leave blank as well.
(-)       (-)       (-)
2         1         1
3         1         1
----- SSOutList: The next line(s) contains a list of output parameters that will be output in
<rootname>.SD.out or <rootname>.out. -----
"M2N1MKxe, M2N1MKye" - The local side-to-side and fore-aft bending moments at node 1 of member 3 (located at
0 m, i.e. MSL).
"M1N1MKxe, M1N1MKye" - The local side-to-side and fore-aft bending moments at node 1 of member 2 (located at
-10 m, i.e. half way between MSL and mudline).
"-ReactFXss, -ReactFYss, -ReactFZss" - Base reactions: fore-aft shear, side-to-side shear and vertical forces at the mudline.
"-ReactMXss, -ReactMYss, -ReactMZss" - Base reactions: side-to-side, fore-aft and yaw moments at the mudline.
END of output channels and end of file. (the word "END" must appear in the first 3 columns of this line)

```

F SubDyn Input File for Monopile with $t_w=0.05$ m

```

NRELOffshrBsline5MW_OC3Monopile_SubDyn_AF2t005
----- SubDyn v1.01.x MultiMember Support Structure Input File -----
OC3 Monopile configuration (pile only).
----- SIMULATION CONTROL -----
False      Echo          - Echo input data to "<rootname>.SD.ech" (flag)
"DEFAULT"  SDDeltaT        - Local Integration Step. If "default", the glue-code integration step will be used.
3          IntMethod   - Integration Method [1/2/3/4 = RK4/AB4/ABM4/AM2].
True      SttcSolve   - Solve dynamics about static equilibrium point
----- FEA and CRAIG-BAMPTON PARAMETERS-----
3          FEMMod     - FEM switch: element model in the FEM. [1= Euler-Bernoulli(E-B); 2=Tapered E-B (unavailable);
3= 2-node Timoshenko; 4= 2-node tapered Timoshenko (unavailable)]
3          NDiv       - Number of sub-elements per member
True      CBMod       - [T/F] If True perform C-B reduction, else full FEM dofs will be retained. If True, select
Nmodes to retain in C-B reduced system.
0          Nmodes     - Number of internal modes to retain (ignored if CBMod=False). If Nmodes=0 --> Guyan Reduction.
1          JDampings  - Damping Ratios for each retained mode (% of critical) If Nmodes>0, list Nmodes structural
damping ratios for each retained mode (% of critical), or a single damping ratio to be applied to all retained modes. (last
entered value will be used for all remaining modes).
---- STRUCTURE JOINTS: joints connect structure members (~Hydrodyn Input File)---
6          NJoints   - Number of joints (-)
JointID   JointXss    JointYss      JointZss [Coordinates of Member joints in SS-Coordinate
System]
(-)      (m)         (m)           (m)
6        0.00000    0.00000      -44.22820
5        0.00000    0.00000      -25.00000
1        0.00000    0.00000      -20.00010
2        0.00000    0.00000      -10.00000
3        0.00000    0.00000      0.00000
4        0.00000    0.00000      10.00000
----- BASE REACTION JOINTS: 1/0 for Locked/Free DOF @ each Reaction Node -----
1          NReact    - Number of Joints with reaction forces; be sure to remove all rigid motion DOFs of the
structure (else det([K])=[0])
RJointID  RctTDXss  RctTDYss     RctTDZss  RctRDXss  RctRDYss  RctRDZss  [Global Coordinate System]
(-)      (flag)  (flag)      (flag)    (flag)    (flag)    (flag)
6        1      1      1      1      1      1      ""
----- INTERFACE JOINTS: 1/0 for Locked (to the TP)/Free DOF @each Interface Joint (only Locked-to-TP implemented thus far
(=rigid TP)) -----
1          NInterf   - Number of interface joints locked to the Transition Piece (TP): be sure to remove all rigid
motion dofs
IJointID  ItfTDXss  ItfTDYss     ItfTDZss  ItfRDXss  ItfRDYss  ItfRDZss  [Global Coordinate System]
(-)      (flag)  (flag)      (flag)    (flag)    (flag)    (flag)
4        1      1      1      1      1      1
----- MEMBERS -----
5          NMembers  - Number of frame members
MemberID  MJointID1 MJointID2    MPropSetID1 MPropSetID2  COSMID
(-)      (-)      (-)          (-)          (-)          (-)
1        1      2      1      1
2        2      3      1      1
3        3      4      1      1
4        5      1      5      5
5        6      5      6      6
----- MEMBER X-SECTION PROPERTY data 1/2 [isotropic material for now: use this table for circular-tubular
elements] -----
6          NPropSets - Number of structurally unique x-sections (i.e. how many groups of X-sectional properties are
utilized throughout all of the members)
PropSetID YoungE      ShearG      MatDens      XsecD      XsecT
(-)      (N/m2)    (N/m2)      (kg/m3)      (m)        (m)
1        2.10000e+11  8.08000e+10  8500.00      6.000000    0.050000
2        2.10000e+11  8.08000e+10  8500.00      6.000000    0.027000
3        2.10000e+11  8.08000e+10  8500.00      3.870000    0.019000
4        2.10000e+14  8.08000e+14  1.00         1.000000    0.010000
5        1.41930e+11  5.45890e+10  8500.00      6.000000    0.050000
6        1.88600e+12  7.25380e+11  8500.00      6.000000    0.050000
----- MEMBER X-SECTION PROPERTY data 2/2 [isotropic material for now: use this table if any section other than
circular, however provide COSM(i,j) below] -----
0          NXPropSets - Number of structurally unique non-circular x-sections (if 0 the following table is ignored)
PropSetID YoungE      ShearG      MatDens      XsecA      XsecAsx    XsecAsy    XsecJxx
XsecJyy    XsecJ0
(-)      (N/m2)    (N/m2)      (kg/m3)      (m2)        (m2)        (m2)        (m4)        (m4)
(m4)
----- MEMBER COSINE MATRICES COSM(i,j) -----
0          NCOSMs    - Number of unique cosine matrices (i.e., of unique member alignments including principal axis
rotations); ignored if NXPropSets=0 or 9999 in any element below
COSMID    COSM11    COSM12    COSM13    COSM21    COSM22    COSM23    COSM31    COSM32    COSM33
(-)      (-)      (-)      (-)      (-)      (-)      (-)      (-)      (-)      (-)
----- JOINT ADDITIONAL CONCENTRATED MASSES-----
0          NCmass    - Number of joints with concentrated masses; Global Coordinate System
CMJointID JMass      JMXX      JMYX      JMZZ
(-)      (kg)      (kg*m^2)  (kg*m^2)  (kg*m^2)
----- OUTPUT: SUMMARY & OUTFILE -----
True      SSSum      - Output a Summary File (flag).It contains: matrices K,M and C-B reduced M_BB, M-BM, K_BB,
K_MM(OMG^2), PHI_R, PHI_L. It can also contain COSMs if requested.
False     OutCOSM    - Output cosine matrices with the selected output member forces (flag)
False     OutAll     - [T/F] Output all members' end forces

```

NRELOffshrBsline5MW_OC3Monopile_SubDyn_AF2t005

```

3 OutSwTch - [1/2/3] Output requested channels to: 1=<rootname>.SD.out; 2=<rootname>.out (generated by
FAST); 3=both files.
True      TabDelim - Generate a tab-delimited output in the <rootname>.SD.out file
1 OutDec  - Decimation of output in the <rootname>.SD.out file
"ES11.4e2" OutFmt  - Output format for numerical results in the <rootname>.SD.out file
"A11"     OutSFmt - Output format for header strings in the <rootname>.SD.out file
----- MEMBER OUTPUT LIST -----
2 NMOutputs - Number of members whose forces/displacements/velocities/accelerations will be output (-) [Must
be <= 9].
MemberID  NOutCnt  NodeCnt [NOutCnt=how many nodes to get output for [< 10]; NodeCnt are local ordinal numbers from the
start of the member, and must be >=1 and <= NDiv+1] If NMOutputs=0 leave blank as well.
(-)      (-)      (-)
2        1        1
3        1        1
----- SSOuList: The next line(s) contains a list of output parameters that will be output in
<rootname>.SD.out or <rootname>.out. -----
"M2N1MKxe, M2N1MKye" - The local side-to-side and fore-aft bending moments at node 1 of member 3 (located at
0 m, i.e. MSL).
"M1N1MKxe, M1N1MKye" - The local side-to-side and fore-aft bending moments at node 1 of member 2 (located at
-10 m, i.e. half way between MSL and mudline).
"-ReactFXss, -ReactFYss, -ReactFZss" - Base reactions: fore-aft shear, side-to-side shear and vertical forces at the mudline.
"-ReactMXss, -ReactMYss, -ReactMZss" - Base reactions: side-to-side, fore-aft and yaw moments at the mudline.
END of output channels and end of file. (the word "END" must appear in the first 3 columns of this line)

```

G SubDyn Input File for 12 m × 6 m Caisson

```

NRELOffshrBsline5MW_OC3Monopile_SubDyn_AF2CaissonD12L6
----- SubDyn v1.01.x MultiMember Support Structure Input File -----
OC3 Monopile configuration (pile only).
----- SIMULATION CONTROL -----
False      Echo          - Echo input data to "<rootname>.SD.ech" (flag)
"DEFAULT"  SDDeltaT             - Local Integration Step. If "default", the glue-code integration step will be used.
           3 IntMethod   - Integration Method [1/2/3/4 = RK4/AB4/ABM4/AM2].
True       SttcSolve    - Solve dynamics about static equilibrium point
----- FEA and CRAIG-BAMPTON PARAMETERS -----
           3 FEMMod      - FEM switch: element model in the FEM. [1= Euler-Bernoulli(E-B); 2=Tapered E-B (unavailable);
3= 2-node Timoshenko; 4= 2-node tapered Timoshenko (unavailable)]
           3 NDiv        - Number of sub-elements per member
True       CBMod        - [T/F] If True perform C-B reduction, else full FEM dofs will be retained. If True, select
Nmodes to retain in C-B reduced system.
           0 Nmodes      - Number of internal modes to retain (ignored if CBMod=False). If Nmodes=0 --> Guyan Reduction.
           1 JDampings   - Damping Ratios for each retained mode (% of critical) If Nmodes>0, list Nmodes structural
damping ratios for each retained mode (% of critical), or a single damping ratio to be applied to all retained modes. (last
entered value will be used for all remaining modes).
---- STRUCTURE JOINTS: joints connect structure members (~Hydrodyn Input File)---
           6 NJoints     - Number of joints (-)
JointID    JointXss      JointYss              JointZss [Coordinates of Member joints in SS-Coordinate
System]
(-)        (m)          (m)                  (m)
   6       0.00000      0.00000             -57.40000
   5       0.00000      0.00000             -25.00000
   1       0.00000      0.00000             -20.00010
   2       0.00000      0.00000             -10.00000
   3       0.00000      0.00000              0.00000
   4       0.00000      0.00000             10.00000
----- BASE REACTION JOINTS: 1/0 for Locked/Free DOF @ each Reaction Node -----
           1 NReact      - Number of Joints with reaction forces; be sure to remove all rigid motion DOFs of the
structure (else det([K])=0)]
RJointID   RctTDXss     RctTDYss             RctTDZss   RctRDYss   RctRDZss   [Global Coordinate System]
(-)        (flag)      (flag)              (flag)     (flag)     (flag)
   6       1          1                  1          1          1 ""
----- INTERFACE JOINTS: 1/0 for Locked (to the TP)/Free DOF @each Interface Joint (only Locked-to-TP implemented thus far
(=rigid TP)) -----
           1 NInterf     - Number of interface joints locked to the Transition Piece (TP): be sure to remove all rigid
motion dofs
IJointID   ItfTDXss     ItfTDYss             ItfTDZss   ItfRDYss   ItfRDZss   [Global Coordinate System]
(-)        (flag)      (flag)              (flag)     (flag)     (flag)
   4       1          1                  1          1          1
----- MEMBERS -----
           5 NMembers    - Number of frame members
MemberID    MJointID1    MJointID2            MPropSetID1 MPropSetID2  COSMID
(-)        (-)      (-)                  (-)         (-)         (-)
   1       1        2              1           1           1
   2       2        3              1           1           1
   3       3        4              1           1           1
   4       5        1              5           5           5
   5       6        5              6           6           6
----- MEMBER X-SECTION PROPERTY data 1/2 [isotropic material for now: use this table for circular-tubular
elements] -----
           6 NPropSets   - Number of structurally unique x-sections (i.e. how many groups of X-sectional properties are
utilized throughout all of the members)
PropSetID   YoungE          ShearG              MatDens     XsecD        XsecT
(-)        (N/m2)      (N/m2)              (kg/m3)     (m)          (m)
   1       2.10000e+11  8.08000e+10        8500.00    6.000000    0.060000
   2       2.10000e+11  8.08000e+10        8500.00    6.000000    0.027000
   3       2.10000e+11  8.08000e+10        8500.00    3.870000    0.019000
   4       2.10000e+14  8.08000e+14        1.00       1.000000    0.010000
   5       1.84360e+11   7.09100e+10        8500.00    6.000000    0.060000
   6       1.09590e+13   4.21480e+12        8500.00    6.000000    0.060000
----- MEMBER X-SECTION PROPERTY data 2/2 [isotropic material for now: use this table if any section other than
circular, however provide COSM(i,j) below] -----
           0 NXPropSets  - Number of structurally unique non-circular x-sections (if 0 the following table is ignored)
PropSetID   YoungE          ShearG              MatDens     XsecA        XsecAsx     XsecAsy     XsecJxx
XsecJyy    XsecJ0
(-)        (N/m2)      (N/m2)              (kg/m3)     (m2)         (m2)        (m2)        (m4)        (m4)
           (m4)
----- MEMBER COSINE MATRICES COSM(i,j) -----
           0 NCOSMs     - Number of unique cosine matrices (i.e., of unique member alignments including principal axis
rotations); ignored if NXPropSets=0 or 9999 in any element below
COSMID     COSM11     COSM12     COSM13     COSM21     COSM22     COSM23     COSM31     COSM32     COSM33
(-)        (-)      (-)      (-)      (-)      (-)      (-)      (-)      (-)      (-)
----- JOINT ADDITIONAL CONCENTRATED MASSES -----
           0 NCmass     - Number of joints with concentrated masses; Global Coordinate System
CMJointID  JMass        JMXX          JMYX          JMZZ
(-)        (kg)      (kg*m^2)     (kg*m^2)     (kg*m^2)
----- OUTPUT: SUMMARY & OUTFILE -----
True       SSSum        - Output a Summary File (flag).It contains: matrices K,M and C-B reduced M_BB, M-BM, K_BB,
K_MM(OMG^2), PHI_R, PHI_L. It can also contain COSMS if requested.
False      OutCOSM     - Output cosine matrices with the selected output member forces (flag)
False      OutAll      - [T/F] Output all members' end forces

```

NRELOffshrbaseline5MW_OC3Monopile_SubDyn_AF2CaissonD12L6

```

3 OutSwitch - [1/2/3] Output requested channels to: 1=<rootname>.SD.out; 2=<rootname>.out (generated by
FAST); 3=both files.
True TabDelim - Generate a tab-delimited output in the <rootname>.SD.out file
1 OutDec - Decimation of output in the <rootname>.SD.out file
"ES11.4e2" OutFmt - Output format for numerical results in the <rootname>.SD.out file
"A11" OutSFmt - Output format for header strings in the <rootname>.SD.out file
----- MEMBER OUTPUT LIST -----
2 NMOutputs - Number of members whose forces/displacements/velocities/accelerations will be output (-) [Must
be <= 9].
MemberID NOutCnt NodeCnt [NOutCnt=how many nodes to get output for [< 10]; NodeCnt are local ordinal numbers from the
start of the member, and must be >=1 and <= NDiv+1] If NMOutputs=0 leave blank as well.
(-) (-) (-)
2 1 1
3 1 1
----- SSOutList: The next line(s) contains a list of output parameters that will be output in
<rootname>.SD.out or <rootname>.out. -----
"M2N1MKxe, M2N1MKye" - The local side-to-side and fore-aft bending moments at node 1 of member 3 (located at
0 m, i.e. MSL).
"M1N1MKxe, M1N1MKye" - The local side-to-side and fore-aft bending moments at node 1 of member 2 (located at
-10 m, i.e. half way between MSL and mudline).
"-ReactFXss, -ReactFYss, -ReactFZss" - Base reactions: fore-aft shear, side-to-side shear and vertical forces at the mudline.
"-ReactMXss, -ReactMYss, -ReactMZss" - Base reactions: side-to-side, fore-aft and yaw moments at the mudline.
END of output channels and end of file. (the word "END" must appear in the first 3 columns of this line)

```

H MLife Input File for the Regular Monopile

```

----- Fatigue_ImprovedAF -----
----- MLife version 1.0 Input File -----
Test #01 Baseline test
----- Job Options -----
true      EchoInp      Echo input to <rootname>.echo as this file is being read.
false     StrNames     Use channel names following a "$" instead of numbers when specifying channels in this
input file.
false     OutData      Output modified data array after scaling and calculated channels. (currently unavailable)
"%11.3g"  RealFmt      Format for outputting floating-point values.
"AF2"     RootName     Root name for output files.
----- Input-Data -----
0         TitleLine    The row with the file title on it (zero if no title is available).
7         NamesLine   The row with the channel names on it (zero if no names are available or are specified
below).
0         UnitsLine   The row with the channel units on it (zero if no units are available or are specified
below).
9         FirstDataLine The first row of data.
0         NumChans    The number of channels in each input file.
ChanTitle ChanUnits  Scale  Offset  PSF_Type NumCols rows of data follow. Title and units strings must be 10
characters or less.
----- Calculated Channels -----
0         NumChan     The number calculated channels to generate.
1234567890 Seed      The integer seed for the random number generator (-2,147,483,648 to 2,147,483,647).
Col_Title Units  Equation Put each field in quotes. Titles and units are limited to 10 characters. NumCChan rows
of data follow.
----- Load Roses -----
0         nLoadRoses  The number of load roses to generate.
Rose Name Units  Channel1 Channel2  nSectors
----- Time and Wind Speed -----
1         TimeChan   The channel containing time.
2         WSChan     The primary wind-speed channel (used for mean wind speed and turbulence intensity, 0 for
none).
----- Statistics and Extreme Events -----
true      DoStats     Generate statistics of all the channels.
false     WrStatsTxt  Write the stats to a text file?
false     WrStatsXLS  Write the stats to an Excel file?
0         NumSFChans Number of channels that will have summary statistics generated for them.
SFChans   List of channels that will have summary statistics generated for them. Must number NumSFChans.
----- Distributions -----
false     UserDistrib User defined distribution? true = load user-specified distribution, false = only use
Weibull wind distribution
1.97     WeibullShape Weibull shape factor. If WeibullShape=2, enter the mean wind speed for WeibullScale.
11.31    WeibullScale Weibull scale factor. If WeibullShape<>2. Otherwise, enter the mean wind speed.
3        WSin        Cut-in wind speed for the turbine.
25       WSout      Cut-out wind speed for the turbine.
40       WSmx       Maximum wind speed value for the wind-speed bins.
2        WSMxBinSize Maximum width of a wind-speed bin.
0        nDistribVars Number of independent variables in the user-specified distribution, ignored if
UserDistrib = false
""       DistribName  Filename of the user-supplied distribution table, ignored if UserDistrib = false
----- Fatigue -----
1        nFatigueChannels The number of rainflow channels. Next six lines ignored if zero.
0.0      FiltRatio     The fraction of the maximum range of each channel used as a cutoff range for the
racetrack filter. Use zero for no filter.
630720000 DesignLife   Number of seconds in the design lifetime (20 years = 630720000 seconds).
1        Availability Fraction of the design life the turbine is operating when winds are between Vin and
Vout
false     BinCycles    Bin the rainflow cycles?
0.5      UCMult      Multiplier for binning unclosed cycles. (0 discards, 1 counts as a full cycle)
true     DoShortTerm Compute simple (unweighted) damage-equivalent loads and damage rates.
true     DoLife      Do lifetime-related calculations?
true     DoAggregate Compute a DELs and a damage result based on an aggregate of all the input files (does
not use the wind speed distribution)
true     WrShortTermTxt Write short-term results to plain-text files?
true     WrShortTermXLS Write short-term results to an Excel workbook?
true     WrLifeTxt   Write lifetime results to plain-text files?
false    WrLifeXLS   Write lifetime results to an Excel workbook?
1        EquivalentFrequency The frequency of the damage equivalent load (Hz)
true     DEL_AsRange true = report DELs as a range value, false = report as a one-sided amplitude
3        DEL_Type    1 = fixed mean, 2 = zero mean, 3 = both
2        GoodmanFlag 0 = no Goodman correction, 1 = use Goodman correction, 2 = compute results with and
without Goodman correction
Channel# NSlopes SNSlopeLst BinFlag MaxBinWidth/Number TypeLMF LUlt Binwidth not used when BinCycles is
false. nFatigueChannels rows of data follow. LUlt >> LMF
53      1          5          BW          100.0      AM          746386667
1        nGroups     Number of fatigue groups
Group Name NChannels ChannelList
"Basic" 1 1
----- Input Files -----
1        FileFormat  Format of input files. 1 = FAST ascii, 2 = FAST binary
11 1.1 1.3 1.5 1.7 (Weibull-Weighted Normal Operation: NumNormFiles, PSF1, PSF2, PSF3, PSF4)
"AF2_LC2.out"
"AF2_LC3.out"
"AF2_LC4.out"

```

Fatigue_ImprovedAF

```
"AF2_LC5.out"  
"AF2_LC6.out"  
"AF2_LC7.out"  
"AF2_LC8.out"  
"AF2_LC9.out"  
"AF2_LC10.out"  
"AF2_LC11.out"  
"AF2_LC12.out"  
6 1.1 1.3 1.5 1.7 (Weibull-Weighted Idling: NumIdleFiles, PSF1, PSF2, PSF3, PSF4)  
"AF2_LC1.out"  
"AF2_LC13.out"  
"AF2_LC14.out"  
"AF2_LC15.out"  
"AF2_LC16.out"  
"AF2_LC17.out"  
0 1.2 1.3 1.4 1.6 (Discrete Events: NumDiscFiles, PSF1, PSF2, PSF3, PSF4)  
==EOF==  
DO NOT REMOVE OR CHANGE. MUST COME JUST AFTER LAST LINE OF VALID INPUT.
```